UNIVERSITY OF CALIFORNIA, MERCED

WATER QUALITY IN FORESTED MOUNTAIN STREAMS: AN INVESTIGATION INTO SEDIMENT PRODUCTION, SEDIMENT TRANSPORT, AND SOURCE WATERS IN HEADWATER CATCHMENTS OF THE SIERRA NEVADA, CALIFORNIA

A dissertation submitted in partial fulfillment of the requirements
for the degree of Doctor of Philosophy

by

Sarah Elizabeth Martin

in

Environmental Systems
School of Engineering

Committee Members:

Roger C. Bales, Chair
Asmeret Asefaw Berhe
Martha H. Conklin
Joseph W. Wagenbrenner

2017

The dissertation of Sarah Elizabeth Martin is approved, and it is acceptable in quality and form for publication on microfilm and electronically:

Professor Martha H. Conklin, Advisor	Date
Associate Professor Asmeret Asefaw Berhe	Date
Research Scientist. Joseph W. Wagenbrenner	Date
Professor Roger C. Bales, Chair	Date

University of California, Merced

2017

Table of Contents

Table of Figures

Table of Tables

Acknowledgements

There are so many people I would like to acknowledge to who helped make this work a reality. First and foremost, I would like to recognize and thank my advisor Martha Conklin, for sharing her knowledge and creativity and for pushing me to think about the big picture. I am grateful for her patience and encouragement when progress was slow, but also for her enthusiasm in exploring new ways to think about the data. I have come to value her as a mentor and friend over the years we've worked together.

Thanks to Roger Bales for his spot-on questions that pushed me to improve my research and for his careful editing that has made me a better writer. I also want to acknowledge and thank the rest of my committee Asmeret Asefaw Berhe and Joe Wagenbrenner for their many hours spent reviewing this dissertation and serving on my oral defense committee.

This work would not have happened without the help of Patrick Womble, Phil Saksa, and Tyler Patel. Phil and Patrick made the *many* long drives and the wet cold/sweltering hot days of fieldwork enjoyable. I am grateful and thankful for their hard work and positive attitudes. I don't know how many water samples Tyler Patel helped filter, but I know we couldn't have finished them without his help!

I am also appreciative to Glen, Ryan, Peter, Bob, Fengjing, Matt, Michael, and the rest of my Mountain Hydrology Group colleagues for the thoughtful science discussions. It was immensely helpful being able to bounce ideas off you and get your perspective. A huge thanks to Xiande Meng too for his technological genius!

I would like to thank the Sierra Nevada Adaptive Management Project team as well. I am so glad I got to see this project through in its entirety. Everyone's dedication and enthusiasm were unbelievable. The communication and public relations skills I have learned from working with you all have been extremely helpful.

Finally, I am so grateful to my parents, Christopher and Carol Martin, who dragged me (usually willingly) out camping and hiking since before I could walk and inspired in me a love of science and the natural world. You always told me if I work hard I can do whatever I set out to do. I would not be here without your support! And last, but not least, an extra special thanks to Jason Segal for his infinite patience, support and cheerleading during the final push to finish this work. Thanks for believing in me!

This work as part of the Sierra Nevada Adaptive Management Project (SNAMP) is funded by USDA Forest Service Region 5, USDA Forest Service Pacific Southwest Research Station, US Fish and Wildlife Service, California Department of Water Resources, California Department of Fish and Game, California Department of Forestry and Fire Protection, and the Sierra Nevada Conservancy.

The text of this dissertation includes reprints of materials as they appear in Water and in Geomorphology. The co-author's listed in these publications directed and supervised research which forms the basis for the dissertation. Permission to use copyrighted material has been granted.

Vita

Education

Ph.D. Environmental Systems. University of California, Merced. 2017.
Advisor: Martha Conklin, Professor of Engineering

M.S. Environmental Systems. University of California, Merced. 2009.
Advisor: Roger Bales, Professor of Engineering

B.A. Geology; Environmental Studies. Ohio Wesleyan University. 2004.

Publications

Martin, S. E., & Conklin, M. H. (2018 *in press*). Tracking channel bed resiliency in forested mountain catchments using high temporal resolution channel bed movement. *Geomorphology*, *301*, 68–78. https://doi.org/10.1016/j.geomorph.2017.10.026

Conklin, M. H., Bales, R. C., Saksa, P. C., Martin, S. E., & Ray, R. (2015). Appendix E: Water Team Final Report. *Learning How to Apply Adaptive Management in Sierra Nevada Forests: An Integrated Assessment. Final Report of the Sierra Nevada Adaptive Management Project (P. Hopkinson and J.J. Battles, Eds.)*, 104.

Conklin, M. H., Bales, R. C., Saksa, P. C., Martin, S. E., Ray, R., Tobin, B., & Womble, P. (2015). *Sierra Nevada Adaptive Management Project Water-Team Update*.

Martin, S. E., Conklin, M. H., & Bales, R. C. (2014). Seasonal accumulation and depletion of local sediment stores of four headwater catchments. *Water (Switzerland)*, *6*(7), 2144–2163. https://doi.org/10.3390/w6072144

Conklin, M. H., Bales, R. C., Ray, R., Martin, S. E., Saksa, P. C., & Womble, P. (2012). *Sierra Nevada Adaptive Management Project Water-Team Field Activities, Methods and Results*.

Martin, S. E. (2009). *Comparison of in-stream sediment sources and assessment of a bank migration model for headwater catchments in the Central Sierra Nevada, California*. University of California, Merced.

Abstract

The work presented herein examines how and to what extent turbidity, channel bed movement and stream source water ratios change over different temporal scales in four forested mountain headwater catchments in the Sierra Nevada, California. This work focuses on the water quality topics of sediment and source waters as part of a larger study on the effects of forest fuels treatments. No effects on water quality were expected because treatments were set far back from the stream channel and relatively light (8.0% and 7.5% decrease in mean Leaf Area Index (LAI) for the northern and southern site respectively). Therefore, this work was designed to characterize sediment and source waters rather than explore treatment impacts. In doing so important insights were gained around sediment and stream water sources.

Sediment movement was found to be highly episodic and tied to low-frequency, short-duration discharge events with pronounced seasonality. Turbidity hysteresis patterns indicated localized (bed and banks) sediment sources that were mobilized quickly but became progressively depleted. Continuous measurement of channel bed elevations in the thalweg pointed to seasonal mobilization (connectedness) of sediment during winter, a gradual depletion through spring and early summer, and disconnectedness in low flow season when material builds up again at the base of banks mirroring patterns seen in the turbidity hysteresis loops. Stream water chemistry data showed higher concentrations during base flow, which was exacerbated by consecutive years of drought. The high base flow ion concentrations were tied to high ratios of groundwater. End-member mixing analysis showed that wet and dry years had similar source water ratios during high flow (winter and spring) but during the low flow season (late summer), a shift toward higher ratios of groundwater was seen for drought years. Recent tree mortality observed across the Sierra Nevada after four consecutive years of drought underscores the critical role of groundwater in maintaining baseflow and sustaining forest ecosystems. Better understanding of sediment processes, source water contributions, and drought effects in small, forested, mountain, headwater catchments provides an important foundation for sustainable land use management, more effective channel restoration design, and improved mitigation of downstream water quality.

This dissertation *Water Quality in Forested Mountain Streams: An Investigation into Sediment Production, Sediment Transport, and Source Waters in Headwater Catchments of the Sierra Nevada, California* by Sarah Elizabeth Martin, is submitted in partial fulfillment of Doctor of Philosophy in Environmental Systems from the University of California, Merced (Martha H. Conklin, advisor; Roger C. Bales, committee chair).

Chapter 1. Introduction

Background

Headwater streams make up the majority of the stream network in both drainage area and river miles (MacDonald and Coe, 2007; US Environmental Protection Agency, 2017). Due in part to their close connectedness to the landscape and groundwater, headwater streams are corridors for both water and pollutants to reach downstream water bodies (US Environmental Protection Agency, 2017). Hydrologic and biogeochemical processes in headwater streams control the timing and longitudinal distance of chemical transport to higher order streams and rivers (Alexander et al., 2007).

Over half the annual water supply in the state of California originates in the Sierra Nevada, with downstream aquatic ecosystems, and applications such as hydropower, agriculture, and municipal water supplies dependent on this high-quality water (Kattelman et al., 1983, Sierra Nevada Conservancy, 2011, Saksa, 2015). Threats to water quality in the Sierras, which come mainly in the form of increased sediment loading, jeopardize the stability of downstream resources.

Uncertainty in the face of climate change poses a further threat to these systems with increased variability in amount and timing of snow and rain. Climate change may already be leading to more intense drought, wildfires, and pest outbreaks in the Sierra Nevada, with the potential to significantly affect land cover, runoff, and water quality. Lindner *et al*. (2010), in their study of European forests, found that Mediterranean regions were particularly vulnerable to increased drought and wildfire risk with climate change. In the face of rapid change, it is no longer possible to rely on past conditions to provide adequate models for current and future management (Millar et al., 2007). As drought and extreme events are predicted to increase, new data from mountain regions (including the Sierra Nevada) particularly susceptible to the effects of these changes are especially important (Bales, 2006, Lindner et al., 2010). This work adds to that knowledge of forested, mountain, headwater systems by providing a better understanding of sediment movement patterns and water sources to streams, the connection between in-stream sediment movement and catchment flow paths, and the effects extended drought may have on these water sources.

Sediment production and sediment transport play a key role in nutrient cycling, weathering rates, contaminant transport, stream water quality, aquatic-habitat quality, and water-supply/flood-control infrastructure (Snyder et al., 2004; Gathard Engineering Consultants, 2006). It has been well documented that overland flow in undisturbed landscapes in the mountain west is rare, and sediment delivery to streams from overland flow is minimal, only occurring during extreme storm events, shortly after major land disturbances such as logging and/or fire, or in conjunction with poorly built/maintained roads (Haupt, 1967; Stafford, 2011; de Koff et al., 2006). Infiltration and sub-surface water delivery to streams, represents "normal" conditions within the watershed and it

stands to reason then that sediment in streams is mainly from reworking of channel bed and bank material; but a better understanding of the patterns and variability of sediment processes in small, forested, mountain, headwater catchments is necessary as a foundation for sustainable land use management, improved channel restoration design, and better mitigation of sediment's downstream effects.

The research presented aims to answer the following questions: 1) What are the seasonal and event level turbidity patterns and their implications to sediment production and transport in forested mountain headwater streams of the Sierra Nevada, 2) What are the patterns of channel bed movement in these systems and implications for sediment sources and channel bed stability, and 3) How does drought affect stream water chemistry and source water ratios?

The Sierra Nevada Adaptive Management Project

This work is part of the Sierra Nevada Adaptive Management Project (SNAMP), a multidisciplinary assessment of the effects of forest fuels management on a wide array of ecosystem variables. SNAMP was conceived "in response to uncertainty about forest fuels management in the Sierra Nevada and the controversy resulting from the United States Forest Service's 2004 Sierra Nevada Framework that established the current legal boundaries for management prescriptions in the Sierra Nevada national forests" (SNAMP Science Team, 2015). The goal of SNAMP was to assess the impacts of the U.S. Forest Service's Strategically Placed Land Area Treatments (SPLATs) on the ecosystem variables of water, forest health, and wildlife and to evaluate and promote the interaction between the public and agency stakeholders. To do so, a six-part science team was formed focusing on specific ecosystem variables or subject areas. Teams included Wildlife teams studying the California Spotted Owl and Pacific Fisher, a Fire and Forest Health Team looking at fire history, forest structure, and predictive fire models, a Public Participation Team studying and facilitating interaction between stakeholders, a Spatial Team collecting and analyzing extensive spatial data for this project, and a Water Team, (of which the work presented here was a part) looking at changes to water quality and changes in the amount and timing of water moving through the study catchments.

General study design

A Before-After-Control-Impact (BACI) design was adopted for this project, thus two sets of paired study watersheds were chosen for instrumentation and study. The original study design consisted of seven years, which included 3 of pre-treatment and 3 of post-treatment. However, significant delays in the implementation of treatments, limited the post-treatment period to only 2013 as part of the SNAMP project and heavily weighting the study toward pre-treatment data. Some measurements were continued past 2013 and those results are presented here. Hydrologic models were used to project water

quantity parameters into the future, however modeling was not feasible for water quality parameters and instead the focus was placed on characterization of the watersheds and their observed response (SNAMP Science Team, 2015)

Contents summary

This dissertation consists of six chapters. The first two and the last are an introduction and conclusion for this work in its entirety. Chapter 1, the introduction is intended to set the general context of this work including background information on the Sierra Nevada Adaptive Management Project. Chapter 2 presents additional information on the study sites that is not included in subsequent chapters. Chapter 6, pulls together findings presented here and discusses how the three papers fit together. This work is then placed in the broader context of water quality and forest management. Finally, some recommendations are given for next steps and suggestions on the direction of future research and management efforts in these systems.

Chapters 3, 4, and 5 are written as stand-alone journal manuscripts intended for publication. At the time of submission, the material in Chapter 3 has been published (Martin, et al., 2014) and Chapter 4 is in press (Martha and Conklin, 2018 in press). Chapter 3 focuses on the suspended sediment data set from water years 2010 through 2012. It explores the seasonal patterns of turbidity and uses event level turbidity-discharge hysteresis analysis to determine the sediment sources that contribute to storm event turbidity. A conceptual model for sediment source and transport is proposed based on the findings.

Chapter 4 explores patterns of bedload movement using load-cell pressure sensors that have been relatively untried in forested, mountain, headwater systems. Methods for data collection with these sensors are presented and the feasibility/reliability of these sensors in this type of environment is touched on. Event, seasonal, and inter-annual patterns of channel bed accumulation and depletion are considered. A conceptual model that builds on the model from Chapter 3 is presented, which links sediment sources along the channel margins to patterns of channel bed fill and scour in the thalweg. This model helps to explain the seasonal and annual patterns seen in both turbidity and bedload.

Finally, Chapter 5 shifts gears slightly and focuses on water chemistry data from this study. This dataset extends from water years 2010 through 2014 allowing for comparison of both above average and below average precipitation years. water chemistry and source water ratios are examined in terms of seasonal differences as well the effects of three years of consecutive drought. Finally, the importance of groundwater during baseflow and especially during baseflow of drought years is discussed in terms of forest health and ecosystem vulnerability to climate change.

References

Alexander, R. B., Boyer, E. W., Smith, R. A., Schwarz, G. E., & Moore, R. B. (2007). The role of headwater streams in downstream water quality. *Journal of the American Water Resources Association*, *43*(1), 41–59. https://doi.org/10.1111/j.1752-1688.2007.00005.x

Bales, R. C., Molotch, N. P., Painter, T. H., Dettinger, M. D., Rice, R., & Dozier, J. (2006). Mountain hydrology of the western United States. *Water Resources Research*, *42*(8), 1–13. https://doi.org/10.1029/2005WR004387

Bateman, P. C. (1989). *Geologic map of the Bass Lake quadrangle, west-central Sierra Nevada, California*.

Conklin, M. H., Bales, R. C., Ray, R., Martin, S. E., Saksa, P. C., & Womble, P. (2012). *Sierra Nevada Adaptive Management Project Water-Team Field Activities, Methods and Results*.

Conklin, M. H., Bales, R. C., Saksa, P. C., Martin, S. E., & Ray, R. (2015). Appendix E: Water Team Final Report. *Learning How to Apply Adaptive Management in Sierra Nevada Forests: An Integrated Assessment. Final Report of the Sierra Nevada Adaptive Management Project (P. Hopkinson and J.J. Battles, Eds.)*, 104.

Conklin, M. H., Bales, R. C., Saksa, P. C., Martin, S. E., Ray, R., Tobin, B., & Womble, P. (2015). *Sierra Nevada Adaptive Management Project Water-Team Update*.

de Koff, J. P., Graham, R. C., Hubbert, K. R., & Wohlgemuth, P. M. (2006). Prefire and postfire erosions of soil nutrients within a chaparral watershed. *Soil Science*, *171*(12), 915–928. https://doi.org/10.1097/01.ss.0000235231.02063.c2

Gathard Engineering Consulting. (2006). *Klamath River Dam and Sediment Investigation*. Seattle, Washington. Retrieved from https://www.fws.gov/yreka/kri/gecfinalreport.pdf

Haupt, H. F. (1967). Infiltration, overland flow, and soil movement on frozen and snow-covered plots. *Water Resources Research*, *3*(1), 145–161. https://doi.org/10.1029/WR003i001p00145

Kattelmann, R. C., Berg, N. H., & Rector, J. (1983). The potential for increasing streamflow from Sierra Nevada watersheds. *Journal of the American Water Resources Association*, *19*(3), 395–402. https://doi.org/10.1111/j.1752-1688.1983.tb04596.x

Lindner, M., Maroschek, M., Netherer, S., Kremer, A., Barbati, A., Garcia-Gonzalo, J., Seidl, R., Delzon, S., Corona, P., Kolstrom, M., Lexer, M. J., Marchetti, M. (2010). Climate change impacts, adaptive capacity, and vulnerability of European forest ecosystems. *Forest Ecology and Management*, *259*(4), 698–709. https://doi.org/10.1016/j.foreco.2009.09.023

MacDonald, L. H., & Coe, D. (2007). Influence of Headwater Streams on Downstream Reaches in Forested Areas. *Society of American Foresters*, *53*(2), 148–168. Retrieved from http://www.ingentaconnect.com/content/saf/fs/2007/00000053/00000002/art00005

Martin, S. E., & Conklin, M. H. (2018 *in press*). Tracking channel bed resiliency in forested mountain catchments using high temporal resolution channel bed movement. *Geomorphology*, *301*, 68–78. https://doi.org/10.1016/j.geomorph.2017.10.026

Martin, S. E., Conklin, M. H., & Bales, R. C. (2014). Seasonal accumulation and depletion of local sediment stores of four headwater catchments. *Water (Switzerland)*, *6*(7), 2144–2163. https://doi.org/10.3390/w6072144

Millar, C. I., Stephenson, N. L., & Stephens, S. L. (2007). Climate change and forest of the future: Managing in the face of uncertainty. *Ecological Applications*, *17*(8), 2145–2151. https://doi.org/http://dx.doi.org/10.1890/06-1715.1

Saksa, P. (2015). Forest management, wildfire, and climate impacts on the hydrology of Sierra Nevada mixed-conifer watersheds, 127.

Saucedo, G. J., & Wagner, D. L. (1992). *Geologic map of the Chico quadrangle.*

Saxton, K. E., & Rawls, W. J. (2006). Soil water characteristic estimates by texture and organic matter for hydrologic solutions. *Soil Science Society of America Journal*, *70*(5), 1569–1578. https://doi.org/10.2136/sssaj2005.0117

Sierra Nevada Conservancy. (2011). California's Primary Watershed. Retrieved June 23, 2014, from http://www.sierranevada.ca.gov/our-region/ca-primary-watershed

SNAMP Science Team. (2015). Learning adaptive management of Sierra Nevada forests: An integrated assessment. *Sierra Nevada Adaptive Management Project*.

Snyder, N. P., Rubin, D. M., Alpers, C. N., Childs, J. R., Curtis, J. A., Flint, L. E., & Wright, S. A. (2004). Estimating accumulation rates and physical properties of sediment behind a dam: Englebright Lake, Yuba River, northern California. *Water Resources Research*, *40*(11), 1–19. https://doi.org/10.1029/2004WR003279

Stafford, A. K. (2011). *Sediment Production and Delivery from Hillslopes and Forest Roads in the Southern Sierra Nevada, California*. Colorado State University.

US Environmental Protection Agency. (2017). Headwater Streams Studies. Retrieved November 11, 2017, from https://www.epa.gov/water-research/headwater-streams-studies

USDA Natural Resource Conservation Service. (2013). NRCS Web Soil Survey. Retrieved March 11, 2015, from http://websoilsurvey.sc.egov.usda.gov/App/WebSoilSurvey.aspx

Chapter 2. Site descriptions

Sites in this study are characterized by a Mediterranean climate with a distinct wet and dry season. Catchments are located in the rain-snow transition zone, with snow making up 40 to 60 percent of average annual precipitation. Winters in the Sierra are typically warm and wet with the historical average for peak snow pack accumulation occurring around April 1. Annual precipitation varies widely; data for this study were collected in years of high, average, low, and extremely low total precipitation. Study streams were typically perennial but in recent low water years sections went intermittent during summer low flows. Timing of precipitation and subsequent size and duration of the snow pack also varied greatly with some years seeing high precipitation early in the water year and late spring storms bringing a substantial portion of the annual precipitation in other years. Precipitation patterns are covered in substantial detail in the following chapters as it relates to water quality, sediment, and source water data.

Study sites include a total of four paired catchments (two at each site) in the central Sierra Nevada, California. The northern site, which takes its name from the Last Chance treatment project is located in Placer County 24 km northeast of Foresthill, California. The southern site named from the Sugar Pine treatment project is in Madera County approximately 5 km east of Fish Camp, California (Figure 2.1). Both study sites are managed by the USDA National Forest Service with historic and present-day land uses including, grazing, timber production, hunting, recreation, and conservation.

Effort was made to choose catchments with comparable physiographic characteristics, including, elevation, perennial streamflow (during normal water years), stream gradients, hillslope gradients, aspects, vegetation types, canopy closures, tree size distributions, and proximity to each other.

Speckerman Creek and Big Sandy Creek were chosen as study catchments for the Sugar Pine (southern) site (Figure 2.1). Both catchments are located off Jackson Road. The Speckerman catchment outlet intersects Jackson Road approximately 5.6 km from Highway 41 intersection and the upper watershed starts on the northwest side of Speckerman Mountain. The Big Sandy catchment outlet is located at the crossing of Forest Service Road 5S22 near the FS 5S22-Jackson Road intersection in Big Sandy Campground. The watershed extends northeast from the catchment outlet. Outlet coordinates are given in Table 4.1.

At the Last Chance (northern) study site, Bear Trap Creek and Frazier Creek were chosen (Figure 2.1). The Frazier Creek outlet is at the crossing of Forest Service Road 44 approximately 4.7 miles north of the intersection of FS 44 and Mosquito Ridge Rd. The outlet for Bear Trap Creek is approximately 5.2 miles north of the Frazier outlet, also along FS 44. The upper watershed of the two sites border each other east of the catchment outlets.

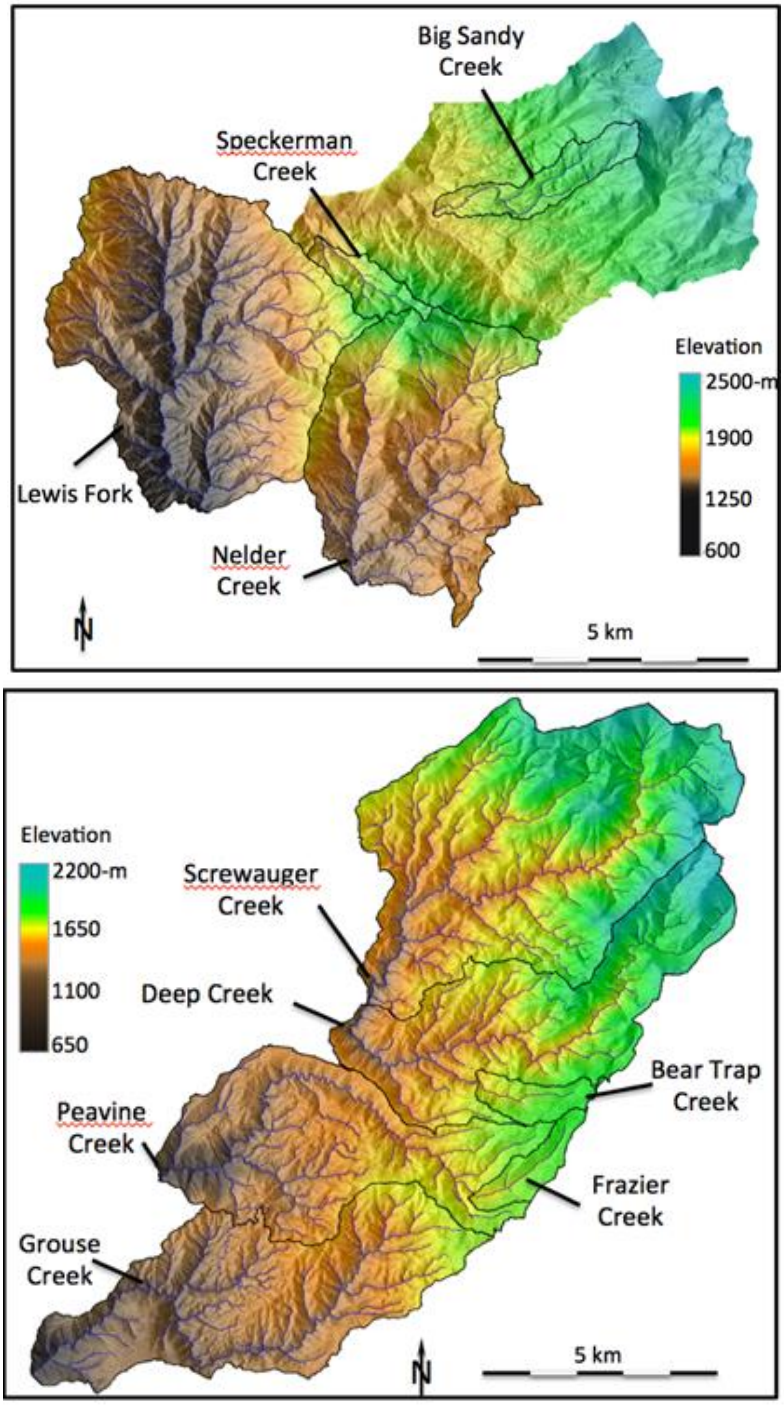

Figure 2.1. Sierra Nevada Adaptive Management Project study sites (SNAMP Science Team, 2015)

Study catchments ranged in size from 1.62 to 2.47 km^2 with Speckerman being the smallest catchment, Big Sandy being the largest and Frazier and Bear Trap intermediate sizes (Table 2.1). Watersheds ran roughly east to west, with north and south facing hillslopes on either side of the channel (Figure 2.1, Table 2.1). Catchment outlet elevations were slightly higher at the southern sites (Table 2.1).

Table 2.1. Watershed physiographic characteristics

	Big Sandy Creek	**Speckerman Creek**	**Bear Trap Creek**	**Frazier Creek**
Outlet elevation (m)	1778	1719	1560	1605
Area (km^2)	2.47	1.62	1.76	1.68
Aspect	southwest	northwest	southwest	west
Soils	Loamy sand/sand	Loamy sand/sand	Sandy loam/ loam	Sandy loam/ loam
Geology	tonalite	tonalite	Miocene-Pliocene andesitic volcanics; sandstones, siltstones/slates	Miocene-Pliocene andesitic volcanics; sandstones, siltstones/slates

Both the northern and southern study sites consist mainly of a mixed conifer forest type with live oak-pine forest type playing a lesser role at the southern site. In the north, Bear Trap was 100% mature mixed-conifer classification and Frazier was 95% mature mixed conifer. For the southern catchments, Speckerman contained 82% mature mixed conifer and 18% live oak-pine forest while Big Sandy had 56% mature mixed conifer and 33% live oak-pine (Saksa, personal communication, Nov 11, 2017). Canopy closures for mature mixed conifer forest types were 60-70% and 10-25% for live oak-pine forest type (SNAMP Science Team, 2015).

White fir (Abies concolor), Douglas-fir (Pseudotsuga menziesii), incense cedar (Calocedrus decurrens), sugar pine (Pinus lambertiana), ponderosa pine (Pinus ponderosa), and California black oak (Quercus kelloggii) are the key tree species found at the Last Chance site. The Sugar Pine site similarly has White fir (Abies concolor) incense cedar (Calocedrus decurrens), sugar pine (Pinus lambertiana), ponderosa pine (Pinus ponderosa), and California black oak (Quercus kelloggii), but lacks Douglas-fir (Pseudotsuga menziesii). The Sugar Pine firesheds also include a grove of giant sequoia (Sequoiadendron giganteum). Riparian hardwood species and woody and herbaceous shrubs are present in varying density patches at both study sites. Dominate shrub species were mountain whitethorn (Ceanothus cordulatus), deerbrush (Ceanothus integerrimus),

and greenleaf manzanita (Arctostaphylos patula)). Additional details on the study firesheds and the extended wildlife study areas can be found in the SNAMP Final Report. (SNAMP Science Team, 2015).

Soil depths ranged from 0 to 1.5 m across all sites with most of the watersheds averaging around 0.75 m. Typical of much of the Sierra Nevada, soils tended to have high infiltration capacities (DeByle, 1970). Texture analysis was performed on limited soil samples taken at soil moisture instrument locations for the full soil profile. Data from the analysis indicated loams and sandy loams for the northern study site and sands, loamy sands, and sandy loams at the southern site (Figure 2.2). Estimates of soil porosities were made using the USDA Agricultural Research Service Hydrology and Remote Sensing Laboratory SPAW model (USDA Agricultural Research Service, n.d.). This model is based on equations from Saxton and Rawls (2006) relating texture to bulk density. Assumed values of 2.65 g/cm3 for particle density, and 1% for organic matter. Sand and clay content were obtained from the soil texture analysis and estimated organic matter was based on data from California Soil Resource Lab, (n.d.). Soil porosity was found to be high, estimated in the 40-45% range (Figure 2.3)

At the southern site, the dominant soils were well drained and derived from granitic parent material. Common soil types at these sites included Ledford family, Entic xerumbrepts, Chaix and Chawanakee variant. The dominant soils at the northern site were also well draining, but were derived from a mix of metamorphic, metasedimentary, and volcanic parent material. Common soils at the northern study site included Crozier, Cohasset, Deadwood, Hurlbut, Mariposa, and McCarthy family soils. Rock outcrops were also common at both the northern and southern sites. (California Soil Resource Lab, n.d.).

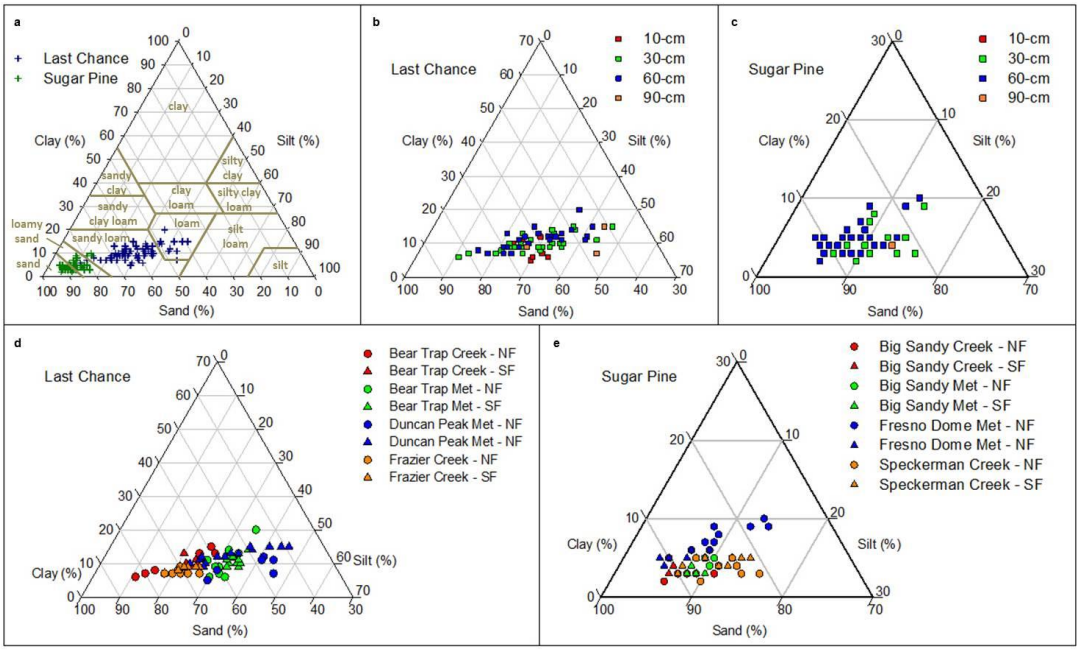

Figure 2.2. Soil texture analysis for samples collected at soil moisture locations (SNAMP Science Team, 2015).

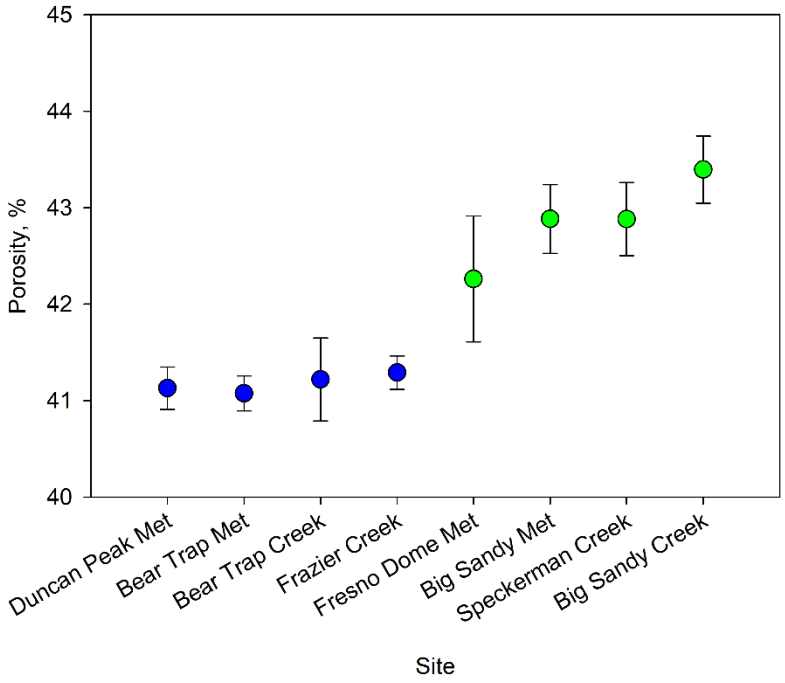

Figure 2.3. Soil porosity estimates for watershed and meteorological station soil samples.

All four watersheds are dominated by a step-pool channel type. Secondary channel types at the southern site are pool-riffle and at the northern sites plane bed type. Additionally, Bear Trap has some scattered bedrock outcrops that locally influence channel type.

Sediment sizes were slightly smaller at the southern sites, with the D_{50} at in-stream instrument locations in the sand range for Big Sandy and the small gravel range for Speckerman. These sites had a substantial fines fraction (silt and clay) with large boulders and woody debris constraining the geomorphology. The D_{50} value for Frazier Creek at the northern site was in the small gravel range, but unlike Speckerman, had a much lower fraction of fines. Bear Trap's D_{50} for the instrument site was in the medium to large gravel range and also had a very low fines fraction. Both northern catchments had considerably larger portion of cobble throughout the watershed. Large woody debris constrained the geomorphology in both catchments, with bedrock outcrops additionally playing a role at Bear Trap. Southern site sediments tended to be more a spherical shape characteristic of granitic rock, while the northern site sediments were more a planar shape representative of the metamorphic rocks in the area.

Table 2.2. Channel geomorphic characteristics

	Big Sandy Creek	**Speckerman Creek**	**Bear Trap Creek**	**Frazier Creek**
Channel type	Step-pool and pool-riffle	Step-pool and pool-riffle	Step-pool and plane bed; some bedrock	Step-pool and plane bed
Dominant bed material	Sand, gravel, boulder	Sand, gravel, cobble	Gravel, cobble	Gravel, cobble
Geomorphic element	Boulder, LWD	LWD	Bedrock, LWD	LWD

In-stream depth, temperature, conductivity, dissolved oxygen, and sediment measurements were collected in the study catchments along with snow depth and soil moisture measurements on the adjacent stream banks. Four meteorological stations were instrumented for this study on open ridges near the study catchments. Instruments measured wind speed/direction, temperature, relative humidity, precipitation, and solar radiation along with snow depth and soil moisture on the adjacent north and south facing hillslopes. Stations were placed at elevations similar to catchment outlets and to the upper watersheds for the northern and southern study sites. A conceptual diagram of site instrumentation locations from this study are shown in Figures 2.4 to 2.7. Additional details on instrumentation and data collection are given in subsequent chapters as well as in the SNAMP Final Report. (SNAMP Science Team, 2015).

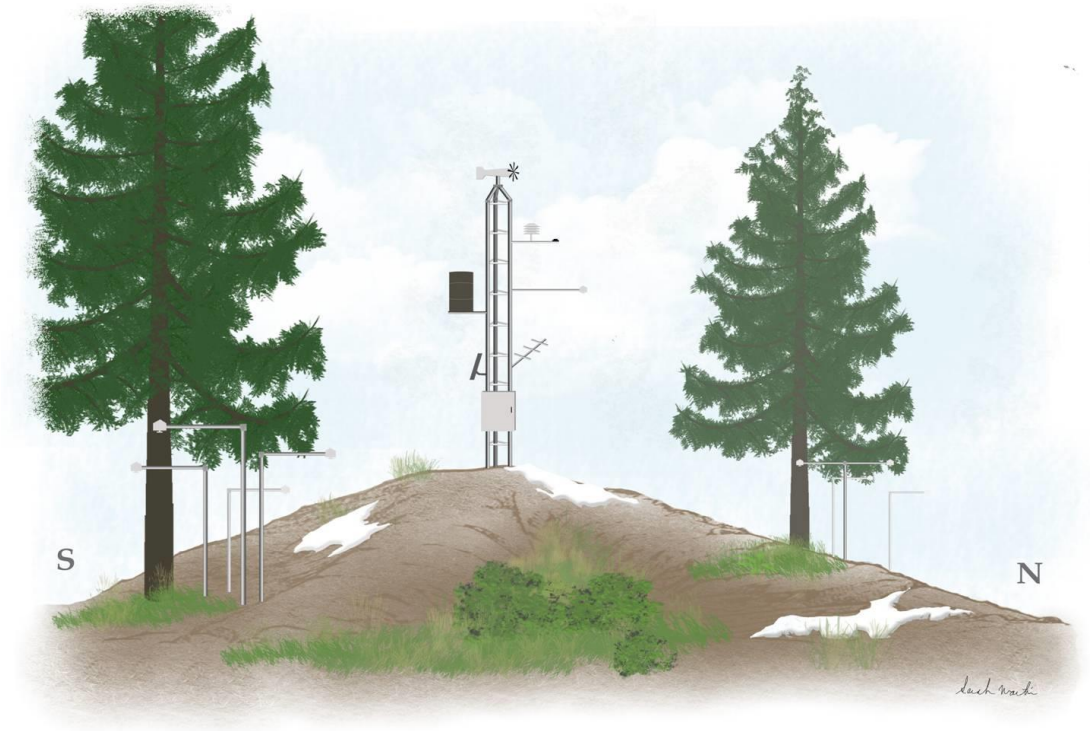

Figure 2.4. Conceptual diagram of meteorological station instrumentation.

Figure 2.5. Conceptual diagram of stream instrumentation.

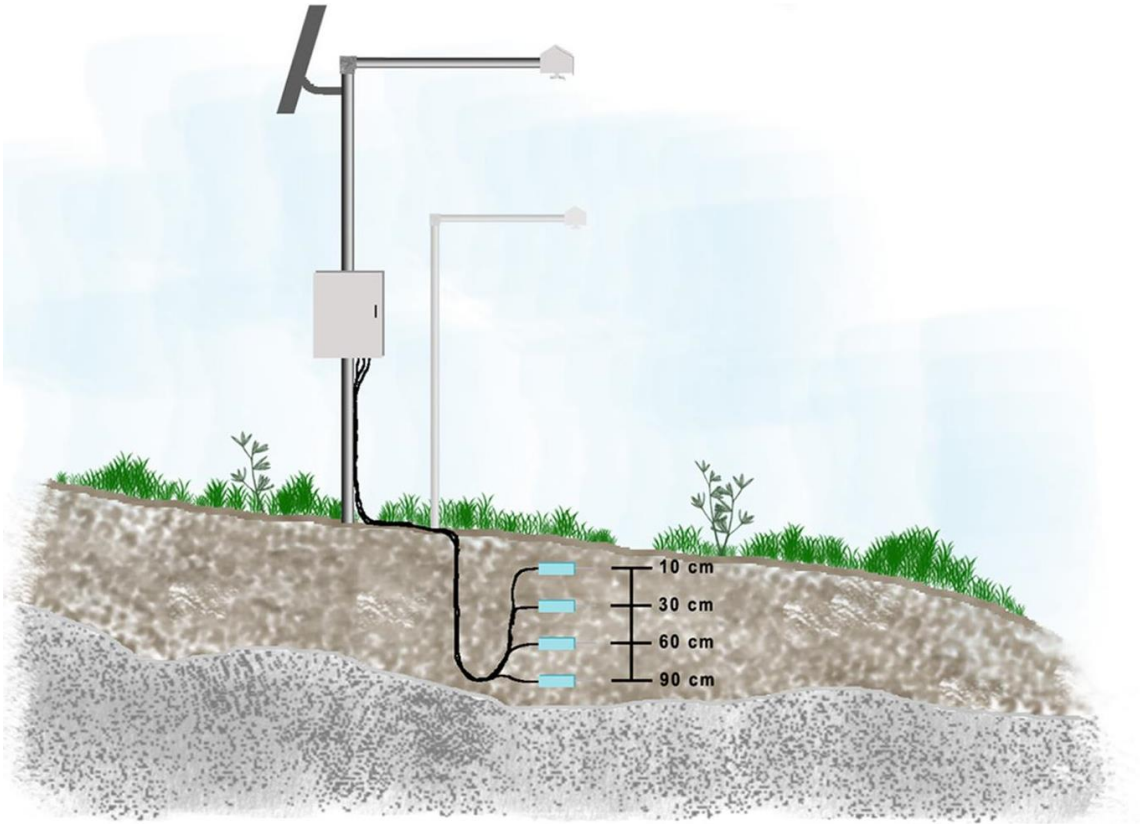

Figure 2.6. Diagram of instrumentation at a hillslope node showing snow depth and soil moisture sensors. Nodes were located on hillslopes adjacent to stream instruments and meteorological stations.

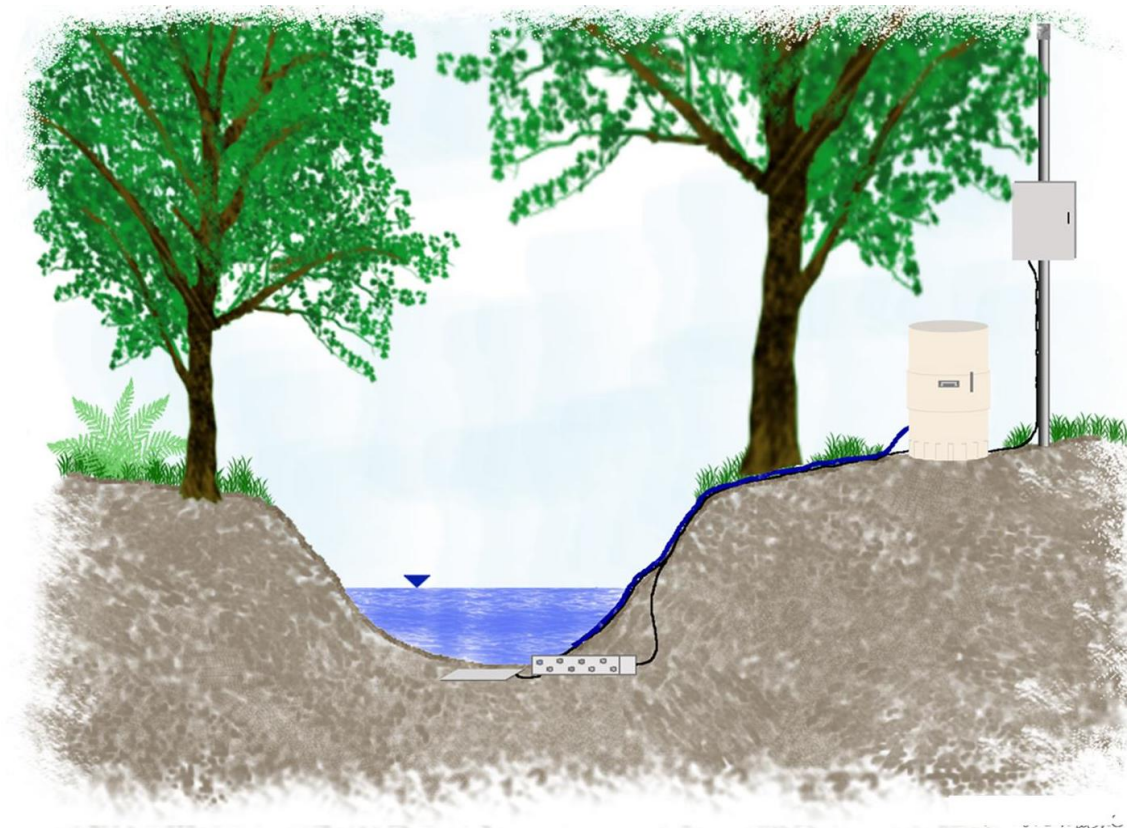

Figure 2.7. Diagram of stream instrumentation sites. In-stream instruments include multi-parameter YSI sonde, ISCO automated sampler, Solinst pressure transducers, and load-cell pressure sensors.

References

California Soil Resource Lab. (n.d.). SoilWeb: An Online Soil Survey Browser. Retrieved December 6, 2017, from https://casoilresource.lawr.ucdavis.edu/gmap/

DeByle, N. V. (1970). *Infiltration in Contour Trenches in the Sierra Nevada*. Ogden, UT.

Saxton, K. E., & Rawls, W. J. (2006). Soil water characteristic estimates by texture and organic matter for hydrologic solutions. *Soil Science Society of America Journal*, *70*(5), 1569–1578. https://doi.org/10.2136/sssaj2005.0117

SNAMP Science Team. (2015). Learning adaptive management of Sierra Nevada forests: An integrated assessment. *Sierra Nevada Adaptive Management Project*.

USDA Agricultural Research Service. (n.d.). Hydrology and Remote Sensing Laboratory. Retrieved December 6, 2017, from https://www.ars.usda.gov/northeast-area/beltsville-md/beltsville-agricultural-research-center/hydrology-and-remote-sensing-laboratory/

Chapter 3. Seasonal Accumulation and Depletion of Local Sediment Stores of Four Headwater Catchments

Sarah Martin *, Martha Conklin and Roger Bales
(Published July 23, 2014 in *Water*)

Abstract

Seasonal turbidity patterns and event-level hysteresis analysis of turbidity verses discharge in four 1 km^2 headwater catchments in California's Sierra Nevada indicate localized in-channel sediment sources and seasonal accumulation-depletion patterns of stream sediments. Turbidity signals were analyzed for three years in order to look at the relationships between seasonal turbidity trends, event turbidity patterns, and precipitation type to stream sediment production and transport. Seasonal patterns showed more turbidity events associated with fall and early to mid- winter events than with peak snow-melt. No significant turbidity patterns emerged for periods of snow melt *vs*. rain. Single event hysteresis loops showed clockwise patterns were dominant suggesting local sediment sources. In successive discharge events, the largest turbidity spike was often associated with the first but not necessarily the largest discharge event-indicating seasonal depletion of local sediment stores. In multi-peaked discharge events, hysteresis loops shifted from clockwise to linear or random patterns suggesting that localized sediment stores are being used up and sufficient flow energy must be reached to start entraining the more consolidated bank/bed sediment or that dominant sediment sources may be shifting to less localized areas such as hill slopes. A conceptual model with phases of accumulation and transport is proposed.

Keywords: hysteresis; sediment; snowmelt; storm event; turbidity

Introduction

This research analyzes the seasonal turbidity and event-level hysteresis patterns of turbidity *versus* discharge in four 1 km^2 headwater catchments in the Sierra Nevada, California. Turbidity events in this region are reported to be infrequent and of short duration (Mazurkiewicz et al., 2011). Turbidity event patterns can vary on multiple time scales as the controlling factors on erosion and sediment transport vary. Understanding the patterns of turbidity events and source areas of sediment within watersheds will allow managers to better target erosion-control measures and to better plan for turbidity-related impacts to downstream water quality.

Fine sediments that remain in suspension and cause turbidity signals in streams can come from hillslope or in-channel sources. On hillslopes and floodplains, the relevant sediment production processes may include soil creep, rain splash, overland flow, bioturbation, and snow creep (Leopold et al., 1995). In-channel processes that can act on banks include mass failure, freeze thaw cycles, drying and crumbling, fluvial erosion during high flows, and bioturbation (Leopold et al., 1995). In-channel erosion processes that act on the channel bed are generally a form of fluvial erosion (*i.e.*, re-suspension or vertical incision). Previous work in stream systems similar to those in this study has suggested that in-channel erosion of the bed and banks are the more important processes in forested mountain headwater catchments (Stafford, 2011).

Turbidity and suspended sediment are controlled not only by discharge but also by erosion and transport processes causing accumulation and depletion of sediment that can vary spatially and temporally within a watershed or event (Doomen et al., 2008). The processes which factor into producing a turbidity signal often depend on the interplay between physical watershed features (*i.e.*, gradient, soil porosity, and vegetation cover), sediment availability, precipitation attributes (*i.e.*, amount, intensity, rain *vs*. snow) and antecedent moisture conditions of the soil. Because of these additional controls on turbidity, typical rating curves based on linear regressions between discharge and suspended sediment concentrations tend to perform poorly for predicting turbidity or sediment loads (Langlois et al., 2005; Doomen et al., 2008; Rodriguez-Blanco et al., 2010; Gao and Josefson, 2012).

The offset of turbidity or suspended sediment peaks from discharge peaks, termed hysteresis effect, can provide insight into sediment movement within watersheds. Hysteresis analysis has long been established as a technique for examining sediment source areas or processes in a wide range of watershed sizes and types based on the shape of discharge-sediment hysteresis loops. The temporal relationship between the turbidity peak and the discharge peak can indicate the proximity of the sediment source and whether sediment depletion is occurring (Wood, 1977; Williams, 1989). Early papers by Wood (1977) and Williams (1989) identified a hysteresis effect and related each hysteresis type to physical processes in the streams. Hysteresis loops are classified into five types (Williams, 1989). Clockwise patterns are produced when turbidity peaks occur before discharge peaks indicating a localized sediment source and/or depletion of the source. Counterclockwise patterns occur when turbidity peaks occur after discharge peaks, indicating a more distant sediment source, a discharge threshold that must be reached to entrain consolidated bank sediments, or a rainfall threshold required to initiate overland flow. Linear patterns, where peaks occur simultaneously, imply a sediment source at an intermediate distance, a lower entrainment threshold, or a continuous supply of sediment. Figure eight and complex patterns typically occur when there are multiple sediment source locations or multiple erosion processes acting concurrently.

Over the past several decades, a significant amount of research has been done on the relationships between precipitation, discharge, and sediment transport. However, much of this work has been focused on individual discharge events (Sadeghi et al., 2008; Granger et al., 2011; Wilson et al., 2012), or has been in predominately agricultural areas (Doomen et al., 2008; Soler et al., 2008; Rodriguez-Blanco et al., 2010; Granger et al., 2011; Gao and Josefson, 2012; Wilson et al., 2012), in small hillslope plots (Granger et

al., 2011) or in areas with drastically different physiographic and climatic regimes (McDonald and Lamoureux, 2009; Fang et al., 2011; Gao and Josefson, 2012). A few longer studies looking at multiple time scales have shown considerable temporal variation in sediment patterns. McDonald and Lamoureux (2009) found significant temporal variation in suspended sediment transport in High Arctic catchments that was linked to snow melt. Rodriguez-Blanco *et al*. (2010) found for agricultural basins in Spain that at the event scale sediment peaked before discharge, at the seasonal time scale sediment yield decreased through the season, and at the annual scale yield was linked to the percentage of the year that large events occurred. For a medium sized basin in Central New York, Gao and Josefson (2012) found event and seasonal patterns to be too complex to identify sources or processes but they did show that in their system, event sediment was generally supply limited. Iida *et al*. (2012) looked at hysteresis patterns associated with snow melt in a temperate mountain catchment in Japan. They found that more sediment moved during the snow melt season than the rest of the year and that a shift from clockwise to counter-clockwise hysteresis patterns occurred as the snow melt season progressed. Fang *et al*. (2011) found differences in the sediment-discharge hysteresis patterns between the hillslope plot (clockwise) and small basin scales (counterclockwise) that implied a hillslope source area in the Loess Plateau of China. Headwater and larger order basins in southeast Australia were studied by Smith and Dragovich (2009) who suggested that differences in sediment patterns were due to rates of sediment transfer to larger order basins.

Work in small, forested mountain catchments with a Mediterranean climate has been limited. Seeger *et al*. (2004) showed for a basin in the central Spanish Pyrenees that seasonal differences in hysteresis loop patterns were tied to antecedent conditions within the basin. In their work in the Lake Tahoe region, Langolis *et al*. (2005) showed fairly consistent clockwise sediment-discharge patterns for the snow melt season, but did not look at other seasons.

An understanding of sediment in small headwater catchments in mountain areas is important as they are a main water source and often a dominant sediment source area (Sierra Nevada Conservancy, 2011). This is especially true in California where 60 percent of the water comes from the Sierra Nevada and most of the major river systems contain dams where storage area can be greatly reduced by accumulating sediment (Sierra Nevada Conservancy, 2011). Several case studies on California reservoirs have shown that the fine sediment fraction (silt, clay, and sand), which can cause turbidity in headwater reaches, accounts for the majority of accumulated sediment in reservoirs (Snyder et al., 2004; Gathard Engineering Consulting, 2006). Sediment and sediment transport also play a key role in nutrient cycling, aquatic-habitat quality, flood-control and water-supply infrastructure, and contaminant transport (Dunne and Leopold, 2002). Knowing where the sediment source areas are located for a given event and how the source areas may change on an event, seasonal, or annual time scale can provide insight into what types of erosion processes dominate within a watershed. Identification of sediment source areas, transport patterns, and erosion processes can aid in managing watersheds and mitigating sediment driven watershed degradation. This information can help policy makers and land/water managers target erosion prone areas or erosion prone time periods with control efforts such as Best Management Practices. A better

understanding of sediment sources and their event, seasonal, and annual variability can also aid sediment and water-quality modeling in catchments. Finally, an understanding of how sediment transport is affected by seasonal conditions (*i.e.*, snow cover) is key to planning for seasonal precipitation changes associated with climate change.

The aim of this study was to use high-temporal-scale discharge, turbidity, and precipitation data from forested mountain catchments to address the following questions: (1) What are the seasonal trends in turbidity patterns? What do these patterns imply about sediment production and sediment transport throughout the water year in these catchments? (2) What are the turbidity patterns associated with individual storm events? What do these patterns imply about sediment sources and sediment transport? (3) How does the source of water (*i.e.*, rain, snow-melt, and rain on snow) to the stream affect the discharge and turbidity response of the stream? What does this imply about water flow pathways and sediment movement in the catchments?

Methods

Study Area

Field sites for this study consist of a northern and southern site, each with two headwater catchments. The southern site (Sugar Pine) is located in the Merced River basin near Fish Camp, CA and the northern site (Last Chance) is located in the American River basin near Foresthill, CA (Figure 3.1).

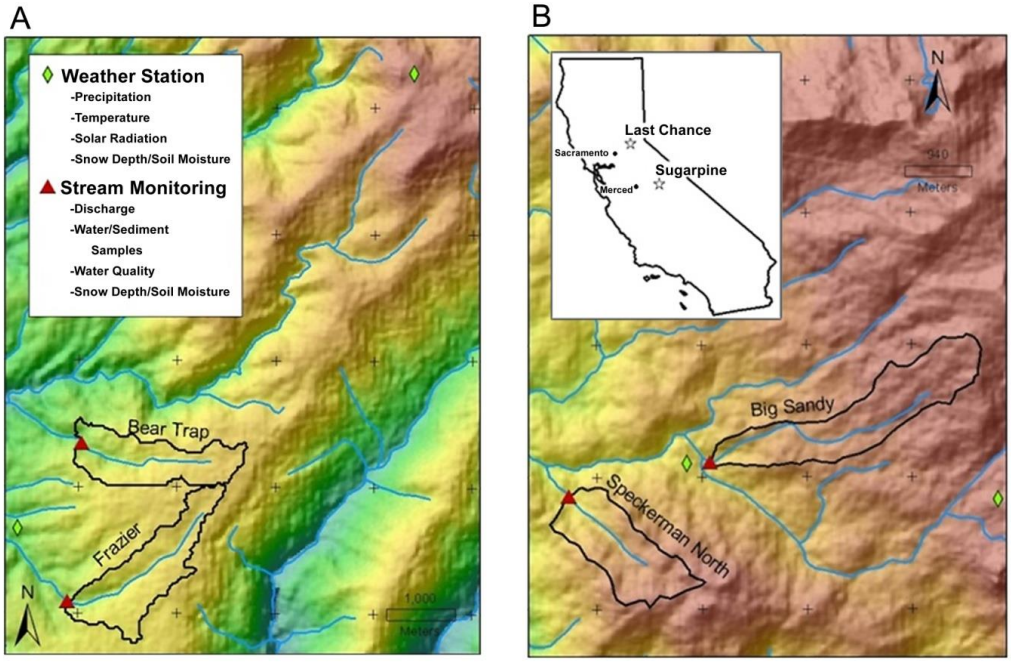

Figure 3.1. Map of Last Chance (A) and Sugar Pine (B) study areas.

The two catchments at the Last Chance site are Frazier Creek and Bear Trap Creek. The catchments at the Sugar Pine site are Big Sandy Creek and Speckerman Creek. The paired catchments were chosen based on comparable size, gradient, discharge, aspect, and vegetation cover (Table 3.1). All catchments have perennial streams located on the western slope of the Sierra Nevada. The study area is characterized by a Mediterranean climate with a distinct wet and dry season and is located in the rain-snow transition zone, with snow making up roughly 40 to 60 percent of average annual precipitation.

Table 3.1. Study watershed characteristics.

Attribute	Frazier Creek	Bear Trap Creek	Big Sandy Creek	Speckerman Creek
River basin	American	American	Merced	Merced
Elevation (m)	1605	1580	1778	1719
Area (km^2)	1.68	1.76	2.47	1.62
Geology	Andesitic volcanics; sandstones/ siltstones/slates	andesitic volcanics; sandstones/ siltstones/slates	tonalite	tonalite
Soil texture	sandy loam/loam	sandy loam/loam	loamy sand/sand	loamy sand/sand
Vegetation	mixed conifer	mixed conifer	mixed conifer	mixed conifer
Annual precipitation (cm)[a]	120–255	120–255	83–214	83–214

[a.] Annual precipitation range for study met stations' period of operation WY 2008–WY 2013.

Instrumentation

Two meteorological stations were also located at each site at elevations similar to the upper portion of the basins and to the catchment outlets. Lower meteorological stations were at 1755 m and 1590 m, while upper elevation meteorological stations were at 2176 m and 2112 m for Sugar Pine and Last Chance sites respectively. Meteorological stations were located on flat open ridges with snow and soil-moisture sensors located adjacent to meteorological stations on north-facing and south-facing hillslopes. Stream instrumentation was located along a relatively low-gradient response reach where sediment scour and deposition are likely to occur.

Turbidity was measured *in situ* at 15-min intervals using 6136 optical turbidity sensors from Yellow Springs Instruments (YSI) mounted on 6920 YSI multiparameter sondes that were either self-logging or attached to a CR1000 datalogger from Campbell

Scientific. Sondes were switched from internal battery power to a solar panel and external battery source partway through WY 2011 due to issues with battery failure. At that time, 600OMS YSI sondes outfitted with a 6136 YSI optical turbidity sensor, were co-located with the 6920 sondes for data redundancy and backup. The 6136 YSI sensor uses a near infrared LED to illuminate a sample of the water column and measures back-scattered light with an adjacent photodiode. The range of the sensor is 0 to 1000 NTU (Yellow Springs Instruments). Anti-fouling wipers are installed on the sensors to prevent buildup of sediment or algae on the optical ports. Wipers ran before each data collection and were replaced as needed every two to three months.

Stream stage was measured at two locations using pressure sensors. At the upstream location, stream stage was measured using a depth sensor calibrated for shallow depth deployments and built into the 6920 YSI sonde. At the downstream location, slightly upstream of the culvert marking the outlet of each catchment, stage was measured using a Solinst Levelogger Gold pressure transducer. The two stage measurements were located 100 to 300 m apart.

Snow depth was measured at all instrument nodes and meteorological stations using Judd ultrasonic depth sensors. Meteorological station sensors were mounted on the meteorological tower and hillslope sensors mounted on the end of an L-shaped rigid metal conduit structure approximately 3 m high. Sensors were positioned so that the surface of the transducer was parallel to the ground. 1–6 sensors were deployed at each hillslope node. They were located on upper or lower banks near the stream sites and under canopy, under drip edge or in the open for several different tree species at the nodes adjacent to meteorological stations. Snow depth was measured at the meteorological stations on hourly intervals for the beginning of the study and changed to 15-min intervals in WY 2011. Hillslope snow measurements were taken at 15-min intervals for the full period of record. Each snow-depth value represents an average of multiple measurements taken over that time interval.

Decagon Devices ECH_20 TM soil temperature and moisture sensors were installed at hillslope sensor nodes and were collocated with snow-depth sensors. Nodes were sited on the north- and south-facing hillslopes adjacent to the meteorological station ridges and on the north- and
south-facing banks adjacent to the stream instrumentation. Sensor installation depths ranged from 10 to 90 cm but were generally confined to 30 and 60 cm due to the shallow nature of the soils. Each node consisted of 6 to 12 soil-moisture sensors.

Precipitation was measured at meteorological stations using a Handar 444B tipping-bucket rain gage. Each tipping-bucket assembly was mounted on the meteorological tower 4.5 to 5 m above the ground. Because the rain gages at the study sites were unshielded and unheated, data from nearby rain gages were used to supplement site data. The nearby station precipitation data were used because of the higher accuracy associated with shielded, heated gages in windy or sub-freezing conditions. For the northern sites the US Bureau of Reclamation Blue Canyon station was used and for the southern sites US Bureau of Reclamation Chilkoot Meadow and US Army Corps of Engineers Westfall stations were used.

Bank erosion pins were used to measure rates of bank erosion in the southern catchments according to methods outlined in Martin (2009). Attempts were made to

install erosion pins in the northern sites, but the stream beds and banks were too rocky (cobble, boulder, and bedrock) to insert rebar pins. Bank-pins were installed in the summer of 2008 and resurveyed each year in late summer or early fall.

A typical bank-pin station consisted of rebar bank pins placed horizontally into the banks perpendicular to the channel and a rebar toe pin pounded vertically into the channel bottom in line with the bank pins. At each station, a bank profile survey was measured with a vertical rod at the base of the toe pin and with a horizontal rod, measuring the distance to the bank at all the slope breaks (changes in bank angle). For each slope break point, a horizontal distance and vertical height were recorded. Locations (vertical stationing) of each bank pin and the distance it stuck out from the bank were also recorded.

Data Analysis

Turbidity data were manually checked to remove any erroneous spikes due to maintenance of sensors, sampling in the stream, or periods when the 6920 Sonde was buried in sediment. To reduce background sensor noise the turbidity data were filtered to remove any values less than 5 NTU. The remaining values were considered actual turbidity events and were used in analysis.

Stage data were manually cleaned, barometrically corrected, and then gap filled. Manual cleaning involved removing any erroneous values due to sensor maintenance or other field activities and adjusting stage levels if a sensor was redeployed at a new depth. Using data collected at the lower meteorological stations with a Solinst Barologger Gold, barometric corrections were performed. Gaps were filled using a linear regression if data were missing for time periods less than 3 hours. The two stage sensors within each stream correlated well so if gaps were more than 3 hours duration, data from the other stage instrument within the same stream were used to gap fill. Occasionally, as in Bear Trap Creek WY 2011 there was overlap in the gaps from the two instruments and gap filling was not possible.

Rating curves were created for each catchment using manual discharge measurements and processed stage data; these were used to calculate discharge. The manual measurements were taken using a slug-tracer dilution method on a monthly to bimonthly basis (Moore, 2003). Attempts were made to capture the full range of high-flow and low-flow events, though site access made the high-flow measurements more difficult. Sediment hysteresis loops were created by plotting turbidity *vs*. discharge for each event. Turbidity spikes not associated with a discharge peak were not included in the analysis. Graphs were visually inspected and classified into clockwise, counterclockwise, linear, figure eight, or complex hysteresis shape categories (Wood, 1977; Williams, 1989).

A two-week running average was computed for the discharge records to represent the background level (non-storm event) discharges. These running averages were used in determining the number of storm events per season and per hysteresis pattern by counting events that were more than 0.10 m^3/s above background flows. Flow intensity was calculated by determining the difference between the peak and the background discharge.

High flow events were defined as the top three largest discharge events per water year per catchment. Data from Bear Trap creek in WY 2011 were left out of analysis due to the large gap in data during winter and spring. For this analysis, fall is defined as from the first fall rain events to the beginning of persistent snow. Early to mid-winter comprises from the first persistent snow to peak snowpack accumulation. Melt season comprises from peak accumulation to full melt out of the snow pack, and base flow refers to the period from full melt of snowpack to first fall rain.

Hysteresis loops were generated for all turbidity events greater than 1 h in duration according to methods described by Wood (1977) and Wilson (2012). These loops were categorized based on the direction and pattern of the loop. Then loops were compared by season and watershed.

Snow-depth values were manually cleaned to remove spikes that occur during periods of precipitation due to the signal bouncing off falling snow or rain. The cleaned data was gap filled using a linear regression for gaps less than 1 day. Data for each node were then averaged and a daily average node value calculated.

A precipitation separation between rain and snow was computed on the nearby met station precipitation data using snow-depth data from the study-site meteorological station. For a given day with precipitation, if snow depth at the study sites increased, the precipitation was assumed to be mainly snow, and the nearby station precipitation record was classified as snow for that day. If precipitation at the nearby sites did not accompany a snow-depth increase at the study sites, that precipitation was assumed to be rain. Snow-density data from nearby US Bureau of Reclamation snow-pillow sites were used to compute snow water equivalent (SWE) for the stream and meteorological station locations according to the method outlined in Liu *et al*. (2013). The Blue Canyon station was used for the northern site and a combination of the Chilkoot Meadow and Poison Ridge stations for the southern site. Data was obtained through the California Department of Water Resources California Data Exchange Center. From the snow-depth and SWE data reported by these pillows, a daily snow-density product was calculated. A linear regression line was fitted to the data and a general relationship between water year day and snow density was found. This relationship was applied to the site-average daily snow depths at the study site meteorological stations and stream sites to calculate the daily SWE. A snowmelt product was calculated for each site from the calculated SWE. If SWE decreased from one day to the next it was assumed that melt was occurring, and a SWE-based snowmelt record was created from the values.

Post processing of soil moisture included manually cleaning data from each sensor to remove erroneous values and averaging the instruments at each node to produce a single record. Node data were then aggregated from 15 min data to 24 h average values. Contiguous 24 h average values were compared and where that change was positive, it was assumed that soil moisture was increasing due to rain or snowmelt. The positive 24 h changes due to rain were filtered out using the rain record and the remaining values represented a snowmelt record (i.e., the soil moisture increase due to snowmelt). The soil moisture derived snow melt was compared to a SWE derived snow melt product with the two methods showing good agreement for days with and without snow melt. The SWE-based product was chosen for analysis because it was a more direct measurement of

snowpack water loss without influences such as vegetation uptake, or groundwater input from upslope areas.

Results and Discussion

WY 2010 and WY 2011 were above average years, and WY 2012 was below average. The percentage of the average historical April 1 snow course SWE was calculated for two snow courses: Poison Meadow near the southern sites (elevation 2070 m) and Huysink near the northern site (elevation 2010 m) (Table 3.2). A Sierra Nevada wide percentage of average was included for comparison. Big Sandy Creek and Frazier Creek had an average of 0.023 m^3/s and 0.038 m^3/s higher flows than their paired catchments, but pairs are similar in timing of events (Figure 3.2). The largest discharge events generally occurred during the early to mid-winter or snow melt seasons with the exception of an early fall rain event in WY 2011 that produced particularly high discharges in Big Sandy creek. Turbidity events vary greatly in magnitude for WY 2010 to WY 2012 and not all storm events produced a turbidity signal (Figure 3.2).

Table 3.2. Percentage of mean April 1 snow pack SWE for Poison Meadow snow course, Huysink snow course, and Sierra Nevada range average for WY 2010 through 2012.

Water Year	Poison Meadow	Huysink	Sierra Nevada[a]
2010	168%	101%	143%
2011	206%	114%	144%
2012	47%	56%	55%
mean SWE [b] (standard deviation)	65 (40) cm	111 (41) cm	

[a.] Data from CA Department of Water Resources

[b.] Values are based on 68 years of 1 April snow pack data at Poison Meadow and 75 years at Huysink.

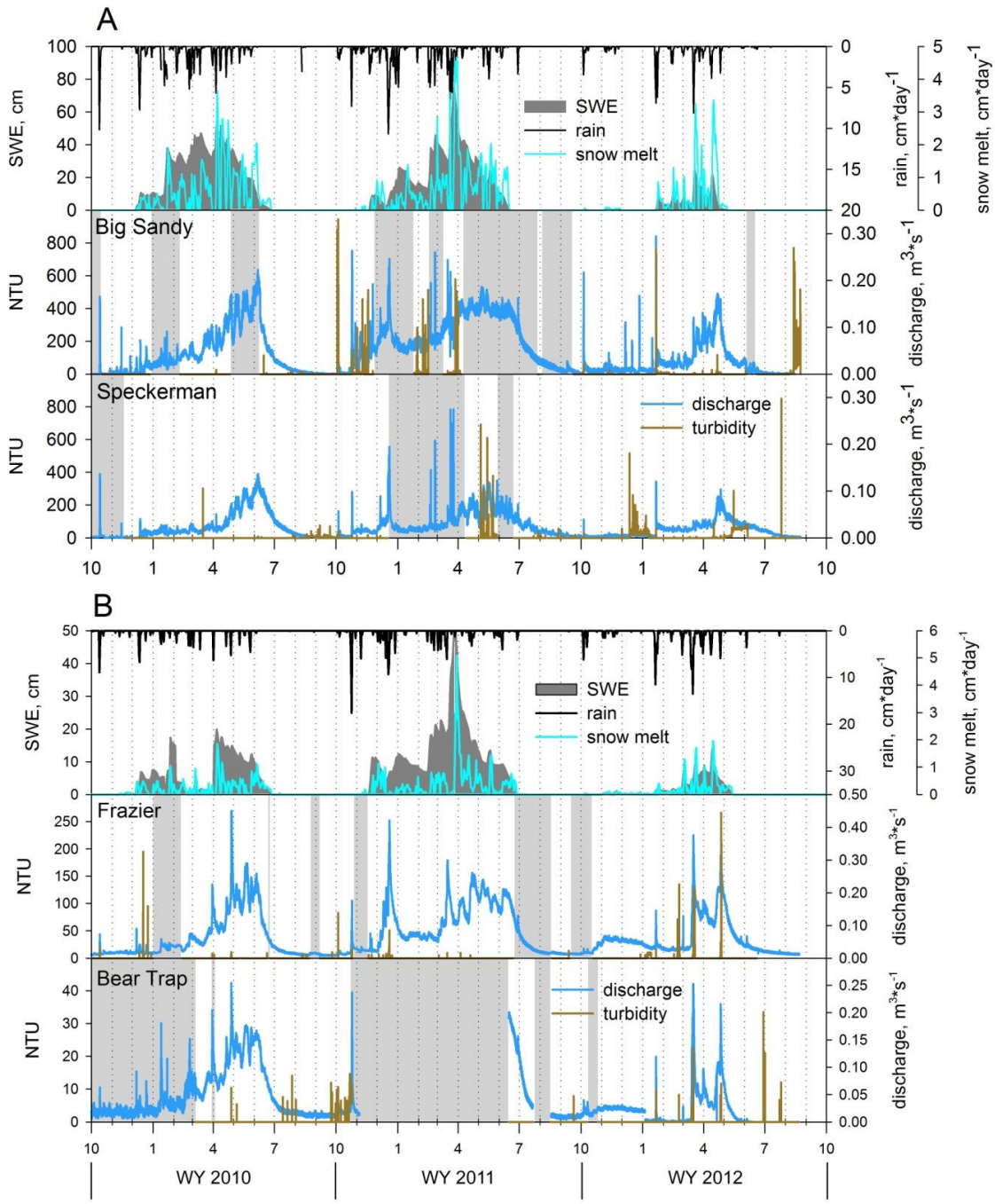

Figure 3.2. Precipitation, discharge, and turbidity data for (A) Sugar Pine and (B) Last Chance sites for WY 2010–WY 2012. Snow values are averaged across the study area. The light grey shaded areas indicate periods when turbidity data were not available.

It was found that in all four watersheds, fall flow events were most likely to produce turbidity signals compared to events in other seasons, with a progressive reduction in percentage of events producing a turbidity signal seen through the water year (Table 3.3, Figure 3.2). The fall discharge events were more likely to produce turbidity signals even though the largest storms typically do not occur during that season. A number of factors could lead to this pattern, such as fall events occurring after a summer dry period, when loose sediment can accumulate at the toe of channel banks or on near channel soil surfaces, so there is more material available to transport (Martin, 2009). In early fall, there also may be some hydrophobicity of dry soils leading to a portion of runoff being moved as overland or very shallow surface (duff layer) flow and more material reaching the stream (Burch et al., 1989; Shakesby et al., 1993). Finally, fall's larger turbidity signals may be due to the fall rain events representing the most abrupt discharge increases (Table 3.4, Figure 3.2). If it is assumed that at steady background discharge levels all transportable sediment at that flow level has been moved, then any increases in flow from that level likely means more sediment will be moved. The greater the increase from background levels, the greater the amount of additional sediment that can be transported due to increased flow energy. Though there are somewhat larger flows during spring events than fall events, the non-event, background flow in spring is fairly high so there is less of an increase in flow with each event, and therefore less of an increase in flow erosivity and fluvial entrainment. Data show that fall discharge events had the highest average flow increases and were almost double the average flow increase of snow melt period discharges (Table 3.4). These results are consistent with those of Duvert *et al*. (2010), Rodriguez-Blanco *et al*. (2010), and Seeger *et al*. (2004) who observed that there are significant seasonal differences in sediment transport and that turbidity is not only tied to the absolute value of the event discharge but also to event intensity.

Table 3.3. Percentage of flow events producing turbidity and number of flow events by season for all catchments.

Season	**Percentage of flow events that produce a turbidity signal**	**Number of large flow events[a]**
Fall	84.2%	0
Early/Mid winter	55.6%	11
Snow melt	49.0%	18
Base flow	44.4%	4

[a.] Large flow events consist of the three largest discharge events of each water year for each stream.

Table 3.4. Intensity values for discharge peaks ($m^3 s^{-1}$) by season.

Season	Average Intensity Values[a] for Discharge Peaks (Standard Deviation)	Number of Peaks [b]	Number of Measurement Days [c]
Fall	0.11 (0.06)	17	536
Early/Mid Winter	0.10 (0.05)	60	1501
Snow Melt	0.06 (0.04)	52	743
Base Flow	0.06	1	1156

[a] Intensity values equal the peak discharge values minus the background discharge as defined by 15 day running average.

[b] Discharge peaks are defined as peaks where intensity values are greater than 0.04 m^3/s.

[c] Measurement days are the number of days summed by the four watersheds minus the days when no data was collected.

When multiple discharge events occurred in succession**,** the largest turbidity spike was often associated with the first event rather than the largest event. An example of this pattern can be seen in the fall 2010 Speckerman turbidity and discharge data (Figure 3.3). During this fall rainy season, the largest turbidity peak was associated with the first set of rain events, even though those events produced a relatively small discharge response. As the season progressed discharge peaks became larger, but turbidity peaks became smaller.

The reduction in peak turbidity values throughout a season is likely related to a seasonal depletion of sediment stores (Sadeghi et al., 2008; Rodriguez-Blanco et al., 2010). At the beginning of certain seasons there are stores of easy to transport sediment in the channel. The first storm moves a large portion of sediment out of the local area and with each successive storm and associated transport, less and less loose, easy to move sediment is available. This "first flush" is a common phenomenon and has been reported by numerous researchers across a wide range of watershed sizes (0.3 km^2 to 311 km^2), elevations (120 m to 3340 m above sea level), and precipitation regimes (seasonal snow dominated to year-round rain dominated) (Duvert et al., 2010; Iida et al., 2012; Gao and Josefson, 2012; Wilson et al., 2012). In the study catchments, the "first flush" signal occurs strongest during early fall rainstorms.

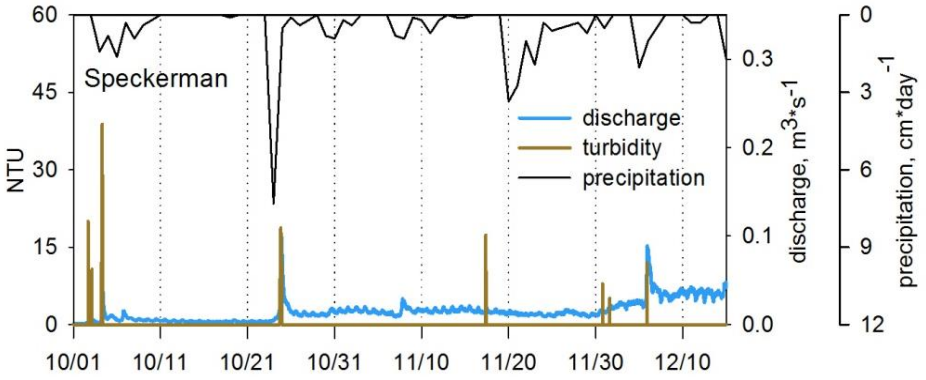

Figure 3.3 Turbidity, discharge, and precipitation data from Speckerman Creek for the fall rainy season, WY 2011.

Peak turbidity values ranged widely in all seasons (Figure 3.2). Snow melt season had the highest average values for turbidity peaks and fall had the next highest average values (Table 3.5). Early/mid-winter and base flow seasons had similar average values and they were the lowest values of the four seasons. Interestingly, even though the snow melt season had the highest average values, it had the lowest maximum value of all the seasons (Table 3.5).

Table 3.5. Peak event turbidity values (NTU) by season.

Season	Average peak event values (standard deviation)	Median peak event value	Min peak event value	Max peak event value
Fall	76 (218)	12.2	5	946
Early/Mid winter	36 (107)	9.6	5	763
Snow melt	92 (172)	11.9	5	692
Base flow	35 (120)	11.5	5	850

Higher average peak turbidity values but lower max peak turbidity values for the snow melt season compared to fall indicates that there is less variation in sediment events within the snow melt season. Average peak turbidity values likely tend to be higher due to the snow melt season having high background flow levels. Higher discharge events mean greater flow energy and therefore greater potential to transport sediment in an event. Other potential explanations are (i) there may be rain-on-snow events that produce a high runoff response; (ii) preferential flow paths through the snowpack may produce concentrated channelized flow at the soil- snowpack interface and facilitating the rapid transport of hillslope sediment to the stream; (iii) saturated soil conditions may increase the likelihood of overland flow that can transport sediment directly to the stream; (iv) snow related erosion processes may produce a store of loose material that is easy to

transport; or (v) differences in the particle size class of sediment transported can result in differences in NTU values. (Yellow Springs Instruments; Zachar, 1982). The high sand content in the soils within the study catchments and low erosion rates on undisturbed hillslopes in the Sierra Nevada suggest overland flow is not a likely explanation for the seasonal differences (Stafford, 2011). Seasonal variations in transported particle size classes is also an unlikely explanation for the difference because size variations only cause up to 10 NTU fluctuations in data readings for the turbidity sensors used in this study (Yellow Springs Instruments).

The relatively high average event values in fall despite lower discharges were expected because of the intensity of fall discharge events and the in-channel stores of loose sediment. These data match well with findings by Rodriguez-Blanco *et al*. (2010) despite major differences in land use and rainfall patterns between the two studies. These Rodriguez-Blanco *et al*. (2010) authors reported fall having the largest sediment load and runoff (50 percent of the annual) but only 29 percent of the water yield. In their study, the large fall sediment loads were attributed to fall having the highest number of rainfall events as well as to the presence of bare ground in fall due to traditional agricultural practices within their catchments. Results from both the Rodriguez-Blanco *et al.* study and this one suggest there may be strong accumulation/depletion patterns occurring in the summer and fall where a large amount of sediment is available for transport in the early season leading to very large peak turbidity values but sediment stores quickly depleting resulting in a lower average for the fall compared to the snow melt season. It is likely that less accumulation of sediment occurs in the early/mid-winter so the snow melt season had less variation in sediment availability and thus a smaller range for NTU values.

The low average values for early/mid-winter and base flow seasons may suggest that these seasons are both times of sediment accumulation where erosion outpaces transport. Both seasons are characterized by flow being low compared to the season immediately following it. During base flow, channel banks are drying out and crumbling and bio-turbation is at its highest in summer when plants and animals are most active (Leopold et al., 1995). During early and mid-winter, processes such as freeze-thaw cycles and snow creep generate loose sediment from the banks and the nearby hillslopes (Leopold et al., 1995).

Prior research has shown conflicting results on the dominate season for sediment transport, but generally the seasons of highest flow tended to also be the seasons with the highest suspended sediment concentrations. Rodriguez-Blanco *et al*. (2010) showed in a steep, low elevation, 16 km^2 basin in northwest Spain with no seasonal snow, that most sediment events and most suspended sediment load transport occurred in the fall, the season of highest volume of runoff and the highest number of events. Research in a mountainous catchment in Japan which is lower elevation but with a similar snow dominated precipitation pattern as this study's sites found that over 60% of the basins suspended sediment load was transported during the spring snow melt period (Iida et al., 2012). The high spring snow melt sediment load was attributed to increased discharge. Finally, Gao and Josefson (2012) did not see a dominant sediment transport season for a medium sized, low elevation, central New York catchment with patchy seasonal snow cover. Instead they showed that most of the sediment was transported throughout the year

during frequent small events. The differences between their results and those of this study are likely due to differences in the amount and types of precipitation throughout the year. Their catchments had much higher year-round precipitation and high intensity or high-volume rainfall/melt events were not concentrated to a specific time period. Additionally, their study sites comprised of 50% agricultural lands which may have provided a steady year-round hillslope sediment source to the streams. Sites in the current study are most similar to the forested, snow dominated catchments from Iida *et al*. (2012) and share the high spring snow melt turbidity signal. However, the strong summer accumulation–fall depletion cycle and the high intensity of fall rain events result in an additional high turbidity season in fall in this study.

All five types of hysteresis loops were seen in this study (Figure 3.4). When separated by study catchment, it was seen that a clockwise hysteresis loop pattern for individual storm events was dominant for all catchments (Table 3.6) occurring five to ten times more frequently than other patterns. The exception was Bear Trap, which was likely due to significant missing data and was not reflective of a naturally lower proportion of events. These results were as expect because paired streams have similar physical properties and similar discharge responses for a given storm. The mainly clockwise patterned events imply that localized in-channel sources dominate sediment supply in these catchments. One would expect to see this in small mountain catchments because these are typically sediment source areas (Yager et al., 2012).

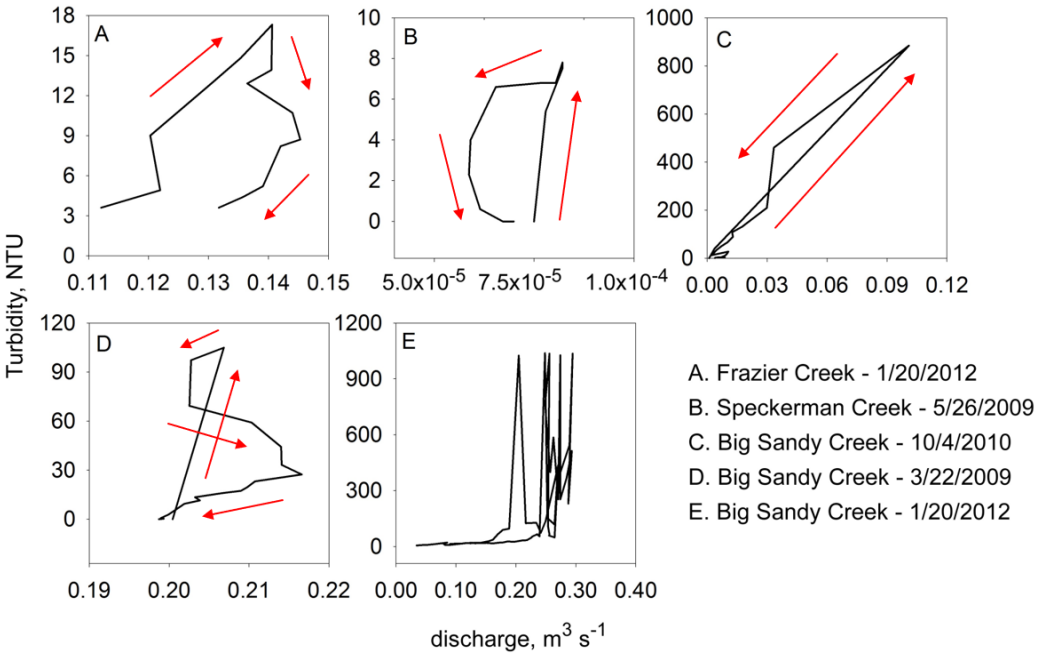

Figure 3.4. Examples of each of the five hysteresis loop shapes seen in the study area (A) clockwise; (B) counter clockwise; (C) linear; (D) figure eight; and (E) complex.

Table 3.6. Number of hysteresis loop patterns for turbidity events.

Hysteresis shape	Big Sandy	Speckerman	Bear Trap	Frazier
Clockwise	14	11	5	16
Counterclockwise	3	3	2	0
Linear	3	1	0	0
Figure Eight	2	4	0	0
Complex	3	1	1	1

Clockwise patterns were the dominant event pattern for all seasons except base flow (Table 3.7). Clockwise events mainly occurred during fall and early/mid-winter. The non-clockwise patterned events that occurred during these seasons were generally associated with multi-rise flow events. Clockwise patterns were also dominant for the snow melt period. The baseflow season's more even distribution of hysteresis patterns is thought to be due to turbidity peaks from buildup of organic matter under extremely low flow conditions and not from the movement of material associated with flow-erosion processes. Supporting evidence turbidity is caused by organic buildup is the fact that many of these spikes occurred without any associated rainfall or discharge rise

Table 3.7. Number of turbidity event hysteresis loop patterns by season at all study catchments.

Hysteresis shape	Fall	Early/Mid-winter	Snow melt	Base flow
Clockwise	18	19	8	1
Counterclockwise	2	2	1	3
Linear	3	0	0	1
Figure Eight	0	2	2	2
Complex	1	3	2	0

The predominance of a clockwise pattern indicates that localized in-channel sources are likely the most important source of sediment in these catchments. Research in other small headwater catchments in the Sierra Nevada suggests that relatively little hillslope material directly reaches the stream and instead sediment comes from the channel bed and banks (Stafford, 2011). In addition, no clear differences in hysteresis patterns are seen between periods of snow cover and periods of open ground in this study further suggesting that hillslope sediment production may play a minimal role in turbidity patterns. Rodriguez-Blanco *et al*. (2010) similarly found clockwise to be the dominant hysteresis pattern suggesting a localized sediment sources. In contrast to these findings, Fang *et al*. (2011) showed clockwise patterns at the hillslope plot scale and counterclockwise patterns at the basin scale suggesting a dominantly hillslope source at various spatial scales on the Loess Plateau of China. The difference in results between this work and Fang *et al*. is likely because their site has some of the highest soil erosion rates in the world with an average annual sediment yield of 22,200 tons per km^2 and

extremely steep slopes of up to 70 degrees (Fang et al., 2011). In comparison, sediment yields in the central Sierra Nevada have been estimated to be around 4.1 tons per km^2 (Stafford, 2011). For these reasons, hillslopes on the Loess Plateau are likely to dominate over channels as a primary sediment source.

The dominance of clockwise hysteresis loops also has implications on flow pathways in the study catchments. Seeger *et al*. (2004) showed that clockwise loops were the most common for small Central Pyrenees catchments and that this pattern occurred under normal runoff conditions. They showed that counterclockwise loops typically only occurred under extremely wet antecedent conditions where overland flow was possible. Additionally, Soler *et al*. (2008) showed that antecedent moisture conditions were important in their dominantly forested catchment where counterclockwise loops were associated with overland flow and implied remote sediment sources within the catchment. The limited number of counterclockwise patterned events along with the characteristically sandy soils suggests that overland flow is extremely rare in typical Sierra Nevada headwater catchments such as the one in this study.

Though clockwise patterns are dominant, that all five hysteresis patterns occur implies there are likely multiple source areas (*i.e.*, in-channel, near channel, or upper hillslopes) and/or multiple source features (*i.e.*, loose material at toe, more consolidated bank material, channel beds with varying degrees of armament) that occasionally come into play. This is to be expected in a mountain catchment with temporal and spatial variations in rainfall, runoff, and discharge. Variations in storm intensities, storm durations, and antecedent conditions result in a range of flow responses and subsequently a variety of hysteresis patterns (Figure 3.4). The linear, counterclockwise, and complex hysteresis patterns are often associated with multiple storm events that occur in short succession. In this study, extended events with multiple discharge peaks showed a shift in hysteresis loop patterns from a clockwise to a more linear pattern with turbidity and discharge peaking concurrently, and then toward a counterclockwise pattern where turbidity peaks after discharge. The first part of this pattern shift is seen in the multi-rise storm sequence shown in Figure 3.5, where the hysteresis loop shape starts off clockwise and becomes progressively more linear. The shifts in hysteresis patterns are indicative of shifts in sediment sources. As local sources become more and more depleted, other sources contribute more to turbidity. The shift in pattern associated with multiple storm events (Figure 3.5) may represent one of two possible scenarios: (1) a shift from loose, easy to erode in-channel material to more cohesive bed/bank material that requires more flow energy to entrain; or (2) a shift from nearby sources (*i.e.*, in-channel stores) to more distant source locations (*i.e.*, upper hillslopes). The more distant sources or more cohesive sources may result in a lag between discharge peaks typical of non-clockwise hysteresis patterns. Lana-Renault *et al*. (2010) and Soler *et al*. (2008) attributed counterclockwise hysteresis patterns in their studies to distant sediment sources or to antecedent conditions that may cause a lag in sediment transport (*i.e.*, subsurface must fill before saturation overland flow can occur). Discharge or precipitation thresholds for the occurrence of counterclockwise hysteresis were not identifiable in this study, however, the number of counterclockwise events was low and with a larger sample size, thresholds may be identifiable.

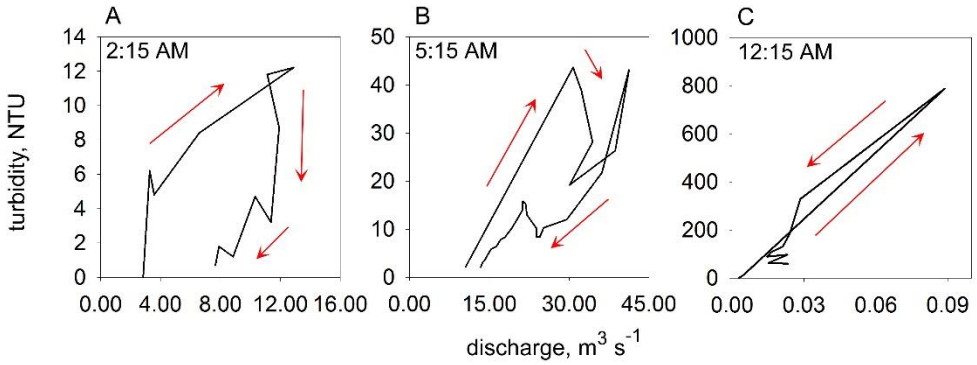

Figure 3.5. Hysteresis pattern progression can be seen within a multi-rise storm event sequence. (A) clockwise; (B) counterclockwise; (C) linear.

Our conceptual model for the accumulation and depletion of localized sediment stores is that during low-flow periods, sediment accumulates at the toe of banks (Figure 3.6). This accumulation period is thought to occur at the seasonal time scale (*i.e.*, summer base flows) as well as event scale (*i.e.*, low flows between discharge peaks). Sediment is entrained and transported downstream during high-flow events, with multiple events in short succession depleting sediment stores (Figure 3.6).

Bank surveys were conducted at the end-of-summer low-flow periods each year. In many of these surveys, a pile of accumulated sediment was observed at the toe of banks and can been seen in the bank-profile plots (Figure 3.7). This accumulated sediment provides supporting evidence to our conceptual model. The stockpiling of sediment in the channel during low-flow periods has been documented in systems of various sizes and hydroclimatic regimes (Doomen et al., 2008; Smith and Dragovich, 2009; Wilson et al., 2012).

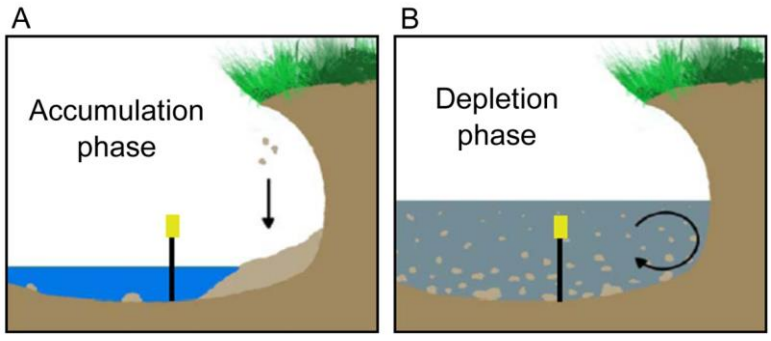

Figure 3.6. A conceptual model of localized sediment processes consisting of (A) an accumulation phase and (B) a depletion phase.

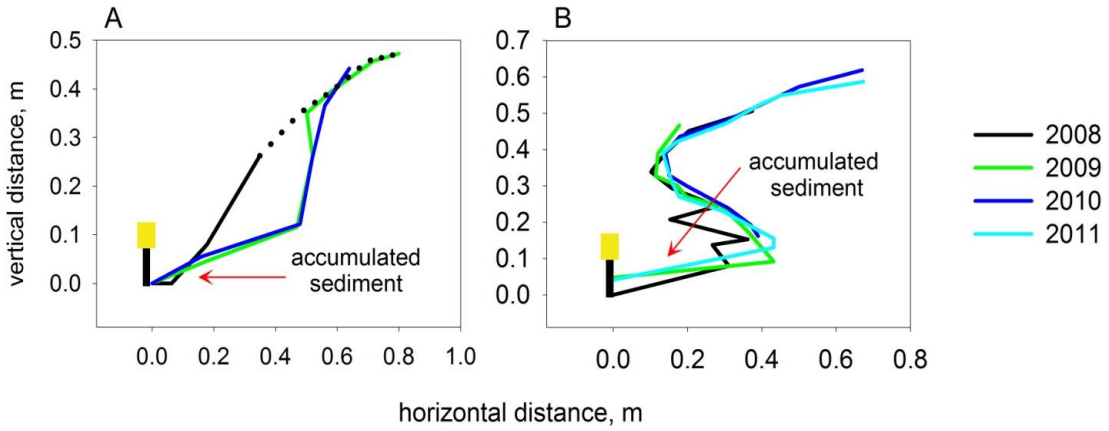

Figure 3.7. Bank pin surveys from (A) Big Sandy and (B) Speckerman showing sediment accumulation at toe of bank slopes.

Conclusions

Turbidity and discharge data collected over three years in four small mountain catchments of the Sierra Nevada showed that localized sources of sediment dominate sediment production and that seasonal and event-scale accumulation and depletion cycles govern sediment transport in these streams. The dominantly clockwise hysteresis patterns in all seasons implied that localized—most likely in-channel—sources supplied the sediment for most events and that overland flow is likely rare. In multiple-rise events or events in short succession-where severe depletion of local sources can occur, the shift in hysteresis shapes to non-clockwise patterns indicated that once localized sources were depleted, more distant or more consolidated sources may come into play. Seasonal reductions in peak turbidity values suggest a seasonal scale of sediment depletion also occurs.

Our conceptual model suggests that material accumulates at the toe of banks through physical erosion during periods of low flow when the stream has little energy to move it. The material is transported during periods of higher flow. These cycles may occur on an event scale as indicated by hysteresis patterns where the event peak is the high-flow depletion phase and inter-event periods the low-flow accumulation phase. This accumulation-depletion pattern also expresses itself on a seasonal scale with fall and snow melt seasons representing depletion phases. Base flow and to a lesser extent, early/mid-winter seasons represent periods of low flow and sediment accumulation.

Knowing the timing and source areas for sediment that causes turbidity will help managers know when and where to focus erosion control measures and structures. Under normal erosion conditions, the importance of in-channel sources over hillslope sources may indicate in-channel sediment control structures such as weirs or check dams rather than hillslope erosion control measures. Alternatively, hillslope sediment control

measures should be limited to cases where significant changes to the system have occurred and hillslope erosion is more likely to overshadow in-channel sources (*i.e.*, fire, roads, logging, or grazing). Additionally, an understanding of the role of snow cover on erosion and turbidity will allow for better planning in the face of a changing snow pack due to climate change. This knowledge will allow management practices to be chosen that will make the most efficient use of erosion mitigation resources.

Acknowledgments

This is SNAMP publication #28. The Sierra Nevada Adaptive Management Project (SNAMP) is funded by USDA Forest Service Region 5, USDA Forest Service Pacific Southwest Research Station, US Fish and Wildlife Service, California Department of Water Resources, California Department of Fish and Game, California Department of Forestry and Fire Protection, and the Sierra Nevada Conservancy. The authors would like to thank California Department of Water Resources, US Forest Service, Sierra Nevada Research Institute, and Sierra Nevada Adaptive Management Project personnel for their support and assistance. Additionally, we would like to thank the two anonymous reviewers for their thoughtful comments which have helped in strengthening this manuscript.

Author Contributions

All three authors chose sampling design and field locations. Sarah Martin set up field sites, conducted field measurements, and analyzed data. Martha Conklin and Roger Bales provided guidance on field measurements and data analysis. Sarah Martin wrote manuscript with guidance and editing assistance from Martha Conklin and Roger Bales.

References

Burch, G. J., Moore, I. D., & Burns, J. (1989). Soil hydrophobic effects on infiltration and catchment runoff. *Hydrological Processes*, *3*, 211–222.

Doomen, A. M. C., Wijma, E., Zwolsman, J. J. G., & Middelkoop, H. (2008). Predicting suspended sediment concentrations in the Meuse River using a supply-based rating curve, *1856*(August 2007), 1846–1856. https://doi.org/10.1002/hyp

Dunne, T., & Leopold, L. B. (2002). *Water in Environmental Planning* (16th ed.). New York, NY, USA: W.H. Freeman and Company.

Duvert, C., Gratiot, N., Evrard, O., Navratil, O., Némery, J., Prat, C., & Esteves, M. (2010). Geomorphology Drivers of erosion and suspended sediment transport in three headwater catchments of the Mexican Central Highlands. *Geomorphology*, *123*(3–4), 243–256. https://doi.org/10.1016/j.geomorph.2010.07.016

Fang, H., Li, Q., & Cai, Q. (2011). Spatial scale dependence of sediment dynamics in a gullied rolling loess region on the Loess Plateau in China. *Environmental Earth Sciences*, *64*(3), 693–705. https://doi.org/10.1007/s12665-010-0889-4

Gao, P., & Josefson, M. (2012). Geomorphology Event-based suspended sediment dynamics in a central New York watershed. *Geomorphology*, *139–140*, 425–437. https://doi.org/10.1016/j.geomorph.2011.11.007

Gathard Engineering Consulting. (2006). *Klamath River Dam and Sediment Investigation*. Seattle, Washington. Retrieved from https://www.fws.gov/yreka/kri/gecfinalreport.pdf

Granger, S. J., Bol, R., Hawkins, J. M. B., White, S. M., Naden, P. S., Old, G. H., … Haygarth, P. M. (2011). Using artificial fluorescent particles as tracers of livestock wastes within an agricultural catchment. *Science of the Total Environment*, *409*(6), 1095–1103. https://doi.org/10.1016/j.scitotenv.2010.12.005

Iida, T., Kajihara, A., Okubo, H., & Okajima, K. (2012). Effect of seasonal snow cover on suspended sediment runoff in a mountainous catchment. *Journal of Hydrology*, *428–429*, 116–128. https://doi.org/10.1016/j.jhydrol.2012.01.029

Lana-Renault, N., Regüés, D., Nadal-Romero, E., Serrano-Muela, M. P., García-Ruiz, J. M., Lana, N., Nadal, E., Serrano, M. P., García, J. M. (2010). Streamflow response and sediment yield after farmland abandonment: results from a small experimental catchment in the Central Spanish Pyrenees. *Revista de Ecología de Montaña*, *165*, 97–114. https://doi.org/10.3989/Pirineos.2010.165005

Langlois, J. L., Johnson, D. W., & Mehuys, G. R. (2005). Suspended sediment dynamics associated with snowmelt runoff in a small mountain stream of Lake Tahoe (Nevada). *Hydrological Processes*, *19*(18), 3569–3580. https://doi.org/10.1002/hyp.5844

Leopold, L. B., Wolman, M. G., & Miller, J. P. (1995). *Fluvial Processes in Geomorphology* (2nd ed.). Mineola, NY, USA: Dover Publications.

Liu, F., Hunsaker, C., & Bales, R. C. (2013). Controls of streamflow generation in small catchments across the snow-rain transition in the Southern Sierra Nevada, California. *Hydrological Processes*, *27*(14), 1959–1972. https://doi.org/10.1002/hyp.9304

Martin, S. E. (2009). *Comparison of in-stream sediment sources and assessment of a bank migration model for headwater catchments in the Central Sierra Nevada, California*. University of California, Merced.

Mazurkiewicz, A., & McGurk, B. (2011). Effect of Snow Covered Area and Delayed Snowmelt on Water Quality and Reservoir Management: 2010 Turbidity Event in Hetch Hetchy Reservoir. In *Proceedings of the 79th Annual Western Snow Conference* (pp. 47–62). Stateline, NV, USA. Retrieved from http://www.westernsnowconference.org/sites/westernsnowconference.org/PDFs/2011Mazurkiewicz.pdf

McDonald, D. M., & Lamoureux, S. F. (2009). Hydroclimatic and channel snowpack controls over suspended sediment and grain size transport in a High Arctic catchment. *Earth Surface Processes and Landforms*, *34*(December 2008), 424–436. https://doi.org/10.1002/esp

Moore, R. D. (2005). Introduction to salt dilution gauging for streamflow measurement Part 3: Slug injection using salt in solution. *Streamline*, *8*(4), 20–23. https://doi.org/10.1592/phco.23.9.1S.32890

Rodríguez-Blanco, M. L., Taboada-Castro, M. M., Palleiro, L., & Taboada-Castro, M. T. (2010). Temporal changes in suspended sediment transport in an Atlantic catchment, NW Spain. *Geomorphology*, *123*(1–2), 181–188. https://doi.org/10.1016/j.geomorph.2010.07.015

Sadeghi, S. H. R., Mizuyama, T., Miyata, S., Gomi, T., Kosugi, K., Fukushima, T., … Onda, Y. (2008). Determinant factors of sediment graphs and rating loops in a reforested watershed. *Journal of Hydrology*, *356*(3–4), 271–282. https://doi.org/10.1016/j.jhydrol.2008.04.005

Seeger, M., Errea, M. P., Beguería, S., Arnáez, J., Martí, C., & García-Ruiz, J. M. (2004). Catchment soil moisture and rainfall characteristics as determinant factors for discharge/suspended sediment hysteretic loops in a small headwater catchment in the Spanish Pyrenees. *Journal of Hydrology*, *288*(3–4), 299–311. https://doi.org/10.1016/j.jhydrol.2003.10.012

Shakesby, R. A., Coelho, C. D. O. A., Ferreira, A. D., Terry, J. P., & Walsh, R. P. D. (1993). Wildfire impacts on soil erosion and hydrology in wet Mediterranean forest, Portugal. *International Journal of Wildland Fire*, *3*(2), 95–110. https://doi.org/10.1071/WF9930095

Sierra Nevada Conservancy. (2011). California's Primary Watershed. Retrieved June 23, 2014, from http://www.sierranevada.ca.gov/our-region/ca-primary-watershed

Smith, H. G., & Dragovich, D. (2009). Interpreting sediment delivery processes using suspended sediment-discharge hysteresis patterns from nested upland catchments, south-eastern Australia. *Hydrological Processes, 23*, 2415–2426. https://doi.org/10.1002/hyp

Snyder, N. P., Rubin, D. M., Alpers, C. N., Childs, J. R., Curtis, J. A., Flint, L. E., & Wright, S. A. (2004). Estimating accumulation rates and physical properties of sediment behind a dam: Englebright Lake, Yuba River, northern California. *Water Resources Research*, *40*(11), 1–19. https://doi.org/10.1029/2004WR003279

Soler, M., Latron, J., & Gallart, F. (2007). Relationships between suspended sediment concentrations and discharge in two small research basins in a mountainous Mediterranean area (Vallcebre, Eastern Pyrenees). *Geomorphology*, *98*, 143–152. https://doi.org/10.1016/j.geomorph.2007.02.032

Stafford, A. K. (2011). *Sediment Production and Delivery from Hillslopes and Forest Roads in the Southern Sierra Nevada, California*. Colorado State University.

Williams, G. P. (1989). Sediment concentration versus water discharge during single hydrologic events in rivers. *Journal of Hydrology*, *111*(1–4), 89–106. https://doi.org/10.1016/0022-1694(89)90254-0

Wilson, C. G., Papanicolaou, A. N. T., & Denn, K. D. (2012). Partitioning fine sediment loads in a headwater system with intensive agriculture. *Journal of Soils and Sediments*, *12*(6), 966–981. https://doi.org/10.1007/s11368-012-0504-2

Wood, P. A. (1977). Controls of variation in suspended sediment concentration in the River Rother, West Sussex, England. *Sedimentology*, *24*(3), 437–445. https://doi.org/10.1111/j.1365-3091.1977.tb00131.x

Yager, E. M., Turowski, J. M., Rickenman, D., & McArdell, B. W. (2012). Sediment supply, grain protrusion, and bedload transport in mountain streams. *Geophysical Research Letters*, *39*(10), 1–5. https://doi.org/10.1029/2012GL051654

Yellow Springs Instruments 6920 V2 Multiparameter Sonde Specifications. (n.d.). Retrieved June 23, 2014, from http://www.ysi.com/media/pdfs/069300-YSI-6-Series-Manual-RevJ.pdf

Zachar, D. (1982). Classification of Soil Erosion. In *Soil Erosion*. Bratislava, Slovakia: Holý, I.M., Ed.; VEDA Publishing House of the Slovak Academy of Sciences.

Chapter 4. Tracking channel bed resiliency in forest mountain catchments using high temporal resolution channel bed movement bedload data

Sarah E. Martin[1] and Martha H. Conklin[*]
(in press, 2018 in *Geomorphology*)

Abstract

This study uses continuous-recording load cell pressure sensors in four, high-elevation (1500–1800 m), Sierra Nevada headwater streams to collect high-temporal-resolution, bedload-movement data for investigating the channel bed movement patterns within these streams for water years 2012–2014. Data show an annual pattern where channel bed material in the thalweg starts to build up in early fall, peaks around peak snow melt, and scours back to baseline levels during hydrograph drawdown and base flow. This pattern is punctuated by disturbance and recovery of channel bed material associated with short-term storm events. A conceptual model, linking sediment sources at the channel margins to patterns of channel bed fill and scour in the thalweg, is proposed building on the results of Martin *et al*. (2014). The material in the thalweg represents a balance between sediment supply from the channel margins and sporadic, conveyor-belt-like downstream transport in the thalweg. The conceptual model highlights not only the importance of production and transport rates but also that seasonal connectedness between the margins and thalweg is a key sediment control, determining the accumulation rate of sediment stores at the margins and the redistribution of sediment from margins to thalweg that feeds the conveyor belt. Disturbance and recovery cycles are observed at multiple temporal scales; but long term, the channel beds are stable, suggesting that the beds act as short-term storage for sediment but are in equilibrium interannually. The feasibility of use for these sensors in forested mountain stream environments is tested. Despite a high failure rate (50%), load cell pressure sensors show potential for high-temporal-resolution bedload measurements, allowing for the collection of channel bed movement data to move beyond time-integrated change measurements — where many of the subtleties of bedload movement patterns may be missed — to continuous and/or real-time measurements. This type of high-temporal-resolution data provides insight into short-term cycles of bedload movement in high gradient, forested mountain streams.

Keywords**:** bedload; load-cell; sediment; transport

Introduction

Along with channel morphology, channel bed movement is a key driver of aquatic habitat quality and abundance. The balance between sediment supply and transport in streams determines overall channel stability and is an important factor in downstream sediment delivery. Globally, small mountainous rivers drain only about 20% of the land area but may account for more than half the global sediment budget (Milliman and Syvitski, 1992). With mounting concerns regarding overgrown forests and the increasing frequency of catastrophic fires, particularly in the southwestern United States (Miller et al., 2009), process understanding of sediment sources and bedload transport in forested mountain catchments is fundamental to predicting how major disturbances such as timber harvesting, fire, road construction/decommissioning, and intense precipitation events impact sediment budgets and downstream water resources.

Bedload movement in streams occurs when the energy of flow along the bed surface exceeds that necessary to entrain bed material particles. Flow energy depends on a number of factors, most importantly discharge, water depth, and turbulence (Leopold et al., 1964). Entrainment depends on flow energy, bed cohesiveness, and mass of the individual particles making up the bed (Leopold et al., 1964). In a generalized pattern of bedload transport, the channel bed sediment begins to move once the discharge threshold for entrainment has been reached. Stream flow moves sediment into (fill) or out of (scour) a cross section as long as material of transportable size is available. As discharge falls, the largest particles drop out first with progressively finer fractions remaining in suspension. High-resolution information about patterns of channel bed sediment movement improves our understanding of transport processes within the catchments, geomorphically effective flows, and seasonal variations within sediment budgets.

Despite forested mountain catchments being an important water and sediment source worldwide (Milliman and Syvitski, 1992), much of sediment transport theory has been developed on lowland systems and with flume work (Traylor and Wohl, 2000). Data sets on gravel-bed streams are often located in upland systems; however, bedload studies in forested mountain catchments have challenges such as episodic high flows, high bed roughness, complicated flow forms (i.e., hydraulic jumps, super critical flows), woody debris structures, and a wide range of particle sizes (Gintz et al., 1996). The challenge is exacerbated by obstacles associated with data collection in remote locations. Historically, estimations of mean transport rates have been hampered by an insufficient number of measurements and/or a long enough sampling program to capture variability (Gomez, 1991; Ziegler et al., 2014). Data sets that are of high temporal resolution and long duration have been lacking in the literature (Gomez, 1991; Bunte et al., 2004; Hedrick et al., 2013; Ziegler et al., 2014). Common field methods involve manual surveys of the stream bed (Kelly, 1992; Traylor and Wohl, 2000; Hassan and Woodsmith, 2004; Heritage and Milan, 2004; Levy et al., 2011; Ryan et al., 2011 ; Recking et al., 2012) or manual bed sediment grab sampling (Carling et al., 1998; Moog and Whiting, 1998; Bunte et al., 2004; Hassan and Woodsmith, 2004; Heritage and Milan, 2004; Muskatirovic, 2008 ; Levy et al., 2011; Ryan et al., 2011 ; Rathburn et al., 2013) and typically are labor intensive and thus of low temporal resolution and/or short duration

(Figure 4.1). Scour chains are frequently utilized in conjunction with channel bed surveys (Hassan and Woodsmith, 2004; Bigelow, 2005; Levy et al., 2011) but can only provide aggregate information at a single point in time. Other methods employ various forms of sediment traps or basins that require manual cleaning or involve extensive and costly apparatus, such as conveyor belt systems, to continuously clear the material (Kelly, 1992; Hassan and Church, 2001; Bond, 2004; Bunte et al., 2004; Schindler Wildhaber et al., 2012; Lucía et al., 2013). These devices have varying degrees of trapping efficiency and sample bias. Studies that seeded luminescent (Thompson et al., 2007) or magnetic tracer particles (Gintz et al., 1996) onto the stream bed have also been used to track bedload movement. These studies integrate movement over set time periods and still have limited temporal resolution as they rely on repeat surveys. A few more recent techniques, such as in situ magnetic detection devices (Carling et al., 1998; Tunnicliffe et al., 2000) or acoustic/impact methods (Hsu et al., 2011; Turowski et al., 2011; Yager et al., 2012), can operate at time scales on the order of 10–100 Hz but are limited in their ability to detect the finer sediment fractions (< 10–32 mm). As Figure 4.1 illustrates, many of the common techniques that can measure the finer particle size fractions tend to be labor-intensive and challenging in getting at temporal resolutions under a day for a significant length of time, an especially problematic situation in flashy or episodic systems. Many of the subtleties of bedload movement within individual storm events may be missed at coarser resolutions. By not extending studies over longer time periods, the ability to look at seasonal variations and patterns in bedload movement is lost (Gomez, 1991).

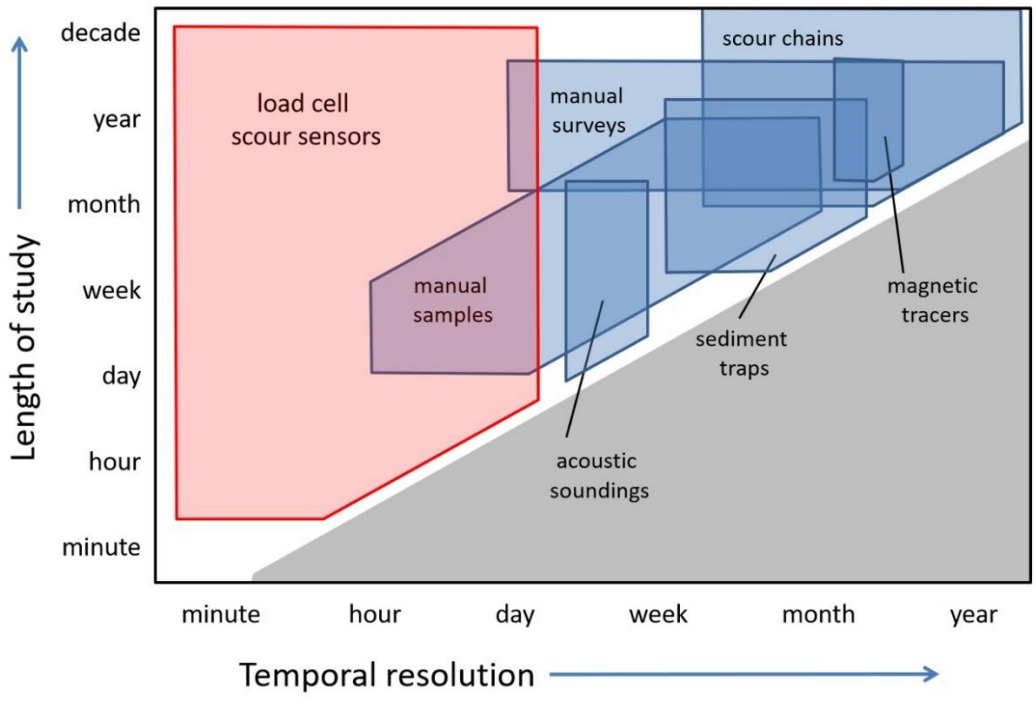

Figure 4.1. Relationship between temporal resolution and duration of study for common channel bed monitoring methods.

High-resolution, long-term data are especially important for forested mountain catchments where the bulk of sediment typically moves during infrequent, short-duration, large events and where seasonal snow coverage may drastically influence erosion and discharge patterns from season to season. A fairly recent development in measuring sediment movement is with load cell pressure sensors (Carpenter et al., 2001; Hamblen, 2003). These sensors allow the collection of high-temporal-resolution data for long periods of time, with relatively low cost and low power consumption (Figure 4.1). Previous testing of load cell pressure sensors, however, has mainly been in low-gradient sand and gravel-bed rivers. Further evaluation and field testing of the sensors is needed to determine their ability to perform in the narrow channel widths, larger substrates, steeper gradients, and flashier discharge events typical of forested, mountain headwater streams. The purpose of this study is to utilize load cell pressure sensors in this type of environment to address the following questions: (i) what are the disturbance and recovery patterns of these streams? At what temporal scales do these patterns occur? (ii) What do the observed patterns imply about channel bed stability and the channel bed as a sediment source? (iii) Are load cell pressure sensors a useful tool in measuring bedload movement in forested mountain streams? (iv) Under what physical stream conditions, if any, does their performance drop?

Methods

Study catchments

This study utilizes two sets of paired headwater catchments, all with perennial streams, located in the rain-snow transition zone of the Sierra Nevada. Sugar Pine site (southern) includes Big Sandy Creek and Speckerman Creek within the South Fork of the Merced River watershed near Fish Camp, California. Last Chance site (northern) consists of Frazier Creek and Bear Trap Creek within the Middle Fork of the American River watershed near Foresthill, California (Figure 4.2). Locations and elevations for catchment outlets and meteorological stations are given in Table 4.1. Meteorological stations were located at elevations that approximate elevations of the top of the catchments and the outlets. Gravel-bed stream channels dominate, but all catchments contain step-pool reaches with large cobble and boulder structure, lower gradient response reaches (storage reaches in which significant geomorphic adjustment occurs) with greater percentages of fine material and large woody debris structures. Southern catchments tend toward more fine material and more cobble and boulder structure. Northern sites are dominated by large gravels and cobble with interspersed bedrock outcrops. Located in the mixed conifer zone on the western slope of the Sierra, these catchments are characterized by a Mediterranean climate having a distinct wet and dry season with snow making up 40 to 60% of average annual precipitation. Annual hydrographs typically peak during snow melt but display high-intensity, short-duration flow events often associated with rain or

rain-on-snow events in fall, winter, and spring. Base flows were on the order of 0.5 L s^{-1}, and spring melt flows were 2–3 orders of magnitude higher.

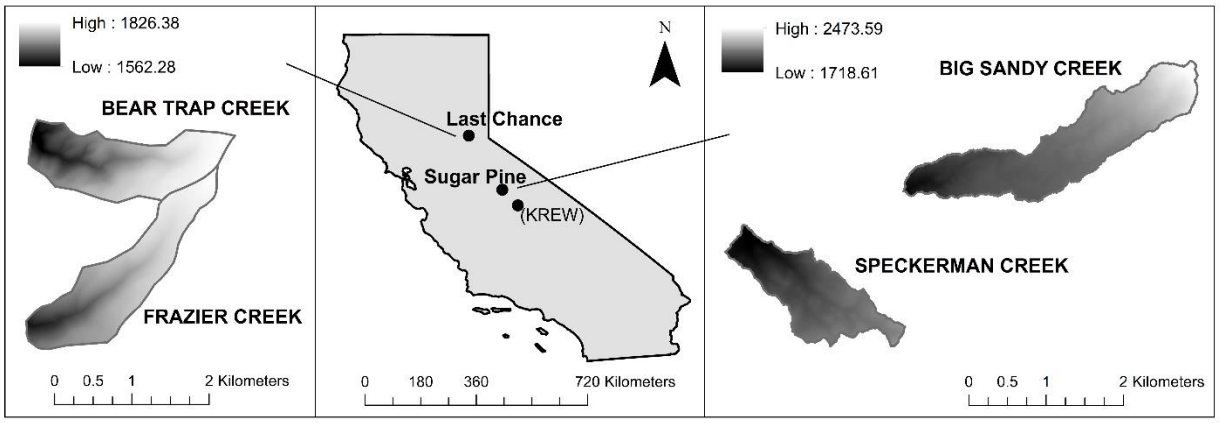

Figure 4.2. Sierra Nevada Adaptive Management Project study watersheds

Table 4.1. Watershed attributes and locations for study catchment outlets and meteorological stations

Site	Instrument cluster	Latitude (north)	Longitude (west)	Area (km^2)	Elevation (m)	Channel gradient[a] (m/m)
Sugar Pine	Big Sandy Creek	37.4684	119.5819	2.46	1780-2010	0.074
	Speckerman Creek	37.4639	119.6051	1.63	1720-2160	0.146
	Big Sandy Met	37.4684	119.5856	--	1755	--
	Fresno Dome Met	37.4638	119.5362	--	2175	--
Last Chance	Bear Trap Creek	39.1067	120.5670	1.76	1560-1830	0.100
	Frazier Creek	39.0851	120.5689	1.68	1610-1830	0.051
	Bear Trap Met	39.0945	120.5769	--	1590	--
	Duncan Peak Met	39.1546	120.5101	--	2112	--

[a] Values for lower 500 m of stream length where instruments are located.

This study period coincided with 3 years of record low precipitation in the Sierra Nevada; during this period, the study streams did not overflow their banks. Sierra-wide April 1 snow water equivalent (SWE), which is considered to generally represent peak snow accumulation, was roughly half that of the long-term average in WY 2012 and WY 2013; in WY 2014, it was only one-third (Table 4.2). Although peak snow pack and annual water yields were fairly similar, WY 2012 and WY 2013 were very different in timing of precipitation. Most of the precipitation in WY 2012 occurred mid- to late-spring. In contrast, WY 2013 had early winter and mid-spring events but very little toward the end of the season. The difference between the water years was more pronounced at the northern study sites. Cumulative totals were not reported for Bear Trap Creek in WY 2014 owing to an incomplete data set (Table 4.2).

Table 4.2. Cumulative discharges at study watersheds and percentage of long-term average April 1 snow water equivalent for the Sierra snowpack

Water year	Cumulative Discharge (10^6 L)				Sierra Nevada snowpack[a] (% of April 1 average)
	Big Sandy	Speckerman	Bear Trap	Frazier	
2012	530	461	951	989	55
2013	674	594	960	880	52
2014	354	325	[b]	487	32

[a] April 1 average data from California Department of Water Resources Cooperative Snow Surveys Program.
[b] Not available.

Soil depths at the northern sites range from 0 to 1.5 m, but typically are 0.75 m or less. The lower portion of both watersheds is characterized by hillslope gradients of 30 to 75%, while the upper hillslopes range from 2 to 30% (USDA Natural Resource Conservation Service, 2013). The Frazier Creek soils consist mainly of loams and gravelly clay loams, with smaller amounts of gravelly sandy loams, alluvium, and rock outcrops (USDA Natural Resource Conservation Service, 2013). Parent material in Frazier is Miocene-Pliocene andesitic pyroclastic flow deposits with some metasedimentary sandstone, siltstone, and slate of the ShooFly Complex (U.S. Geological Survey, 2014). Bear Trap soils mainly are gravelly loams and gravelly sandy loams, with smaller amounts of sandy loams and gravelly clay loams (USDA Natural Resource Conservation Service, 2013). Parent material for Bear Trap Creek is dominated by ShooFly Complex metasedimentary rock with some Miocene-Pliocene andesitic pyroclastic flow deposits (U. S. Geological Survey, 2014). Texture analysis on limited soil samples show loams and sandy loams as the dominant classes for both northern catchments.

At the southern sites, soil depths also range from 0 to 1.5 m with slightly deeper soils at most locations compared to the northern sites (USDA Natural Resource Conservation Service, 2013). Hillslopes in the lower portion of the Speckerman watershed have 35 to 65% gradients and 10 to 45% gradients in the upper watershed. Speckerman soils dominantly are coarse sandy loams, with some rock outcrop, and sandy loams (USDA Natural Resource Conservation Service, 2013). Hillslope gradients in the lower Big Sandy watershed are 10 to 45%, and the upper watershed has hillslope gradients from 20 to 60%. Dominant soils in the Big Sandy catchment are coarse sandy loams and rock outcrops with some sandy loams and loams (USDA Natural Resource Conservation Service, 2013). Parent material in both catchments is Early Cretaceous Bass Lake Tonalite with limited Paleozoic quartzite and phyllite at the top of the catchments (U.S. Geological Survey, 2014). Texture analysis for the southern catchment soil samples show sands, loamy sands, and sandy loams.

Field instrumentation

Field instrumentation and measurements consisted of two load cell pressure sensors (manufactured by Rickly Hydrological) per catchment, collecting bedload data at 15-minute intervals, as well as manual channel geometry and substrate measurements. Load cell pressure sensors were installed in low gradient response reaches to maximize channel bed change captured in the data. These sensors consisted of a 6 cm by 10 cm metal pan with a flexible foil top filled with degassed water and attached to a pressure transducer to form a sealed unit (Figure 4.3A). A second, built-in, pressure transducer was open to the water column. When buried in the stream bed, they can measure the pressure exerted by the sediment sitting on the pan. As scour and fill cycles occur, the load cell pressure sensors record changes in channel bed elevation and movement of channel bed material.

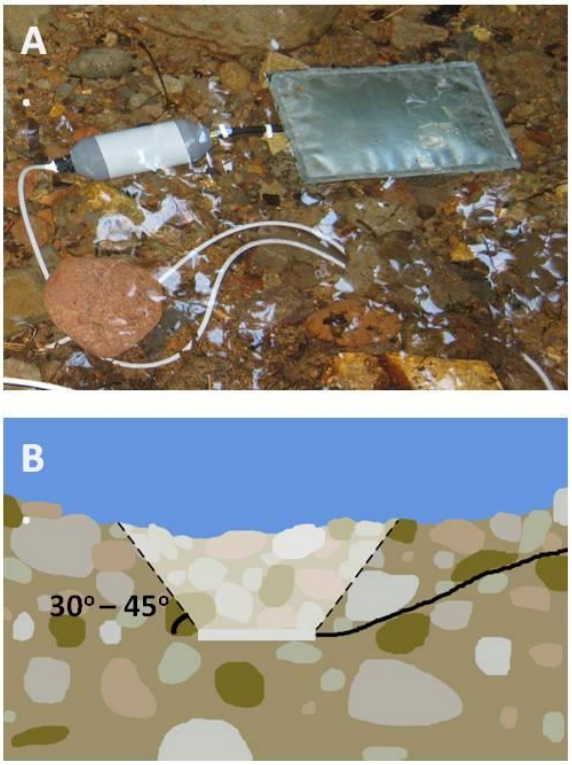

Figure 4.3. (A) Load cell pressure sensor prior to burial. (B) Diagram showing cone of influence above the sensor. The angle of the cone is approximated based on a 30–45° angle of repose.

Load cells were located ~ 500 m upstream of the catchment outlets shown in Table 4.1 for the Sugar Pine site and ~ 50 m upstream of the outlets for the Last Chance site. The two Big Sandy Creek sensors were placed ~ 15 m from each other. Sensors in the other three catchments were co-located.

The load cell pans and transducers were buried horizontally in the channel thalwegs at a depth of 30 to 50 cm below the stream bed surface. Care was taken not to puncture the foil as sediment was replaced on top of the sensor. The BSN 1 sensor was installed at the tail end of a pool, while the remaining sensors were installed in runs. Sediment masses reported are for the material above the load cells and are not integrated across the entire channel width. We assume that most of the material in these systems moves downstream in the thalweg and is therefore measured by the sensors. Detailed channel cross sections were measured manually at the time of sensor installation and annually or biannually thereafter during late summer/early fall low flow. Error in the manual cross section measurements is ± 1 cm in the vertical direction. Additional data on particle size distribution, active channel width, bankfull flow depth, and type of channel morphology at the sensor locations are given in Table 4.3.

Table 4.3. Physical channel characteristics at load cell pressure sensor locations

Sensor	D_{50} (mm)[a]	D_{84} (mm)[a]	% fines[a]	Active channel width (m)	Bankfull flow depth (m)	Channel morphology
BSN 1	6	101	48	2.6	0.5	pool
BSN 2	0.5	4	85	1.4	0.5	run
SPK	12	85	36	1.7	0.3	run
BTP	60	81	8	1.4	0.4	run
FRZ	74	107	8	1.5	0.4	run

[a] Grain size information presented is for subsurface (bulk) samples.

Stream stage was separately measured using a pressure transducer mounted on a YSI multiparameter sonde and/or using a Solinst Levelogger. These data were corrected using barometric data collected at nearby meteorological stations. Rating curves were created using monthly to bimonthly salt-dilution discharge measurements over a 3-year time period.

Calibration and data analysis

The load cell pressure sensors are designed so that the pan transducer sees the pressure from the sediment above it, the water column, and the atmosphere. The side transducer sees only the water column and atmospheric pressure. When the side sensor values are subtracted from the pan sensor values, the difference should be the signal from sediment only. This behavior held in lab tests; but when buried in the streambed, the two transducers unexpectedly tracked each other. We suspect that sediment became packed in the side sensor orifice when buried (despite attempts at screening the opening) and the transducer was effectively seeing some of the bed sediment.

To deal with the lack of reliable side sensor data, manual corrections were made on the pan transducer data using independent, co-located stage and barometric pressure measurements. These data were used to calculate the sediment signal in the continuously recorded data according to the following:

$$S_{sed} = S_{total} - S_{stage} - S_{baro} - c \quad (1)$$

where S_{sed}, S_{total}, S_{stage}, and S_{baro} are the sensor signal for sediment, total pressure, stage, and barometric pressure respectively. The pan constant c is found using known barometric pressure and stage values at the time of calibration when $S_{sed} = 0$. The sediment signal (in mV) was then converted to kg of bed sediment using calibration data and an assumed sediment bulk density of 1.8 g/cm^3. This value was chosen as an intermediary between water 1.0 g/cm^3 and granite 2.65 g/cm^3.

The factory and laboratory calibrations for each pan did not translate well to the field data. Instead, in situ field calibrations, performed at the end of data measurement, were used to determine the relationship between mV of signal and kg of material on each

pan. The decision was made to wait until the end of the study for this calibration to not disturb the sediment during the data collection period. During calibration, pans were unburied but left in place, and known weights were placed on the pans in increments to calibrate. Although in situ field calibrations were only performed from 0 to 13.6 kg, laboratory calibrations were performed over a range of 0 to 70 kg, and the sensors' response remained linear throughout for both calibrations. Manually corrected data from the load cell pressure sensors were compared to calculated values from manual field measurements with a truncated and inverted rectangular pyramid-shaped cone of influence based on assumed 30 and 45° angles of repose using methods from Hamblen (2003) (Figure 4.3B). While the angle of repose will vary based on the size distribution of the bed material, the 30–45° values are thought to cover the range of variation (Glover, 1995).

Results

Load cell pressure sensor data in all four catchments show disturbance and recovery patterns on multiple time scales. An annual pattern was observed where channel bed material built-up during fall and early/mid-winter, followed by gradual scour of material back to a stable equilibrium bed surface elevation during spring and summer, roughly following the pattern of the annual hydrograph (Figure 4.4). A second pattern, of disturbance and recovery occurring on a daily to weekly time scale, punctuated the broad annual pattern and was associated with the more substantial storm events (Figure 4.4; Figure 4.5).

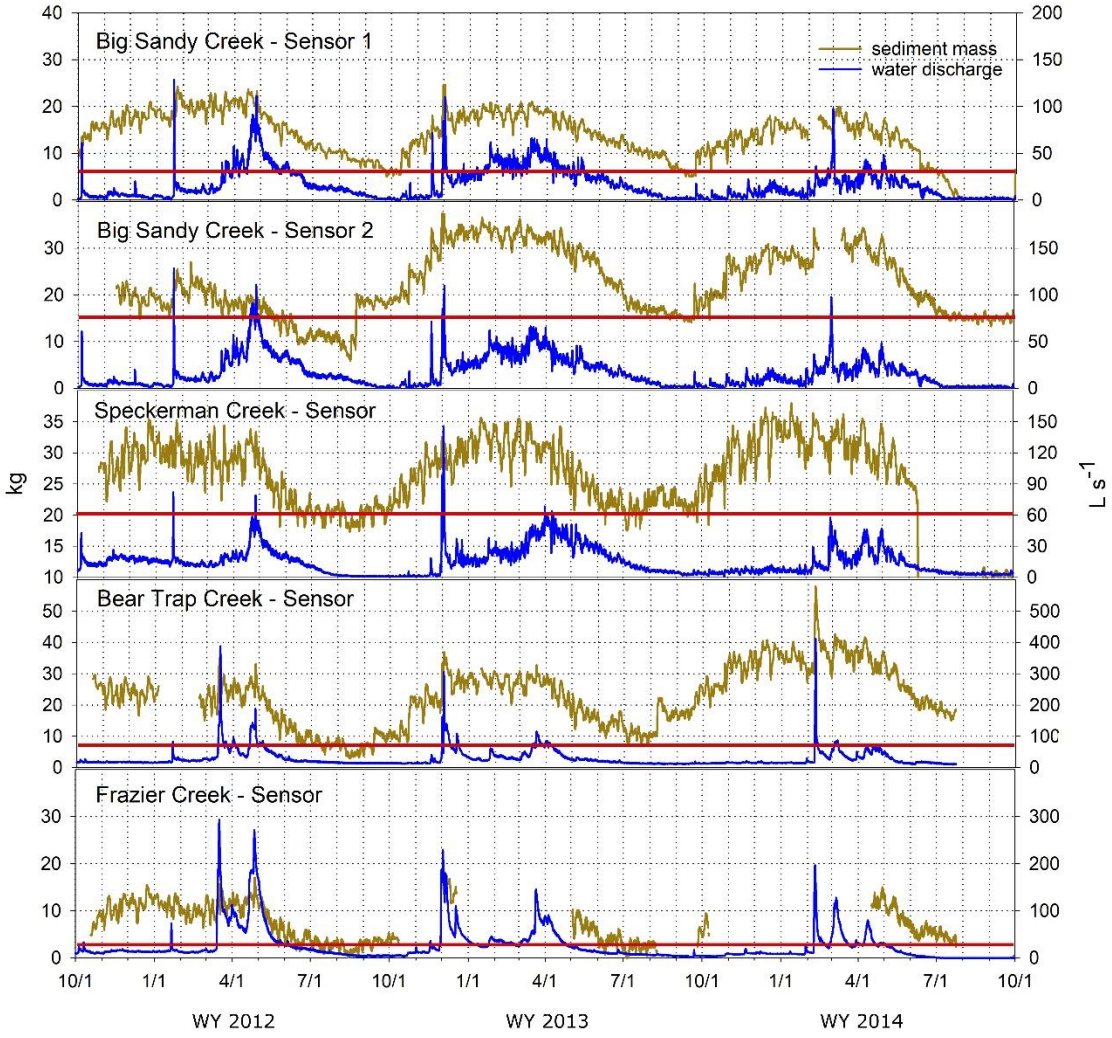

Figure 4.4. Load cell pressure sensor and water discharge data for WY 2012–2014. Red horizontal line approximates annual stable level of channel bed material. Drops in sediment observed at the end of WY 2014 in BSN, SPK, and BTP are because of pans being unburied for calibration measurements.

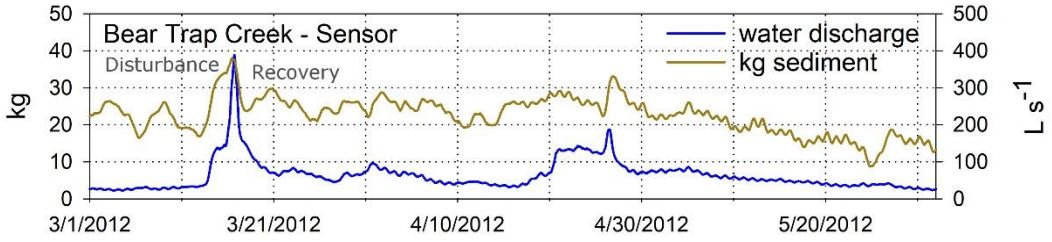

Figure 4.5. Patterns of bedload movement are characterized by abrupt disturbances associated with storm events followed by a more gradual recovery on a day to week time scale. An example of this pattern is shown for a storm event in Bear Trap Creek on 3/16/2012.

The general annual-scale pattern, trended with the annual hydrograph, showing increased accumulation during fall and winter followed by a slow removal back to baseline elevations in the spring and summer. In some years, channel bed material began to build before the background (i.e., nonevent) flows increased significantly (Figure 4.4). As hydrograph drawdown occurred in spring and summer, the amount of bed material overlying the sensors gradually dropped, approaching a stable baseline elevation for the low flow season. This broad pattern appears to be consistent over several years in each catchment (Figure 4.4).

Daily to weekly scale patterns were associated with discharge events (i.e., discharge spikes caused by rain and snowmelt events) and were characterized by an immediate channel bed disturbance followed by a more gradual recovery back to predisturbance levels (Figure 4.5). Discharge events were analyzed by their intensity: defined as the difference between peak discharge for the event and the two-week running average that represents nonevent baseline values. The measured amount of channel bed material moved during the most intense discharge events varied widely from 4.4 to 7.7, 1.4 to 9.1, 5.8 to 27.8, and 1.5 to 8.2 kg for Speckerman Creek, Big Sandy Creek, Bear Trap Creek, and Frazier Creek respectively (Table 4.4). The most intense discharge events (events > 20 L s^{-1} for the southern sites and > 30 L s^{-1} for the northern sites) followed a general trend of increased sediment movement with increased peak discharges, but considerable scatter was observed in the data. The two northern catchments showed a more pronounced trend than the southern catchments; however, the southern catchments had much lower peak event discharges.

Table 4.4. Peak discharge values, sediment movement pattern of scour then fill (S) or fill then scour (F), and the maximum amount of material moved for high discharge intensity events for each load cell pressure sensor.

Sensor	Date	Peak Q	S/F	Max sediment change (kg)
BSN 1	10/5/2011	60.9	F	4.2
BSN 1	1/21/2012	128.8	F	6.6
BSN 1	3/30/2012	57.4	S	1.6
BSN 1	4/21/2012	91.3	F	6.1
BSN 1	4/26/2012	111.1	F	4.5
BSN 1	11/17/2012	71.6	F	5.1
BSN 1	11/30/2012	85.2	F	8.3
BSN 1	12/2/2012	110.2	F	7.6
BSN 1	1/24/2013	62.1	F	3.6
BSN 1	2/28/2014	97.8	S	5.2
BSN 1	4/28/2014	48.6	F	6.0
BSN 2	10/5/2011	60.9	F	7.1
BSN 2	1/21/2012	128.8	F	8.3
BSN 2	3/30/2012	57.4	S	2.3
BSN 2	4/21/2012	91.3	NA	1.4
BSN 2	4/26/2012	111.1	F	3.7
BSN 2	11/17/2012	71.6	F	9.1
BSN 2	11/30/2012	85.2	F	6.5
BSN 2	12/2/2012	110.2	F	6.3
BSN 2	1/24/2013	62.1	F	4.0
BSN 2	2/8/2014	36.5	F	8.5
BSN 2	4/28/2014	48.6	F	7.1
SPK	1/21/2012	82.1	F	4.4
SPK	4/26/2012	78.9	F	7.7
SPK	11/30/2012	98.5	F	5.2
SPK	12/2/2012	145.0	F	7.1
SPK	2/28/2014	57.7	F	5.8
BTP	3/16/2012	388.5	F	21.1
BTP	3/31/2012	97.0	S	6.7
BTP	4/23/2012	142.9	F	6.8
BTP	4/26/2012	187.8	F	10.7
BTP	11/30/2012	161.9	F	16.0
BTP	12/2/2012	306.1	F	9.6
BTP	12/5/2012	140.6	F	5.8
BTP	12/17/2012	108.7	F	6.2
BTP	3/20/2013	115.5	F	5.8
BTP	2/9/2014	413.1	F	27.8
FRZ	1/21/2012	73.3	S	2.1
FRZ	3/16/2012	293.6	F	8.2
FRZ	4/22/2012	182.4	F	3.2
FRZ	4/26/2012	271.3	F	6.6
FRZ	12/17/2012	110.4	F	1.5

Initial deposition of sediment (fill) then recovery (scour) back toward pre-event levels was the most common pattern of sediment movement at the storm event scale. Events where scour occurred first were rare and typically occurred during smaller sediment events (see events labeled S in Table 4.4). All scour then fill event patterns occurred during mid-winter to spring with at least one event of this pattern occurring in every watershed except Speckerman Creek.

The length of recovery time for the channel bed varied from two days to just under two weeks. In some cases, recovery times were cut short by subsequent storm events. A roughly one-to-one correlation was found for the duration of the discharge event and the recovery time of channel bed sediment. This pattern can be seen in Figure 4.5.

In addition to disturbance and recovery patterns associated with storm events, a pattern of regular oscillations in pressure/sediment on a 4- to 10-day temporal scale was observed. These oscillations occurred year-round and did not appear to be associated with changes in discharge, barometric pressure, or temperature. Rough synchronicity was seen in the timing of the oscillation peaks between the two Big Sandy Creek load cell scour sensors. It is assumed that these oscillations are due to physical sediment processes within the stream rather than sensor noise, because measurements were from independent instruments placed in different (though nearby) cross sections.

Using the 15-minute sensor data, all increases in channel bed sediment were summed for the full water year to give an estimate of the amount of total bed material moving through the cross section annually (Table 4.5). This included sediment added to the cross section at all time scales 15 min or greater, including the 4- to 10-day oscillations. Water year 2013 was chosen for the calculations, as it was the most complete year of data. Frazier Creek was not included in the analysis because of data gaps. A second approach was employed by taking the difference between the annual maximum and minimum amount of bed material recorded on the load cell pressure sensors (Table 4.5). These values do not take into account any flux of material in and out of the sensor's cross section at smaller than annual time scales. The 15-minute increase method gives an estimate of throughput of material, providing insights into supply and transport capacity. On the other hand, the min/max difference method provides an estimate of the amount of material built up at peak accumulation of the channel bed. These estimates provide insights into the maximum geomorphic change of the channel bed and the degree to which supply and transport are in/out of sync.

Table 4.5. Bedload transport estimates for WY 2013

Sensor	**Bedload transport – 15-minute increase method (kg km^{-2} y^{-1})**	**Bedload transport - annual min/max difference method (kg km^{-2} y^{-1})**
BSN 1	80	8
BSN 2	100	9
SPK	200	11
BTP	300	17

Calculated amounts of material on the sensors (based off manual cross section measurements) were compared to point measurements from the continuous data (Figure 4.6). The BSN 1 and SPK sensors showed recorded values that fit within the range of the manual measurements. Sensors BSN 2 and FRZ had recorded values that all fell well below the range of manual measurements and two of the three recorded values for BTP fell below the range of the manual measurements.

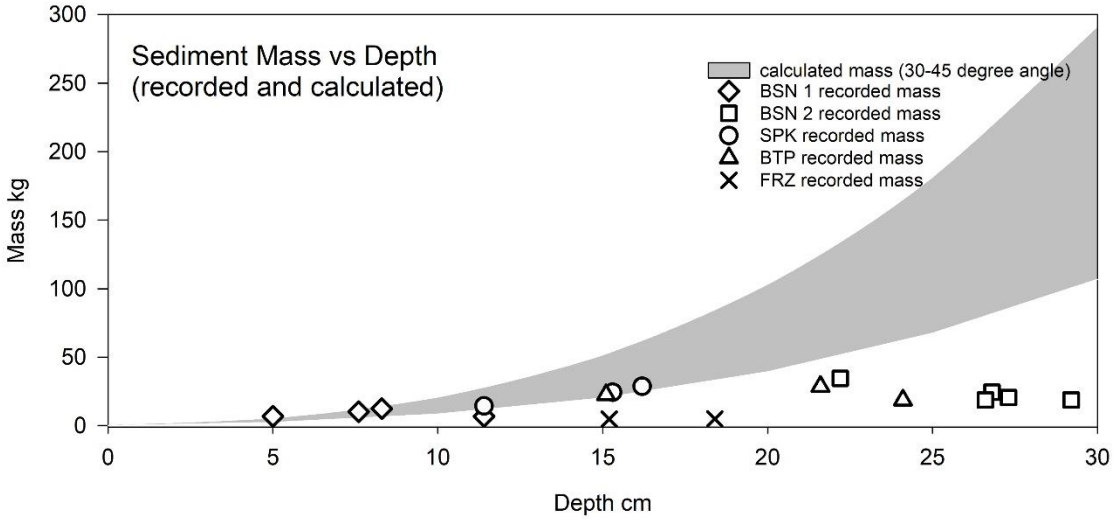

Figure 4.6. Sediment mass on load cell scour sensors vs. depth of sensor. Recorded amounts of sediment on pans are shown by points, and manual calculations of material are shown by the shaded area for a cone of influence that ranges from 30 to 45°.

Failure rate for load cell pressure sensors in the 3 years of this study was 50%. Sensors were determined to have failed when they stopped responding to increases in pressure, or they consistently gave readings that were far out of range (i.e., extremely negative readings). Failure times for sensors varied widely. Of the 10 sensors originally obtained for this study, two failed during initial laboratory testing and were never deployed. Three of the remaining eight sensors deployed in the catchments failed at some point during the 3-year study. Physical characteristics of the channel were measured, such as channel bed sediment size distribution, channel width, and gradient (Table 4.3). These parameters were compared with time until failure, but no relationships were found. Each of the three deployed sensors that fully failed were co-located (i.e., had virtually identical channel properties) with a sensor that remained functional, although it is recognized that sensor and cross section sample size were small and further testing is recommended. Visual inspections of the sensors post-study revealed that failure of the foil on the upper surface of the pan or failure of the solder joint between the foil and pan were common. More robust materials that prevent punctures and leaks in the foil covering of the load cell could drastically improve sensor failure rates. It should be noted that data reported in this study (Table 4.4 and Figure 4.6) are from the functioning rather than the failed

sensors. Despite the inconsistency between recorded and calculated values at some of the functioning sensors, all 5 reported here remained responsive throughout the study period.

Discussion

Load cell pressure sensor performance

Three out of the five functioning sensors show recorded values lower than values calculated from manual cross section measurements. Measurement error from manual surveys was considered as an explanation but could not alone account for the difference. In addition, error of this type is unlikely to have a one-directional bias for all measurements. The most likely cause of the discrepancies is uncertainty in the angle of repose and complications from channel bed and bank structure. While we assume 30 to 45° is a good approximation for the range of possible values, individual channel properties may affect the exact volume of material that the sensor sees. Notably, in cases where recorded values are lower than the manual calculations, the sediment depths are relatively high and/or the active channel widths are relatively narrow.

The BSN 2 sensor, in particular, sits in a narrow cross section (1.4 m active channel width) with a large boulder on one bank and thick vegetation on the other. The sensor was placed relatively deep in the channel bed, in the thalweg, which hugged the left side of the channel. At a depth of 25 cm (similar to sediment depths measured at this location), a cone of influence with a 30° angle of repose is ~ 93 cm wide (56 cm wide for a 45° angle of repose). The thalweg and sensor location was only 27 cm from the boulder. As a result of this asymmetric placement, the cone of influence was likely truncated by the boulder, reducing the effective mass of material weighing on the sensor by 7 to 22%, contributing to the lower than expected recorded sediment values.

In addition to edge effects truncating cones of influence, arching of channel bed materials may occur in channels where a substantial amount of large substrate is present. Compared to other study sites, Bear Trap Creek and Frazier Creek have very few fines (8%) and a high amount of cobble of metamorphic origin, with wide flat shapes characteristic of weathered slate. Material of this size and shape is more likely to stack tightly together and has a higher potential for buttressing support from the sides (arching or partial arching). Additionally, Frazier Creek's sensor is in a relatively narrow section of stream with some large cobble comprising the banks. A combination of a truncated cone of influence and arching of the larger material may have contributed to recorded values being lower than those predicted by the manual calculations.

Sensors BSN 1 and SPK sit in the widest cross sections (2.6 and 1.7 m respectively), at comparatively shallow depths, with substantial fine sediment fractions (45 and 36% respectively), thus nothing impinged on sensor operation and recorded values matched calculated values as expected. A minimum active channel width and fine sediment fraction for the sensors may be indicated based on these results.

Despite challenges such as high failure rates, in situ calibration requirements, and edge effects in narrow channels, load cell pressure sensors show potential as a tool for collecting high-temporal-resolution bedload measurements that provide insight into short-term cycles of bedload movement. The failure rate improved from previous studies (Hamblen, 2003) where hand built sensors of similar design were used in an Arizona sand-gravel bed river and saw failure rates of 6 out of 7 sensors over a 3-month period. Levy *et al.* (2011) installed a single Roctest vibrating wire load cell scour sensor in a large, low gradient river in Ohio for ~ 7 months and did not experience sensor failure. While the Levy *et al*. study had good results using a different type of load cell, sample size was notably small, measurement time was short, and the broad sand-bed river provided ideal conditions for sensor installation.

While it is recognized that a small amount of noise may exist in these systems, it is not likely that the 4–10 day oscillations are caused by sensor noise, and they do not appear related to patterns in discharge, water temperature, or barometric pressure. Alternative explanations to account for the load cell performance were examined, including that seasonal increases in pressure on the load cells could be from increases in subsurface flow to the stream with upwelling flows exerting additional pressure on the pans. Little evidence of overland flow, such as rilling or gullying, was observed in these catchments during site visits; and we can assume that subsurface flow to the stream, through shallow subsurface flows in the soil/saprolite layer or recharge from deeper groundwater, increases when the hydrograph is seasonally high. However, it is unlikely that subsurface flow accounts for a significant portion of the force on the load cell pressure sensors. Even if a high subsurface flow rate of 0.01 cm/s (4.3 m/d) is assumed, the estimated force on the pan caused by the flow would be on the order of 10^{-8} N, a negligible amount. Therefore, the annual change in pressure measured by the load cell pressure sensors is thought to represent actual buildup and scour of the channel bed material. Only a very small fraction of the seasonal change in pressure may be attributed to subsurface flows, and additional work measuring groundwater intrusion rates into the stream channel could verify the exact amount.

Increased water density resulting from increased suspended sediment during high flows was also suggested to explain event level signals from the load cell pressure sensors and the annual rise and fall of channel bed sediment. This is also unlikely to explain these patterns because the duration of suspended sediment transport does not match that of channel bed movement. In these systems, turbidity measurements reveal infrequent and short duration suspended sediment transport on the order of minutes to hours (Martin et al., 2014). Channel bed movement patterns, however, are much broader (on the order of days to weeks) at the event level and entire seasons at the annual level. In addition, no measurable turbidity is seen during much of the spring snowmelt season when load cell pressure sensors measure some of their highest values. It is noted that in systems with higher suspended sediment loads than those in this study, a correction factor may be necessary to account for the changes in fluid density.

The most likely explanation is that these oscillations may be waves of fine sediment moving through the cross section (such as those seen in sand/gravel-bed rivers) or may be a smaller number of large particles rolling into and out of the sensor's view along the bed surface (Gomez et al., 1989; Gomez, 1991; Hoey, 1992). The oscillations

do not appear to affect overall behavior of storm event response-recovery or the annual buildup and return to stable baseline stream bed elevations.

These patterns do highlight the importance of collecting concurrent discharge data so that important events can be recognized and separated from background (nonevent related) patterns. Additional tests on sensor response across a range of pressures and temperatures can help confirm the extent of any possible noise occurring at this scale, and tracer studies tracking individual particle movement would help to verify the presence or absence of waves of material and its periodicity in these systems.

Disturbance-recovery patterns

In these systems, patterns of channel bed sediment movement mirror patterns of discharge, which is characterized by high-intensity, short-duration events overlaid onto a broad, snowmelt-high-flow and summer-low-flow annual hydrograph (Figure 4.4). Abrupt disturbance that appears tied to storm event discharge on the hydrograph characterizes channel bed movement at the hours-days scale (Figure 4.5). These disturbances are followed by a more gradual recovery toward pre-event levels. The general trend of increased sediment movement with increased discharge was expected, as more energetic flows are able to move more and larger bed material. The southern study sites had considerable scatter and a narrower range of discharge values observed compared to the northern sites and thus had a less pronounced trend between discharge and channel bed movement.

The frequency of bedload movement, the discharge-sediment movement relationship at the event level, and the amount of variation in that relationship seen in this study resemble that found in other studies. For example, Gintz *et al*. (1996) used magnetically tagged particles to measure the magnitude and frequency of bedload transport for a large, steep mountain river in Bavaria, Germany. These authors found that bedload moved infrequently, with only a few events per year showing significant transport. Small, short-duration events tended to move fewer particles, to move them shorter distances, and to be less likely to bury the particles than larger events; but as in this study, they observed considerable variation even between events of similar size. They attributed that variability to variations in antecedent sediment availability. In a study by Goode *et al*. (2013), on scour depths of gravel spawning beds for streams in the northern Rocky Mountains of comparable slope, forest cover, and land use to streams in this study, the authors determined the threat of channel bed scour to salmonid species was minimal because channel bed movement events tend to be infrequent and of short duration. Working on the Great Miami River in southwestern Ohio, Levy *et al*. (2011) found scour depth, and thus sediment movement, increased with river stage in a roughly linear relationship. Despite being in a larger, lowland river setting, the Levy *et al*. work similarly showed high amounts of variation in the relationship between scour and stage, with stage representing only 48% of scour variability. For alluvial gravel-bed streams in Idaho, of similar slope and grain size to those in this study, Moog and Whiting (1998) showed increased bedload transport with increased discharge but similarly observed considerable scatter in the relationship between discharge and bedload transport.

On an annual time scale, a pattern was observed in which the channel bed built up during fall and early winter, then gradually scoured back to baseline levels during peak flow and summer drawdown of the annual hydrograph, marking seasonal variations in sediment availability and transport. Martin *et al*. (2014) used clockwise hysteresis patterns of suspended sediment for the streams in this study to show that for the wet and dry water years of their study, the dominant sediment source areas were localized within the channel bed and banks. Their work describes channel banks as the main source for sediment and proposes a conceptual model of seasonal connectedness where loose material accumulates at the base of channel banks during dry season low flows and is entrained and transported during high flow events. Building on the Martin *et al*. (2014) work, a conceptual model for these systems incorporates increased flow in early fall connecting the channel margins with the thalweg as material begins to flush into the thalweg, building up the channel bed above the load cell pressure sensors (Figure 4.7). This very localized reworking of the bed material may be occurring because of increased discharge or increased lateral flows through the banks associated with small precipitation events or with reduced ET as understory plants senesce. A conveyor-belt-type model of channel bed sediment movement in the thalweg, as described by Blum and Tornqvist (2000), is suggested where material gradually moves downstream with each discharge event. In a given cross section, the conveyor belt moves material that was previously in that cross section downstream, and new material moves into the cross section taking its place. Blum and Tornqvist (2000) originally suggested the conveyor belt concept in relation to continental margins; it also fits the observations and scale of this study. The conveyor belt model represents a mode of sediment transport where sediment is moved from upstream sources without significant long-term change to channel bed elevation. Throughout fall and winter, the conveyor-belt-like transport within the thalweg moves material with each successive flow event, but as long as supply from the margins and areas immediately upstream (input of material to the conveyor belt) outpaces downstream transport, the bed elevation increases. Recovery for individual events is sometimes truncated by successive storms aiding the building up of the bed throughout the wet season. In spring, discharge (transport capacity) is high and sediment supplies become depleted resulting in less deposition. Transport finally outpaces supply, and the channel bed gradually scours back to stable base-flow elevations. As flows recede, the margins and thalweg eventually disconnect and material builds up again at the margins through the base-flow period. The change in channel bed elevation throughout the year is a function of the balance between the supply of sediment (amount and connectedness of sources) to the thalweg and the pace of the conveyor belt.

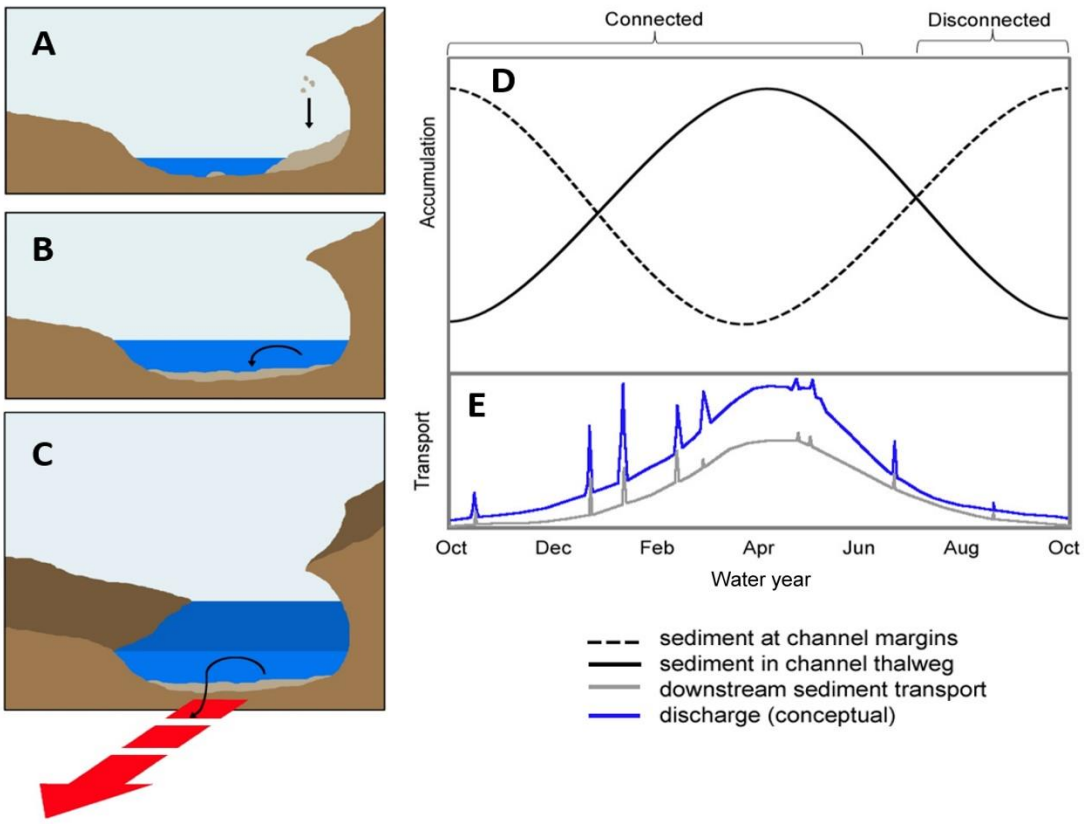

Figure 4.7. A conceptual model for montane streams in the Sierra Nevada, with panel (A) showing sediment production from bank erosion at the channel margins, where the accumulation of sediment is highest toward the end of base flow because the margin and thalweg become disconnected in the dry months except for occasional scattered rain events, allowing material to accumulate. A localized reworking of material within the cross section is shown in panel (B), which begins in early fall and continues through snowmelt (based on Martin et al., 2014). Panel (C) depicts the conveyor-belt-like transport in the thalweg moving material progressively downstream with successive yet sporadic high flow events. Panel (D) graphically represents the timing of these processes. The smoothed solid black line indicates the buildup and scour of material in the thalweg, which is measured by load cell pressure sensors (individual storm events are not depicted on this line). What the sensors see in the thalweg is a balance of erosion processes at the margin, the redistribution of material from margin to thalweg, and the downstream transport of material. Panel (E) represents a conceptual hydrograph for timing and context.

The conceptual model explains the annual buildup and scour of the channel bed as well as the observed scour and fill patterns. In fall and early winter, all events showed deposition of material (fill) then scour. The only events that first scoured the thalweg then began to fill occurred during late winter and spring when supplies are depleted and transport of bed material outpaces supply. While we believe this model can be applied for these streams in typical water years, it may not hold during extreme precipitation events. Additional work simultaneously measuring bed material at the channel edges/base of eroding banks and in the thalweg, and/or tracing of particle pathways, would help verify the model.

The proposed conceptual model can be applied more generally to forested mountain catchments where sediment availability and sediment transport capacity are disconnected or out of sync and show significant variation seasonally. The conclusions of Gintz *et al*. (1996) fit with the model in that they found sediment movement for individual storm events can vary significantly based on the antecedent sediment stores and/or the pace of sediment delivery to the thalweg. The model also holds consistent with annual scale hysteresis trends seen by Moog and Whiting (1998) and incorporates their inference that material accumulates in dry months at the toe of banks.

Bedload transport estimates

Annual bedload transport estimates calculated for WY 2013 are 80–300 kg km^{-2} y^{-1} using the 15-minute increase method and 8–20 kg km^{-2} y^{-1} for the difference between annual maximum and minimum method (Table 4.5). In the current study, both annual bedload transport estimates are made using bedload measured by thalweg load cell pressure sensor, and operate under the assumptions of our conceptual model, i.e., that the majority of bedload gets transported to the thalweg and passes over the load cells; suspended load was not included. The annual minimum and maximum accumulation method estimates the amount of material that builds up (and scours out) each year but does not take into account the throughput of material. The total bedload calculated from 15-minute increase data gives an annual estimate of the amount of material transported by conveyor-belt processes, but this method does not capture situations where sediment moved in and out of the cross section between time steps, so it may represent a minimum value. While they may represent a minimum, values estimated by the 15-minute increase method are within the range expected based on comparison with other studies.

In the nearby King's River Experimental Watershed (KREW), average annual values of sediment transport for WY 2003–2009 range from 200 to 6100 kg km^{-2} y^{-1} across eight study catchments, with a median value of 1150 kg km^{-2} y^{-1} and all but one catchment having mean values under 1700 kg km^{-2} y^{-1} (Hunsaker and Neary, 2012). The KREW catchments are of comparable characteristics (size, elevation, vegetation, precipitation, gradient, etc.) to catchments in the current study, although several of them (including the catchment with the highest mean sediment transport) have headcuts and incised channels upstream the measurement point. The KREW sediment transport values were based on material captured in instream catch basins annually. While these basins may not have had a 100% capture efficiency, they likely trapped the bedload and a

substantial portion of the suspended load, increasing the annual totals (Martin, 2009). Data reported in the KREW watersheds also showed significant variability; standard deviations for WY 2003 to 2009 were as large or larger than the mean annual transport values (Hunsaker and Neary, 2012).

Water year 2014 represents the third consecutive year of drought, so estimates from this study are thought to be more representative of the low end of the range of transport values. The KREW data may better represent longer-term averages as low and high annual precipitation years were captured. The driest year in the KREW study was WY 2007 in which transport values were under 500 kg km^{-2} y^{-1} for even the watershed with the highest transport rates (Hunsaker and Neary, 2012). Analyzing longer periods that also include wet years and/or extreme sediment events (rain-on-snow, post-wildfire, etc.) may result in higher average values for catchments in this study.

Stability and sediment sources

Cycles of disturbance-recovery and trends toward fixed channel bed elevations annually imply that the channel bed is roughly sediment neutral during this study period and that channel beds act as temporary storage for sediment generated elsewhere. Other authors have reported similar findings in terms of temporary scour and fill events but longer-term channel stability. Looking at bedload pulses in flume and field studies, Hoey (1992) indicated that gravel-bed streams are in a state of dynamic equilibrium in regards to bedload processes. In these streams, channel bed disturbance and recovery can occur at a number of temporal scales depending on the combination and scale of erosion and discharge processes. In their review of river morphodynamic studies, Church and Ferguson (2015) stated that hydrologic and erosive phenomena, which are inherently unsteady, result in bedload transport process variability but that the morphology of channels shift toward longer-term stability and equilibrium. As suggested in Bagnold (1973), when sediment supply is out of balance with stream power, channel beds aggrade or degrade. Active downcutting or aggradation, in which the channel bed becomes a sediment source or sink, was not observed over the long term in the streams in this study. Rather, temporary scour and fill cycles were seen that approached stable elevations for each channel cross section by the low flow season. Similar cycles are reported by Hassan and Church (2001) who, using pit traps in a gravel-cobble, snow-dominated stream in British Columbia, showed no generalized mobilization of the local bed material but rather short-term fluxes in bedload transport from sand pulses washing through the cross section from upstream.

Short-term changes seen in the amount of channel bed material are reflective of fluctuations in storage rather than the bed being a true source or sink. Individual particles of sediment move progressively downstream from storage area to storage area (in these systems typically pool or step-pool features). There may be temporary fluxes in the bed elevation at a given cross section as sediment deposits and washes out but no long-term (annual or greater scale) accumulation or depletion of the channel bed for the study period. Hassan and Woodsmith (2004) also reported a relatively stable channel bed (particle sizes greater than the D50 rarely mobilized) for a northern California catchment

and suggested observed changes to bed elevation are because of upstream sediment storage and/or bank collapse. The seasonal connection and disconnection of channel margins and thalweg allow for more material to build up resulting in greater seasonal changes (buildup and scour) of the bed, but the balance between supply and transport maintains the channels' long-term stability.

Conclusions

This work furthers the trial of load cell pressure sensors for collecting channel bed movement data in forested mountain catchments, a physiographic environment where they have not been well tested. Patterns of channel bed movement are evaluated, and a conceptual model is suggested in which sediment production occurs mainly at the channel banks, transport occurs within the thalweg in a conveyor-belt fashion, and the channel margins become disconnected from the thalweg during the low-flow season. This model helps to explain observed patterns, but data collected by load cell pressure sensors in these systems open a host of new questions.

Load cell pressure sensors offer management a tool for high-temporal-scale and/or real-time monitoring of channel bed scour and fill events. While periodic channel bed surveys can answer the question of whether the channel is at long-term equilibrium, higher temporal resolution data are required to begin to estimate how much material is moved. This type of detailed channel bed movement data can inform fisheries management (sediment movement affects spawning reds), land management (mitigating sediment inputs that affects water quality), and reservoir operations (minimizing downstream sedimentation to maximize reservoir lifespan). When looking at the effects of roads, forest treatments, or fire, point-in-time surveys may not capture major changes in throughput of material in the channel. With growing concerns over water supply and recent discussion in California over siting of new reservoirs, an understanding of upstream sediment movement can be invaluable to future land and infrastructure planning with respect to changing land use and climate.

While these sensors are not perfect (50% failure rate), they are promising for use in steep, forested catchments with gravel and small cobble substrates. Additional work is needed on sensor design, defining the range of appropriate physiographic environments, and verification of the conceptual model. Further work to determine more precise geometry, including angles of repose, for the sensor's cones of influence could help to confirm the truncating effects channel bank structures may have on recorded values. Sensor failures in this study did not correlate to any physical channel characteristics but rather appeared to be caused by manufacturing defects and deterioration of sensors. Improvements to sensor robustness may help reduce failure rates in these types of stream systems. A flexible rubberized coating over the entire pan that seals the joints can withstand expected water temperatures and most importantly protects the foil from sharp objects is a suggested design improvement. By placing sensors across full cross sections and employing small measurement intervals (seconds to minutes), these instruments have the potential to provide reasonably good estimates of bedload transport that can help to project reservoir life spans and upstream impacts to hydroelectric operations.

Milliman and Syvitski (1992) showed that basin relief was more highly correlated to sediment production than were factors such as climate and runoff, making basins in this study a robust analogue for a broad range of basins worldwide. Bedload estimates in small mountainous stream environments, such as those in this study, are applicable to high relief basins worldwide and may play an important role in the global sediment budget. Additional data on groundwater intrusion, variations in pore pressure of the stream beds, and particle pathways between the banks and thalweg are especially ripe areas for additional research.

Acknowledgements

This paper is SNAMP publication number 40. The Sierra Nevada Adaptive Management Project is funded by USFS Region 5, USFS Pacific Southwest Research Station, U.S. Fish and Wildlife Service, California Department of Water Resources, California Department of Fish and Game, California Department of Forestry and Fire Protection, and the Sierra Nevada Conservancy. This research was also supported by the US National Science Foundation, through the Southern Sierra Critical Zone Observatory (EAR-0725097). We would also like to thank Phil Saksa, Patrick Womble, and Tyler Patel for their invaluable assistance in data collection and analysis. Finally, we would like to extend a special thanks to our reviewer, Dr. Jon Tunnicliffe, and editor, Dr. Richard Marston, for their careful examination which helped to improve this manuscript.

References

Bagnold, R. A. (1973). The nature of saltation and of "bed-load" transport in water. In *Proceedings of the Royal Society, London. Series A, Mathematical and Physical Sciences* (Vol. 322, pp. 473–504).

Bigelow, P. E. (2005). Testing and improving predictions of scour and fill depths in a northern California coastal stream. *River Research and Applications*, *21*(8), 909–923. https://doi.org/10.1002/rra.863

Blum, M. D., & Törnqvist, T. E. (2000). Fluvial responses to climate and sea-level change: A review and look forward. *Sedimentology*, *47*(SUPPL. 1), 2–48. https://doi.org/10.1046/j.1365-3091.2000.00008.x

Bond, N. R. (2004). Spatial variation in fine sediment transport in small upland streams: The effects of flow regulation and catchment geology. *River Research and Applications, 20*(6), 705–717. https://doi.org/10.1002/rra.787

Bunte, K., Abt, S. R., Potyondy, J. P., & Ryan, S. E. (2004). Measurement of Coarse Gravel and Cobble Transport Using Portable Bedload Traps. *Journal of Hydraulic Engineering, 130*(9), 879–893. https://doi.org/10.1061/(ASCE)0733-9429(2004)130:9(879)

Carling, P. A., Williams, J. J., Kelsey, A., Glaister, M. S., & Orr, H. G. (1998). Coarse bedload transport in a mountain river. *Earth Surface Processes and Landforms, 23*(2), 141–157. https://doi.org/10.1002/(SICI)1096-9837(199802)23:2<141::AID-ESP827>3.0.CO;2-J

Carpenter, M. C., Cluer, B. L., Smith, G. R., Wick, E. J., Lockett, J. L., & Brockner, S. J. (2001). Field trials monitoring sand deposition and erosion on a razorback sucker spawning bar on the Green River near Jensen, Utah, and operation description of load-cell scour sensors. In *Proceedings of the Seventh Federal Interagency Sediment Conference* (pp. 12–15). Reno, NV.

Church, M., & Ferguson, R. I. (2015). Morphodynamics: Rivers beyond steady state. *Water Resources Research, 51*(4), 1883–1897. https://doi.org/10.1002/2014WR016862

Gintz, D., Hassan, M. A., & Schmidt, K. H. (1996). Frequency and magnitude of bedload transport in a mountain river. *Earth Surface Processes and Landforms, 21*(5), 433–445. https://doi.org/10.1002/(SICI)1096-9837(199605)21:5<433::AID-ESP580>3.0.CO;2-P

Glover, T. J. (1995). *Pocket Ref* (Second). Sequoia Publishing.

Gomez, B. (1991). Bedload transport. *Earth. Sci. Rev.*, *31*, 89–132.

Gomez, B., Naff, R. L., & Hubbell, D. W. (1989). Temporal variations in bedload transport rates associated with the migration of bedforms. *Earth Surf. Process. Landforms, 14*, 135–156. https://doi.org/10.1002/esp.3290140205

Goode, J. R., Buffington, J. M., Tonina, D., Isaak, D. J., Thurow, R. F., Wenger, S., … Soulsby, C. (2013). Potential effects of climate change on streambed scour and risks to salmonid survival in snow-dominated mountain basins. *Hydrological Processes, 27*(5), 750–765. https://doi.org/10.1002/hyp.9728

Hamblen, J. M. (2003). *Spatial and Temporal Trends in Sediment Dynamics and Potential Aerobic Microbial Metabolism, Upper San Pedro River Southeastern Arizona*. University of Arizona.

Hassan, M. A., & Church, M. (2001). Sensitivity of bed load transport in Harris Creek: Seasonal and spatial variation over a cobble-gravel bar. *Water Resources Research*, *37*(3), 813–825. https://doi.org/10.1029/2000WR900346

Hassan, M. A., & Woodsmith, R. D. (2004). Bed load transport in an obstruction-formed pool in a forest, gravelbed stream. *Geomorphology*, *58*(1–4), 203–221. https://doi.org/10.1016/j.geomorph.2003.07.006

Hedrick, L. B., Anderson, J. T., Welsh, S. A., & Lin, L.-S. (2013). Sedimentation in Mountain Streams: A Review of Methods of Measurement. *Natural Resources*, *4*, 92–104. https://doi.org/10.4236/nr.2013.41011

Heritage, G. L., & Milan, D. J. (2004). A conceptual model of the role of excess energy in the maintenance of a riffle-pool sequence. *Catena*, *58*(3), 235–257. https://doi.org/10.1016/j.catena.2004.05.002

Hoey, T. (1992). Temporal variations in bedload transport rates and sediment storage in gravel-bed rivers. *Progress in Physical Geography*, *16*(3), 319–338. https://doi.org/10.1177/030913339201600303

Hsu, L., Finnegan, N. J., & Brodsky, E. E. (2011). A seismic signature of river bedload transport during storm events. *Geophysical Research Letters*, *38*(13), 1–6. https://doi.org/10.1029/2011GL047759

Hunsaker, C. T., & Neary, D. G. (2012). Sediment loads and erosion in forest headwater streams of the Sierra Nevada, California. *Revisiting Experimental Catchment Studies in Forest Hydrology*, *353*(July 2011), 195–203.

Kelly, L. A. (1992). Estimating sediment yield variation in a small forested upland catchment. *Hydrobiologia*, *235–236*(1), 199–203. https://doi.org/10.1007/BF00026212

Leopold, L. B., Wolman, M. G., & Miller, J. P. (1964). *Fluvial Processes in Geomrphology*. San Francisco: W.H. Freeman and Co.

Levy, J., Birck, M. D., Mutiti, S., Kilroy, K. C., Windeler, B., Idris, O., & Allen, L. N. (2011). The impact of storm events on a riverbed system and its hydraulic conductivity at a site of induced infiltration. *Journal of Environmental Management*, *92*(8), 1960–1971. https://doi.org/10.1016/j.jenvman.2011.03.017

Lucía, A., Recking, A., Martín-Duque, J. F., Storz-Peretz, Y., & Laronne, J. B. (2013). Continuous monitoring of bedload discharge in a small, steep sandy channel. *Journal of Hydrology*, *497*, 37–50. https://doi.org/10.1016/j.jhydrol.2013.05.034

Martin, S. E. (2009). *Comparison of In-Stream Sediment Sources and Assessment of a Bank Erosion Model for Headwater Catchments in the Central Sierra Nevada, California*. University of California, Merced.

Martin, S. E., Conklin, M. H., & Bales, R. C. (2014). Seasonal accumulation and depletion of local sediment stores of four headwater catchments. *Water (Switzerland)*, *6*(7), 2144–2163. https://doi.org/10.3390/w6072144

Miller, J. D., Safford, H. D., Crimmins, M., & Thode, A. E. (2009). Quantitative evidence for increasing forest fire severity in the Sierra Nevada and southern Cascade Mountains, California and Nevada, USA. *Ecosystems*, *12*(1), 16–32. https://doi.org/10.1007/s10021-008-9201-9

Milliman, J. D., & Syvitski, J. P. M. (1992). Geomorphic/Tectonic Control of Sediment Discharge to the Ocean: The Importance of Small Mountainous Rivers. *The Journal of Geology*, *100*(5), 525–544. https://doi.org/10.1086/629606

Moog, D. B., & Whiting, P. J. (1998). Annual hysteresis in bedload rating curves. *Water Resources Research*, *34*(9), 2393–2399. https://doi.org/10.1029/98WR01658

Muskatirovic, J. (2008). Analysis of bedload transport characteristics of Idaho streams and rivers, *1768*, 1757–1768. https://doi.org/10.1002/esp

Rathburn, S. L., Rubin, Z. K., & Wohl, E. E. (2013). Evaluating channel response to an extreme sedimentation event in the context of historical range of variability: Upper Colorado River, USA. *Earth Surface Processes and Landforms*, *38*(4), 391–406. https://doi.org/10.1002/esp.3329

Recking, A., Leduc, P., Liébault, F., & Church, M. (2012). A field investigation of the influence of sediment supply on step-pool morphology and stability. *Geomorphology*, *139–140*, 53–66. https://doi.org/10.1016/j.geomorph.2011.09.024

Ryan, S. E., Dwire, K. A., & Dixon, M. K. (2011). Impacts of wildfire on runoff and sediment loads at Little Granite Creek, western Wyoming. *Geomorphology*, *129*(1–2), 113–130. https://doi.org/10.1016/j.geomorph.2011.01.017

Schindler Wildhaber, Y., Michel, C., Burkhardt-Holm, P., Bänninger, D., & Alewell, C. (2012). Measurement of spatial and temporal fine sediment dynamics in a small river. *Hydrology and Earth System Sciences*, *16*(5), 1501–1515. https://doi.org/10.5194/hess-16-1501-2012

Thompson, C., Rhodes, E., & Croke, J. (2007). The storage of bed material in mountain stream channels as assessed using Optically Stimulated Luminescence dating. *Geomorphology*, *83*(3–4), 307–321. https://doi.org/10.1016/j.geomorph.2006.02.020

Trayler, C. R., & Wohl, E. E. (2000). Seasonal changes in bed elevation in a step-pool channel, Rocky Mountains, Colorado, USA. *Arctic Antarctic and Alpine Research*, *32*(1), 95–103. https://doi.org/10.2307/1552414

Tunnicliffe, J., Gottesfeld, A. S., & Mohamed, M. (2000). High resolution measurement of bedload transport 1. *Hydrological Processes*, *2643*(February), 2631–2643.

Turowski, J. M., Badoux, A., & Rickenmann, D. (2011). Start and end of bedload transport in gravel-bed streams. *Geophysical Research Letters*, *38*(4), 1–5. https://doi.org/10.1029/2010GL046558

United States Geological Survey. (2014). National Geologic Map Database. Retrieved August 9, 2015, from http://ngmdb.usgs.gov/ngmdb/ngmdb_home.html

USDA Natural Resource Conservation Service. (2013). NRCS Web Soil Survey. Retrieved March 11, 2015, from http://websoilsurvey.sc.egov.usda.gov/App/WebSoilSurvey.aspx

Yager, E. M., Turowski, J. M., Rickenman, D., & McArdell, B. W. (2012). Sediment supply, grain protrusion, and bedload transport in mountain streams. *Geophysical Research Letters*, *39*(10), 1–5. https://doi.org/10.1029/2012GL051654

Ziegler, A. D., Sidle, R. C., Phang, V. X. H., Wood, S. H., & Tantasirin, C. (2014). Bedload transport in SE Asian streams-Uncertainties and implications for reservoir management. *Geomorphology*, *227*, 31–48. https://doi.org/10.1016/j.geomorph.2014.01.015

Chapter 5. The seasonal and drought effects on stream chemistry and source water in forested mountain streams.

Abstract

Five years of continuous and discrete discharge, water quality, precipitation, and water chemistry data from four forested, mountain, headwater catchments in the Sierra Nevada, is used to explore the effects of drought on seasonal source water availability. The study period includes two years of above average precipitation followed three consecutive years of drought. Study catchments contain perennial streams and are characterized by a Mediterranean climate with a distinct wet and dry season. Sites are located in the rain-snow transition zone with snow making up 40 to 60 percent of average annual precipitation. Barring human disturbances such as logging/grazing (compaction) or fire (hydrophobicity), catchment soils have high infiltration capacities.

Springs and seeps maintain baseflow during the summer low-flow season, and shifting chemical signals within the streams indicate an increased importance of sub-surface water sources during drought years. End-member mixing analysis was conducted to identify water source end members. This analysis indicated drought years saw a higher fraction of ground water contributing to streamflow during base flow than in non-drought years, but no discernible difference was seen during the rest of the year. Significant tree mortality seen across the Sierra Nevada in 2015 and 2016 suggests there may not have been enough available water to sustain trees throughout the dry seasons in extended drought years. This fits with our observed shift toward deeper ground water sources (perhaps below the rooting zone of many trees) during the dry seasons of drought years of this study. An understanding of the effects of drought on water sources and flow pathways aids in predicting which areas are most vulnerable and provides a foundation for comprehensive, sustainable land use management in forested, mountain systems.

Introduction

Multiple consecutive years of drought have occurred across much of the western United States in recent years. California has been hit especially hard. The multi-year drought (2012-2016) included the lowest total annual precipitation and the highest annual temperature on record (Diffenbaugh et al., 2014). Long term studies in a wide variety of physiographic regions have demonstrated increased temperatures and decreased discharge over the past 50-100 years (Rood et al., 2008; Mishra and Singh, 2010; Petrone et al., 2010; Reinfelds et al., 2014; Sawaske and Freyberg, 2014; Kang et al., 2016). Climate change is exacerbating the effects of drought as increased temperatures further evaporative demand and water storage challenges.

Rain, snow, and subsurface waters sustain flow in forested, mountain headwater catchments. The ratio of these source waters varies both spatially and temporally with changes in precipitation and storage capacity (Klos et al., in press). Groundwater is a particularly important source in maintaining baseflows and vegetation during the dry season in mountain headwater systems (Blumstock et al., 2015). In California, and many other areas with a distinct dry season, vegetation and wildlife depend on subsurface and baseflow water availability for survival. Source waters and their flow pathways also have implications for nutrient cycling, weathering rates, and sediment transport, which affect stream water chemistry, stream water quality, and health of biotic systems.

The effect of drought can be especially drastic in Mediterranean climates that already experience seasonal extremes in precipitation. Availability of subsurface water during extended droughts can have profound effects on vegetation, forest health, and ecosystem persistence. During the recent California drought, approximately 102 million trees have died in California national forests since 2010 and its estimated that an additional 62 million trees died in 2016 alone as a result of the combined effects of the multi-year drought and bark beetle infestations (US Forest Service, 2017).

The trend toward increasing water scarcity is expected to continue as climate change leads to more variability and climactic extremes (Mishra and Singh, 2010). The decreased precipitation and increased temperatures seen with drought and climate change puts greater stress on forest ecosystems that in some areas may already be water limited in the summer dry season (Klos et al., in press). The effects of climate change and drought are particularly important in forested mountain headwater catchments because they sustain downstream water supplies (Blumstock et al., 2015). Uplands provide a disproportionally large amount of water for the larger systems (Tetzlaff and Soulsby, 2008). A solid understanding of catchment groundwater availability and the persistence of subsurface storage under drought conditions is critical for water conservation planning, flow forecasting, and ecosystem management, but limited work has been done at a seasonal level on the effects of drought on source waters (Sawaske and Freyberg, 2014) Managers need to know how watersheds will respond in low water years as well as how that response might impact forest resources such as water and timber over the short term and overall ecosystem health over the long term.

The aim of this study is to use high-temporal-scale discharge, water quality, and precipitation data in conjunction with periodic water chemistry samples from forested mountain catchments to address the following questions: 1) How do the discharge patterns and water chemistry change during drought conditions? 2) How do the source waters change seasonally in these systems and what are the effects of drought on the source water ratios? 3)What connections are implied between source waters and forest health during consecutive years of drought?

Methods

Field Sites

Field sites consist of two sets of paired, forested, headwater catchments on the western slope of the Sierra Nevada in California. The southern site (Sugar Pine) catchments are Big Sandy Creek and Speckerman Creek, located in the Merced River basin near Fish Camp, CA. The northern site (Last Chance) catchments are Bear Trap Creek and Frazier Creek, located in the American River basin near Foresthill, CA (Figure 5.1; Table 5.1). Each catchment contains a perennial stream and is in the rain-snow transition zone with snow making up 40 to 60 percent of average annual precipitation. The study sites are characterized by a Mediterranean climate with a distinct wet (winter) and dry (summer) season.

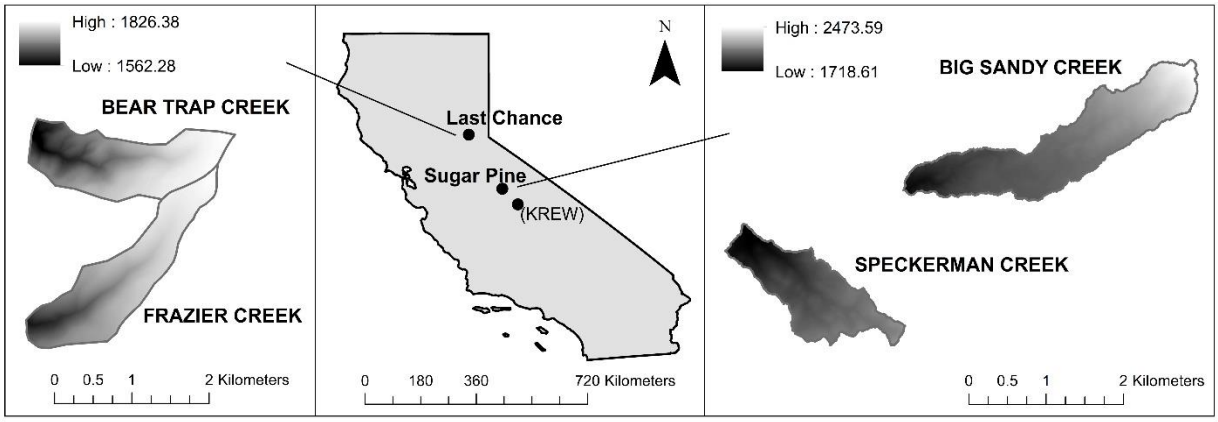

Figure 5.1. Sierra Nevada Adaptive Management Project study site locations

Loam and sandy loam are the dominant soil textures (averaged over the full soil profile) at the northern sites where soil depths range from 0 to 1 m and average about 0.75 m. Soil depths range from 0 to 1.5 m at the southern site with average depths slightly greater than at the northern site. Southern site soils have sand, loamy sand, and sandy loam textures (Table 5.1). The southern site bedrock geology is granitic, while the bedrock geology of northern site is a mix of metamorphics and volcanics (Table 5.1). Detailed soil and geological characterization for these sites can be found in Martin and Conklin (2017 *in press*).

Table 5.1. Watershed physiographic characteristics.

	Big Sandy Creek	Speckerman Creek	Bear Trap Creek	Frazier Creek
Outlet elevation (m)	1778	1719	1560	1605
Area (km^2)	2.47	1.62	1.76	1.68
Aspect	southwest	northwest	southwest	West
Gradient (m/m)	0.074	0.146	0.100	0.051
Soil texture	Loamy sand/sand	Loamy sand/sand	Sandy loam/ loam	Sandy loam/ loam
Geology	tonalite	tonalite	sandstones, siltstones/slates; andesitic volcanics	andesitic volcanics; sandstones, siltstones/slates
Channel type	Step-pool and pool-riffle	Step-pool and pool-riffle	Step-pool and plane bed; some bedrock	Step-pool and plane bed
Dominant bed material	Sand, gravel, boulder	Sand, gravel, cobble	Gravel, cobble (some bedrock)	Gravel, cobble
Geomorphic elements	Boulder, LWD	LWD	Bedrock, LWD	LWD

Data Collection

Slightly upstream from each of the catchment outlets, a Yellow Springs Instruments multiparameter sonde was installed to measure water temperature, conductivity, and stage at 15-minute intervals for the duration of the study period. An additional YSI sonde installed in the Big Sandy, Speckerman, and Bear Trap catchments in WY 2011, provided data redundancy. Redundant sonde data was used to fill gaps due to power failures and burial of the primary sonde by stream sediment. Stream stage and water temperature were measured independently using Solinst pressure transducers near the catchment outlets.

Stream water grab samples for major ions, and stable water isotopes were taken monthly to bi-monthly adjacent to the in-stream instruments (Table 5.2). Manual discharge measurements were taken using a slug-tracer dilution method immediately following water sample collection (Moore, 2003). Attempts were made to capture the full range of high-flow and low-flow events. Ion samples were stored frozen while waiting for filtration and analysis. Isotope samples were collected and stored until analysis in air-free bottles to prevent isotope fractionation.

Major ion samples were filtered (0.45 microns) then split in half for ion chromatography analysis to determine ion concentrations and titration analysis to determine acid neutralization capacity. Isotope samples were processed using integrated-cavity laser spectroscopy (Los Gatos Research DLT-100 Liquid Water Isotope Analyzer) to determine the δ^2H and $\delta^{18}O$ of samples. Sample analysis was conducted by the

University of California, Merced Environmental Analysis Laboratory. Instrument precision for ion samples was 0.01 mM and for isotope samples was 0.8 or less (δ^2H) and 0.3 or less ($\delta^{18}O$).

Table 5.2. Sample descriptions.

Sample Type	Sample Site	Sample Size	Duration	Location Type
Stream water	BSN	30	2010 - 2014	Instrumented transect
Stream water	SPK	27	2010 - 2014	Instrumented transect
Stream water	FRZ	34	2010 - 2014	Instrumented transect
Stream water	BTP	33	2010 - 2014	Instrumented transect
Spring/seep	BSN	1	Oct 2011	Multiple locations within channel
Spring/seep	SPK	8	Jul 2012, Sep 2012	Multiple locations within channel
Rain	BSN Met	1	Aug 2013 (1 month integrated)	Meteorological station
Rain	FRD Met	1	Aug 2013 (1 month integrated)	Meteorological station
Snow	BSN Met	2	Mar 2010, Mar 2012	Snow pit sample
Snow	FRD Met	4	Mar 2010, Apr 2012	Snow pit sample
Snow	BTP Met	2	Mar 2010, Apr 2012	Snow pit sample
Snow	DPK Met	1	Mar 2010	Snow pit sample
Groundwater well	Tenaya Lodge	2	Oct 2014	Drinking water wells from Tenaya lodge (500’ and 900’ depth)
Meadow soil water	KREW P301, B201	2	Oct2009	Piezometer sample
Spring	KREW B201	1	Oct 2009	Spring water sample
Groundwater well	KREW Dinkey Creek, Glen Meadow, Blue Canyon	4	Aug 2008, Oct 2009	Drinking water wells from FS workstations

Snow pack ion and isotope samples were collected during snow surveys conducted in March/April of 2010 and 2012 (Table 5.2). Snow for ion sampling was collecting by inserting a clean pvc tube vertically into the snow pack to obtain depth integrated samples. These snow samples were immediately melted and bottled for filtration and analysis. If multiple tubes were needed for deep snow the samples were combined when melted. Snow isotopes were collected at 10 cm intervals vertically through the snowpack using a 1000 cm^3 snow density cutter. These samples were also immediately melted then bottled.

Major ion and stable water isotope samples were also taken at springs and confluences with side channels in Big Sandy and Speckerman catchments during the summer of 2012. Sampling was repeated at the outlet, confluences, and springs in Speckerman during the fall of WY 2012 (Table 5.2).

Rain samples were collected at the Sugar Pine meteorological stations in 2013 and analyzed for major ions and isotopes (Table 5.2). These samples were integrated over approximately one month and represent 1-3 mm of precipitation that fell in a single event. A thin layer of mineral oil was used to prevent evaporation in the collection container. Two deep groundwater samples were collected and analyzed from two drinking water wells at Tenaya Lodge located 3 and 5 miles from Speckerman and Big Sandy Creeks on 10/3/2014. Sampled wells were 305 meters and 390 meters deep with screening all but the top 30 meters.

Spring, groundwater well, and piezometer samples collected at the Kings River Experimental Watershed (KREW) in 2008 and 2009 were collected for a separate study, but were considered as potential end-members (Table 5.2). Only the October 2008 sample from a 1.5-meter depth piezometer at the P301 meadow was determined to be chemically representative of an end-member for one of the catchments in this study. Liu 2012 presents further details on the KREW study site and sample collection.

Meteorological stations were located at each site at an elevation similar to the paired catchment outlets and to the upper portion of the catchments. These stations measured precipitation, snow depth, and temperature. Precipitation data were additionally obtained from nearby precipitation gages and were used to supplement study site meteorological station data because of the higher accuracy associated with shielded, heated gages in windy or sub-freezing conditions. For the northern sites the US Bureau of Reclamation Blue Canyon station was used and for the southern sites US Bureau of Reclamation Chilkoot Meadow and US Army Corps of Engineers Westfall stations were used (Martin et al., 2014).

Adjacent to the meteorological stations and to the stream instrumentation, snow depth and soil moisture instrument nodes were installed. Sensor nodes were placed on the north and south facing hillslopes adjacent to each meteorological station and on the north and south facing banks adjacent to the stream instruments. Snow depth was measured using Judd ultrasonic depth sensors mounted 1.5 meters above and parallel to the ground. Each node contained 1-6 sensors placed on upper and lower banks near the stream instruments and in under canopy, drip edge, and open locations for various tree species adjacent to the meteorological stations. Decagon Devices ECH20 TM soil temperature and moisture sensors were co-located with snow-depth sensors at the hillslope node locations. Sensors were installed in vertical pits at depths ranging from 10

to 90 cm, with the majority at 30 and 60 cm. Each hillslope node contained 6-12 soil moisture sensors that recorded at 15-minute intervals. Snow and soil moisture data presented in this study are daily, site-wide averages.

At each of the soil moisture sensor locations, 1 L of bulk soil was collected, air dried, and sent to the University of California Analytical Laboratory (UC-ANL) in Davis, CA for texture analysis. Soil particle size was determined by measuring the settling rates of the sample in a sodium hexametaphosphate solution, using a hydrometer to record changes in suspension density (1% detection limit) (Saksa, 2015).

Data Processing/Analysis

Stage data were manually cleaned removing erroneous values due to sensor maintenance or other field activities and adjusting stage levels if a sensor was reset at a new depth. The data was then barometrically corrected using data collected at the lower elevation meteorological stations with Solinst Barologger Gold sensors. Remaining gaps were filled using a linear regression for any missing time periods less than 3 hours. Gaps more than 3 hours duration were filled using data from the other stage instrument within the same stream as there was good correlation between stage sensors within the same stream. For occasional periods where there were concurrent data gaps from both stage instruments, (e.g. Bear Trap Creek WY 2011) gap filling was not possible. Rating curves were created for each catchment using a slug dilution method for manual discharge measurements and processed stage data; these were used to calculate discharge.

A SWE product was created as detailed in Martin *et al*. (2014) and Liu *et al*. (2013) for WYs 2010-2014. Average sitewide daily snow depth data was converted to SWE using Snow-density data from nearby US Bureau of Reclamation snow-pillow sites (Blue Canyon station for northern sites; Chilkoot Meadow and Poison Ridge stations for southern site).

Conductivity, major ions, and stable isotopes were compared by catchment and by water year. End-member mixing analysis (EMMA) using ion and isotope data was performed for each catchment following methods outlined in Hooper (2003) and Liu *et al*. (2008). Study site rain, snow, groundwater and stream water samples were evaluated as potential end-members, as well as end-member samples from the nearby King's River Experimental Watershed (KREW). Because stable water isotopes are conservative, they were used to identify the number of end-members needed for analysis. Under a 1-D model, the distribution of residuals against measured values was strongly linearized for both $\delta^{18}O$ and $\delta^{2}H$. Under 2-D, however, the residual distribution had a random pattern for both $\delta^{18}O$ and $\delta^{2}H$, suggesting 2-D mixing space and three end-members were needed. Solutes having a random pattern under 2-D are considered to be conservative. End-member distances of samples projected by eigenvectors were found for all conservative tracers under a 2-D mixing space to determine the eligibility of a potential end-member. The distance is expressed as the percent of absolute distance to tracer concentration and the shorter the distance the greater the tracer's eligibility as an end-member. Three end-members (2-D mixing space) were selected for each stream using the criteria described in Liu *et al*., 2008 including (i) how well a triangle can be formed to

bound most if not all of stream samples (geometrical criterion); (ii) distance of end-members; and (3) how well stream water chemistry can be recreated for conservative tracers (ideal if slope is 1 and R^2 is 1; otherwise, the closer the better). Summer baseflow discharge and water chemistry data were compared for wet and dry years from WY 2010 to WY 2014. Baseflow was defined as May 15 - Oct 15.

Results

Precipitation

Rain and snow patterns observed in this study were typical of catchments in a snow dominated Mediterranean climate with characteristically hot dry summers and warm, wet winters with substantial snowfall. Rain events in these catchments tend to be episodic - short duration (generally only a few hours) with long recurrence intervals. Rain storms typically occur during spring and fall and account for approximately 30 to 70% of total precipitation (Table 5.3). Winter and spring precipitation is dominated by snow which accumulates throughout these seasons and can reach multiple meters in depth at the elevations in this study. Snow pack Snow Water Equivalent (SWE) typically peaks around April 1 with full melt-out occurring by May or June.

Table 5.3. Annual precipitation comparison

	Big Sandy Creek		**Speckerman Creek**		**Bear Trap Creek**		**Frazier Creek**		**Sierra Nevada wide snow**	**Statewide annual runoff[c]**
Water Year	**Rain %**	**Snow %**	**Rain %**	**Snow %**	**Rain %**	**Snow %**	**Rain %**	**Snow %**	**% of long term average[a]**	**mm**
2010	28	72	41	59	50	50	50	50	143[b]	203
2011	43	57	50	50	58	42	58	42	144	345
2012	35	65	47	53	61	39	61	39	55	141
2013	57	43	62	38	74	27	74	27	52	128
2014	31	69	34	66	79	21	79	21	32	82

[a]. from DWR annual April 1 snow survey press releases. Percent of normal (based on for April 1 statewide snow surveys.

[b]. 2010 had several significant April storms so the May 1 snow survey data are presented for 2010.

[c.] from http://waterwatch.usgs.gov/index.php?r=ca&id=statesum. (100-year average is 224 mm)

Precipitation totals ranged widely for the study period of WY 2010 - WY 2014, which included above average precipitation conditions as well as a multi-year drought. WY 2011 was a fairly wet year at 144 % of normal Sierran snow pack SWE and WY 2012, 2013, and 2014 were considerable dry years at 55%, 52%, and 32%, respectively

(Table 5.3). WY 2010 was an above average year with April 1 Sierran snow pack SWE at 143 % of long term average values. Total precipitation for the southern site ranged from 62 cm in WY 2014 to 202 cm in WY 2011. The northern site ranged from 126 cm in WY 2014 to 275 cm in WY 2011 (Table 5.4).

Table 5.4. Annual precipitation totals.

Water Year	Sugar Pine (cm)	Last Chance (cm)
2010	152	191
2011	202	275
2012	83	160
2013	85	169
2014	62	126

The ratio of snow to rain varied significantly from water year to water year. In WY 2010, 72% of the precipitation in the Big Sandy catchment and 59% in the Speckerman catchment fell as snow, while in both northern catchments the ratio between rain and snow was roughly equal (Table 5.3). Water year 2011 had a slightly lower percentage of snow vs. rain across all catchments indicating the high amount of precipitation for the year was partially due to an increased rain fraction. The percentage of snow in WY 2012 was intermediate between WY 2010 and WY 2011 in the southern catchments and it was only slightly lower than in WY 2011 at the northern site. Though the total precipitation in WY 2013 was very similar to WY 2012, the rain-snow ratios were very different. There was considerably less snow compared to rain in WY 2013. The extremely low water year of 2014 had a fairly high percentage of snow for Big Sandy and Speckerman but was the year with the lowest percentage of snow for Bear Trap and Frazier. Overall the southern sites had a higher percentage of snow than the northern sites across all water years, indicating that storms were colder at the slightly higher elevation southern sites. Differences in ratios existed between catchments at the southern site because the Big Sandy catchment had a greater amount of higher elevation area than did Speckerman. Rain-to-snow ratios were equal between the two northern site catchments due to the two sites having roughly equal elevational distributions.

Discharge

Like precipitation, runoff patterns in this study showed behavior typical of mountain streams in a snow-dominated, Mediterranean climate. In summer and early fall, occasional rain events caused spikes in the discharge hydrographs, but aside from these short duration events, the hydrograph didn't begin to rise significantly until Oct-Nov when the weather cooled, rain increased, much of the understory vegetation began to senesce, and soil moisture rose. A gradual rise in the hydrograph occurred through early to mid-winter while the snowpack grew (Figure 5.2). Because these catchments were

located in the Sierra's rain-snow transition zone, periodic days of warmer air temperatures would melt snow and short-term spikes were observed in the discharge, superimposed on the gradually rising annual hydrograph. As sun angles and air temperatures rose during spring, snowmelt increased and the hydrograph peaked (usually in April to June) (Figure 5.2). If air temperatures were warm enough, rain-on-snow events could occur during winter and spring potentially causing very large spikes in the hydrograph. A gradual drawdown of the hydrograph occurred during summer when weather was typically hot and dry, with flows reaching their lowest points in August and September (Figure 5.2). With the snow pack typically gone by June and rain rarely falling during summer months at these elevations, summer flows were maintained by water stored in the catchments.

Significant differences were seen in the annual hydrographs from water year to water year (Figure 5.2). WY 2010 had several moderate discharge events in the fall, then a gradual, steady rise in the hydrograph to a sharp peak in early June when drawdown began for all watersheds. WY 2011 also had several moderate flow events in fall, but very large events in mid-December led to an abrupt rise in stream discharge and a broad plateau shape to the hydrograph, maintained by several significant flow events throughout the winter and spring. Drawdown started in mid-June of 2011. For the three dry years of WY 2012-14, most of the flow occurred late in the season for WY 2012, a bi-modal hydrograph was recorded (more pronounced at the northern sites) in WY 2013, and extremely low flows throughout all of WY 2014.

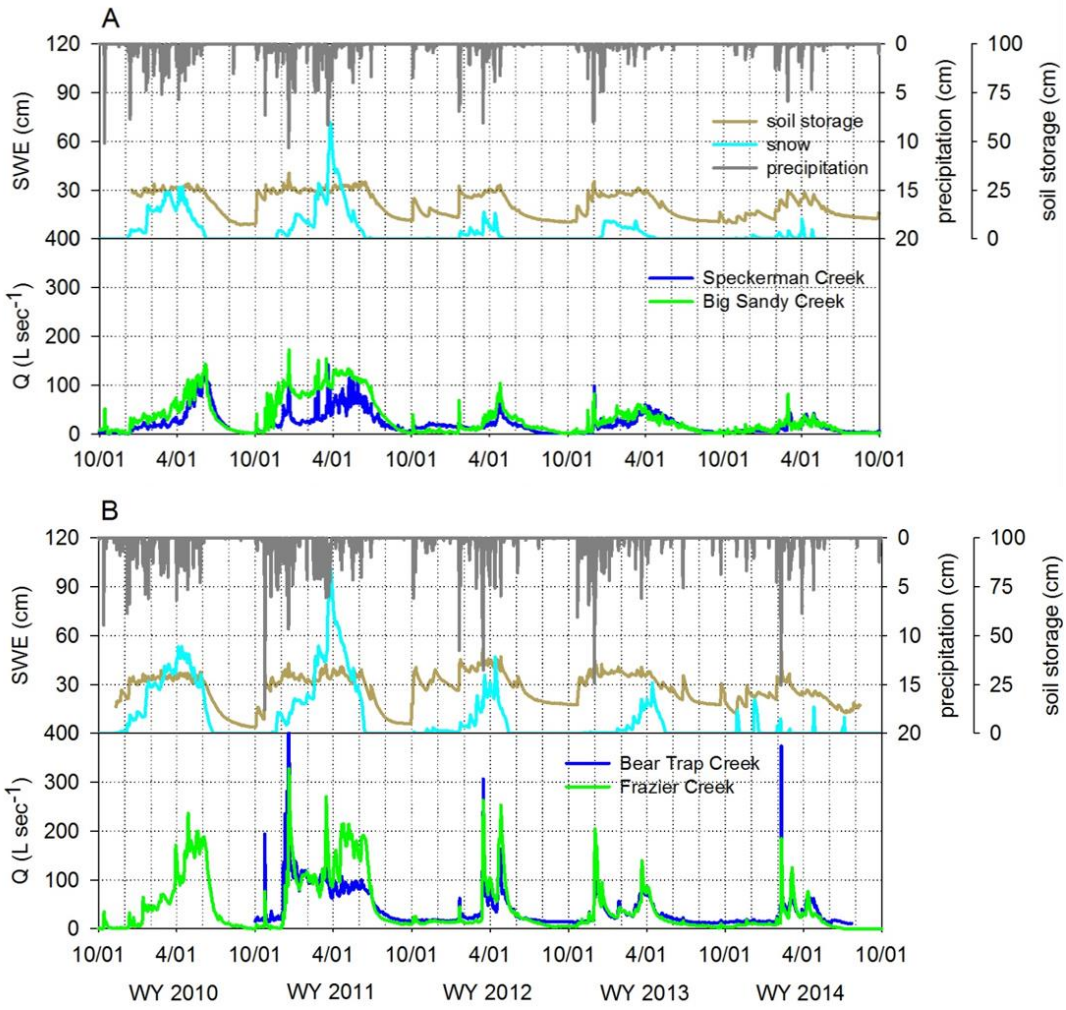

Figure 5.2. Precipitation, snow water equivalent (SWE), soil water storage, and stream discharge observations for (A) Sugar Pine and (B) Last Chance over water years 2010-2014. Precipitation is combined snow and rain from nearby US Bureau of Reclamation and US Army Corps of Engineers with heated precipitation gages (Chilkoot Meadow and Westfall stations for Sugar Pine and Blue Canyon station for Last Chance). Average sitewide snow depth data was converted to SWE using nearby US Bureau of Reclamation snow-pillow sites (Blue Canyon station for northern sites; Chilkoot Meadow and Poison Ridge stations for southern site). Soil moisture data are site-wide averages.

During this study, there were slight differences between the north and south in timing of the largest flow event, but the annual hydrographs peaked and began drawdown at roughly the same time for watershed pairs, and similarly across all catchments (Figure 5.2). While timing was similar, differences in size of discharge events were observed between the study sites. WY 2012 for example saw events in early Oct and mid-January that were much more significant at the southern sites than the northern (Figure 5.2). A large event in mid-March produced the biggest flows of the water year at the northern

sites, but that storm brought minimal increases in flow at the southern sites. All four watersheds also had large multi-day event peaks in late April. These events combined to create a gradually rising hydrograph with a fairly sharp peak for the southern sites and a bi-modal shaped hydrograph for the northern sites. Significant drawdown began at the end of April for all four watersheds in WY 2012. A large event on 12/2/12 brought the highest flows of water year 2013 across all catchments. A smaller mid-December flow event was observed at the northern sites but flow was only minimally impacted at the southern sites. These December events in combination with the mid to late March snow melt peak, gave the hydrographs a bi-modal shape in WY 2013 as well. Drawdown began in early April of that year. Finally, WY 2014 (an extremely dry year) had three significant winter flow peaks in early Feb, early March, and mid-April. The early February event was much more significant for the northern catchments. Aside from these event peaks and drawdowns, the WY 2014 baseline hydrograph remained relatively flat with flows extremely low for the winter/spring season. Drawdown was of short duration, but took place in late April 2014.

Table 5.5. Annual discharge by watershed

	Big Sandy Creek (10^6 L)	**Speckerman Creek (10^6 L)**	**Bear Trap Creek[a] (10^6 L)**	**Frazier Creek (10^6 L)**
WY 2010	1120	825		1588
WY 2011	2284	1136	2236	2584
WY 2012	530	461	951	989
WY 2013	674	594	960	880
WY 2014	354	325		487

[a]. *Discharge totals for Bear Trap Creek could not be calculated for WY 2010 and 2014 due to significant data gaps.*

There were also some notable differences in total annual discharge between catchment pairs (Table 5.5). Differences in total annual discharge between streams were greatest in wet years and more similar in the driest years. Big Sandy's discharge was higher than Speckerman's in all seasons except summer baseflow. Speckerman Creek's total annual discharge was between 50% and 92% of that of Big Sandy. Bear Trap and Frazier were more equal with Frazier having slightly higher baseline (non-event) flows than Bear Trap, but Bear Trap having higher event flows peaks (Figure 5.2). Bear Trap's total annual discharge ranged from 87% to 109 % of Frazier's, with Bear Trap higher compared to Frazier during dry years (Table 5.5).

Though Big Sandy had higher discharges during the fall, winter, and spring, its hydrograph tended to draw down faster and more completely than Speckerman's (Figure 2). Field observations supported this pattern in that Big Sandy had a larger channel and more flow during the winter and spring, but tended to go intermittent during summer baseflow in the dry years of 2012-2014. During the same time period, Speckerman Creek maintained minimal flow in most of its channel. The differences in discharge between Bear Trap and Frazier were not as great as at the southern sites. During most of the year,

Frazier's discharges were only slightly higher than those at Bear Trap. Like Big Sandy, the falling limb of the annual hydrograph was slightly steeper for Frazier, leading to marginally higher baseflow discharges for Bear Trap. Both northern site streams maintained minimal channel flow near catchment outlets, but would go intermittent higher in the catchment during dry year baseflow.

Water Chemistry

Conductivity was inversely related to discharge, with highest annual values during late summer and lowest during peak spring snowmelt. Individual storm events were observed as sharp drops in conductivity, followed by gradually increasing values as discharge drew back down. Stream to stream variation was evident. In general, Speckerman had the lowest values and the narrowest annual range in values (5-20 $\mu S/cm^3$). The other three stream had higher conductivity values and a greater annual range (20-60 $\mu S\ cm^{-3}$) (Figure 5.3). The highest conductivity values during the study period occurred in WY's 2013 and 2014.

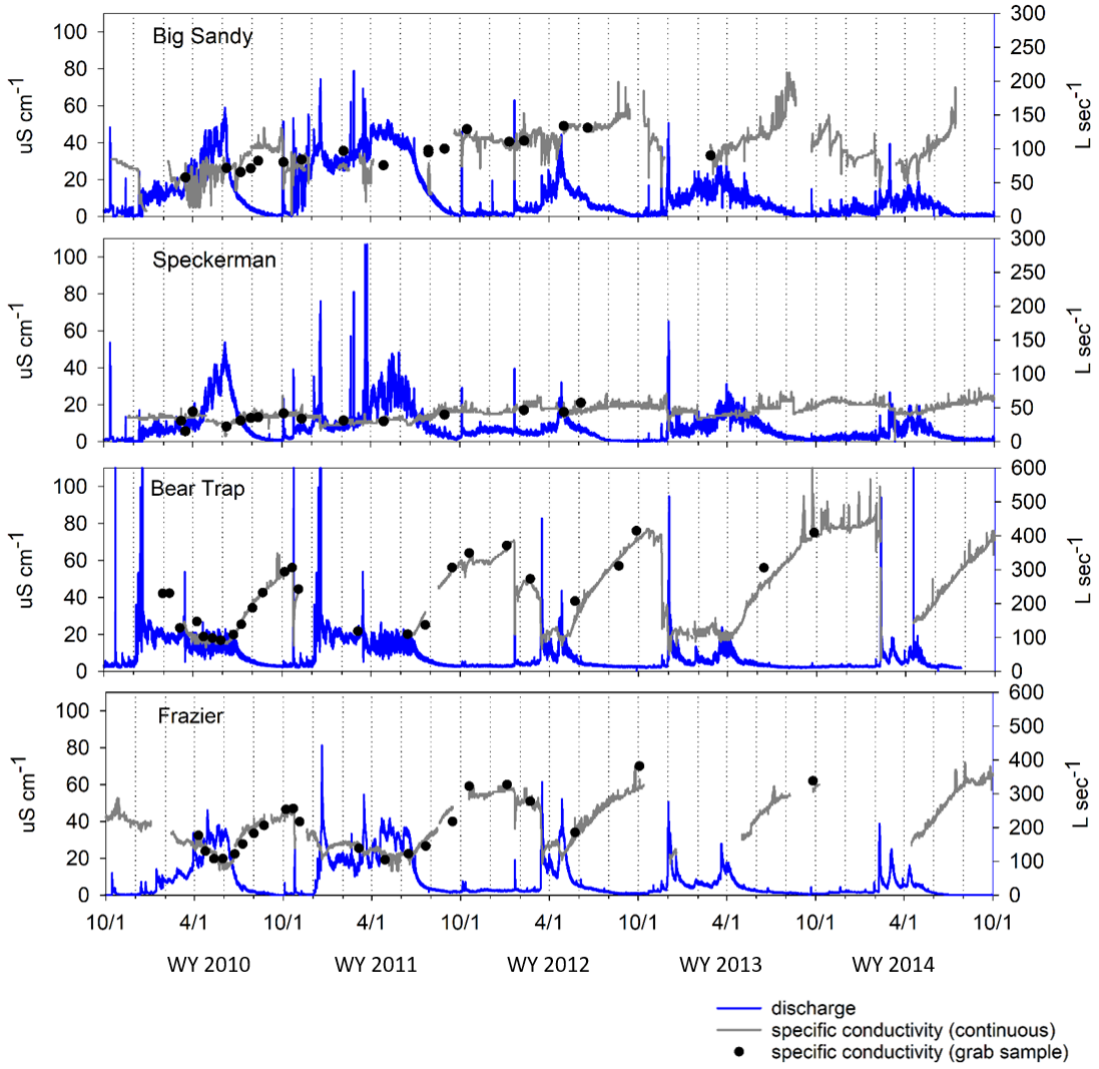

Figure 5.3. Specific conductivity (continuous and manual) plots by watershed for streamflow samples

Like conductivity, Speckerman had mean concentrations for stream water samples that were consistently lower compared to Big Sandy for all ions except Cl^- for which values were essentially the same in both streams (Table 5.6). The relationship between Bear Trap and Frazier varied by ion, with Bear Trap having higher Ca^{+2} values for all other ions measured. Bear Trap had the lowest Na^+ and K^+ of all four streams, and Frazier had the lowest Cl^- and SO_4^{-2}. Snow samples on average had lower ion concentrations than stream samples for all ions, groundwater had higher concentrations (Table 5.6). Rain samples were mixed, but had notably high Cl^- and SO_4^{-2} concentrations compared to stream sample means. The Fresno Dome rain sample had higher ion concentrations than the Big Sandy sample. Spring samples varied depending on the spring and the ion in question.

Table 5.6. Water chemistry summaries

Sample location	**Sample type**	**Number of samples**	**Ca^{+2} (μeqL^{-1})**	**Mg^{+2} (μeqL^{-1})**	**Na^{+} (μeqL^{-1})**	**K^{+} (μeqL^{-1})**	**Cl^{-} (μeqL^{-1})**	**SO_4^{-2} (μeqL^{-1})**	**HCO_3^{-} (μeqL^{-1})**	**δ^2H**	**$\delta^{18}O$**
BSN	Stream flow	30	234.0 (54.5)	64.2 (18.5)	100.5 (33.4)	17.5 (4.6)	7.8 (3.5)	5.7 (1.6)	336.3 (74.3)	-81.5 (7.1)	-11.9 (0.9)
SPK	Stream flow	27	60.4 (8.0)	16.4 (6.2)	82.7 (19.3)	10.3 (2.0)	7.9 (3.9)	1.9 (0.4)	119.4 (26.8)	-81.8 (5.8)	-11.9 (0.8)
BTP	Stream flow	33	289.9 (135.9)	55.1 (20.5)	45.5 (7.7)	4.9 (1.0)	12.7 (6.8)	11.2 (6.5)	321.5 (119.4)	-81.0 (5.7)	-11.8 (0.7)
FRZ	Stream flow	34	195.9 (59.5)	108.7 (44.7)	89.4 (27.7)	18.2 (6.1)	6.7 (4.3)	1.5 (0.4)	349.7 (117.0)	-79.5 (2.7)	-11.5 (0.3)
BSN Met	Snow	2	5.0	0.7	4.0	1.3	3.9	1.4		-85.2	-12.2
FRD Met	Snow	2	5.5	0.5	3.4	0.8	2.7	1.1		-88.2	-12.8
BTP Met	Snow	2	5.0	1.6	8.6	2.1	9.4	1.8		-86.1	-12.7
DPK Met	Snow	2	6.1	2.8	9.4	1.4	9.6	2.5		-89.3	-12.9
BSN Seep 1	Spring	1	257.3	72.9	99.4	17.1	8.2	4.1	373.2	-84.6	-12.4
SPK Seep 1	Spring	1	95.1	24.5	156.6	19.0	12.2	1.3	184.2	-83.8	-12.3
SPK Seep 2	Spring	1	100.3	5.4	127.6	14.9	13.6	1.3		-83.6	-12.2
SPK Seep 3	Spring	1	108.9	25.0	149.9	17.7	11.3	1.8	205.7	-81.1	-11.8
SPK Seep 4	Spring	1	64.2	5.6	92.4	19.8	30.0	3.9	168.2	-83.8	-12.4
SPK Seep 5	Spring	1								-81.6	-11.9
SPK Seep 6	Spring	1								-83.7	-12.4
Tenaya Well 3	Groundwater	1	674.1	122.3	810.1	39.9	257.8	104.0		-90.1	-12.7
Tenaya Well 5	Groundwater	1	575.9	143.7	973.4	46.8	318.2	130.5		-88.5	-12.7
BSN Met Rain	Rain	1	36.9	18.1	28.8	53.8	29.1	81.3		-53.8	-7.0
FRD Met Rain	Rain	1	86.2	33.1	38.6	304.2	48.7	83.7		-50.5	-6.6

When ion concentrations were plotted against conductivity values some significant differences were seen between the four study catchments (Figure 5.4). In general, Speckerman data clustered to the lower left of the plots where conductivity and concentrations were low. The remaining three catchments spanned a greater range (Figure 5.4). Bear Trap had a notably flat slope for the ions Na^+ and K^+ meaning that as conductivity increased, those ion concentrations showed very little change. Similarly, Speckerman had a relatively flat slope for the ion Ca^{+2}. Bear Trap was the only catchment to show increasing SO_4^{-2} concentrations with increasing conductivity. All other catchments had relatively flat slopes for SO_4^{-2}. For Na^+, Big Sandy and Frazier had a similar slope and range of values. Speckerman values also had a slope similar to that of Big Sandy and Frazier, but the data was shifted toward lower conductivities and higher Na^+ concentrations. Relationships for K^+ were very similar to Na^+ except that Speckerman fell roughly on the same line as Big Sandy and Frazier. Bear Trap had a slightly steeper slope and for a given conductivity had higher concentrations than Frazier for the Ca^{+2} ion. Big Sandy Ca^{+2} samples tended to plot intermediate between the two northern catchments and had more scatter.

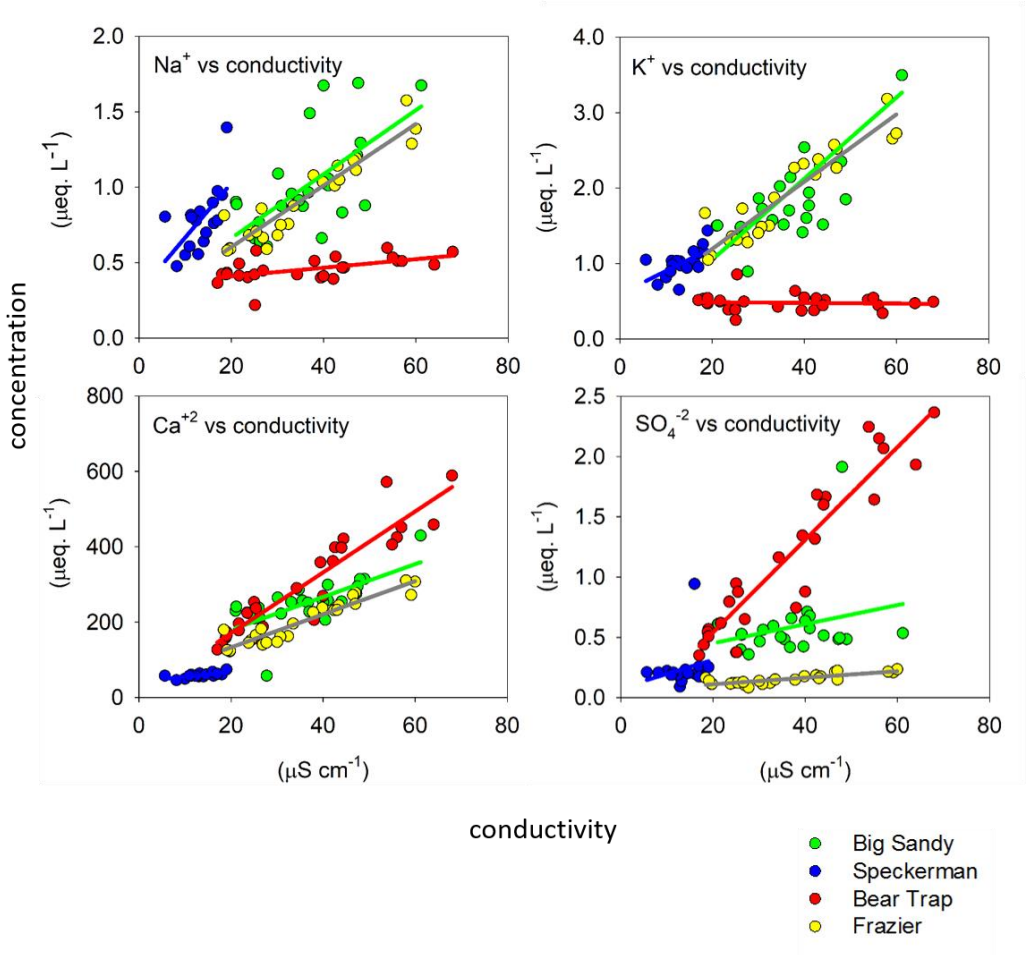

Figure 5.4. Major ions versus concentration plots by watershed for streamflow samples

Mean isotopic ratio values for stream samples were fairly similar across all four watersheds ranging from -81.8 (SPK) to -79.5 (FRZ) for δ^2H and from -11.9 (SPK and BSN) to -11.5 (FRZ) for $\delta^{18}O$ (Table 5.6). Average snow and groundwater isotopic ratios were more negative than the stream sample means, and rain was less negative. Springs varied but were closer to the stream sample means than other sample types.

Individual snow isotope samples showed much greater variation than the stream flow samples (Figure 5.5). Snow samples ranged from -140.7 to -57.8 for δ^2H and from -20.5 to -9.0 for $\delta^{18}O$. Stream samples were more tightly clustered from -104.2 to -58.3 and from-15.2 to -8.4 for δ^2H and $\delta^{18}O$ respectively. When individual stream flow stable isotope samples were compared by watershed, Big Sandy had samples with the most negative isotopic ratio values, followed by Speckerman. Frazier and Bear Trap were the least negative and spanned roughly identical ranges (Figure 5.5). Interestingly, the two southern catchments spanned a wider range than the northern sites with some stream water isotope samples approaching those of the northern catchments. Both the streamflow and snow samples fell on a local meteoric water line (LMWL) which lies above and to the left of the global meteoric water line (GMWL) (Craig, 1961). This LMWL is consistent with other isotope samples throughout the Sierras including those from the Kings River Experimental Watershed (Coplen and Kendall, 2000; R. Lucas, personal communication, Sept 11, 2012).

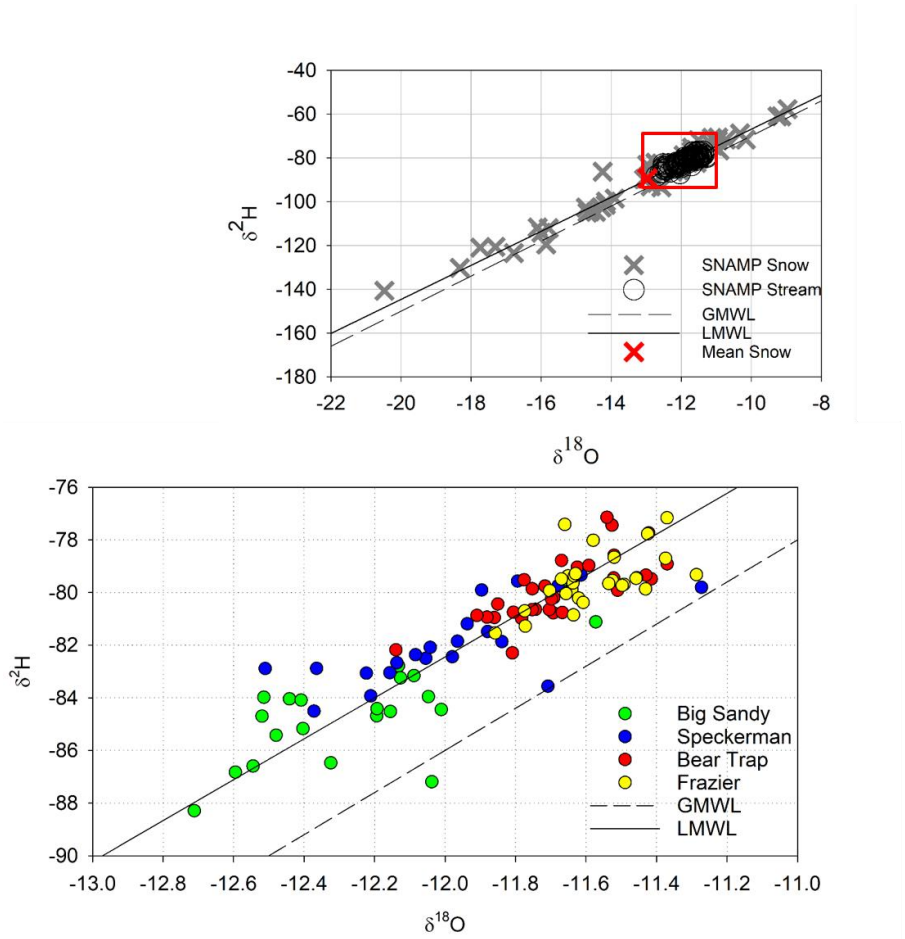

Figure 5.5. Stable water isotope values for A) streamflow and snow samples across all sites; and B) streamflow samples by watershed. Local Meteoric Water Line (LMWL) was calculated from snow, rain, and stream samples from sites in this study and at Kings River Experimental Watershed.

End Member Mixing Analysis

Potential conservative tracers were determined by the distribution of residuals against measured values. Solutes having a random pattern under 2-D are considered to be conservative and are listed in Table 5.7. Figure 5.6 shows mixing diagrams, with summer baseflow stream samples (full snowmelt to start of fall rains) and end-members in terms of principal components 1 and 2. End-Member Mixing Analysis (EMMA) indicates a shift from more precipitation in wet years (blue circles) toward more groundwater in drought years (purple circles). Snow and groundwater were potential end-members for all four catchments. The third end-member varied for each catchment, but samples (especially rain) were limited and additional data points may clarify the nature of this third end-member.

Table 5.7. Conservative tracers in for 1-D and 2-D mixing spaces.

		Residuals Distribution With p > 0.05	
Catchments	**Number of Samples**	**1-D**	**2-D**
Big Sandy Creek	30	None	$\delta\ ^{18}O$, $\delta d^{2}H$, $Ca^{2+,*}$
Speckerman Creek	27	Na^{+}	$\delta\ ^{18}O$, $\delta\ ^{2}H$, Na^{+}, K^{+}
Bear Trap Creek	33	SO_4^{2-}	$\delta\ ^{18}O$, $\delta\ ^{2}H$, Ca^{2+}, SO_4^{2-}
Frazier Creek	34	Ca^{2+}, Na^{+}, K^{+}	$\delta\ ^{18}O$, $\delta\ ^{2}H$, Ca^{2+}, Na^{+}, K^{+}

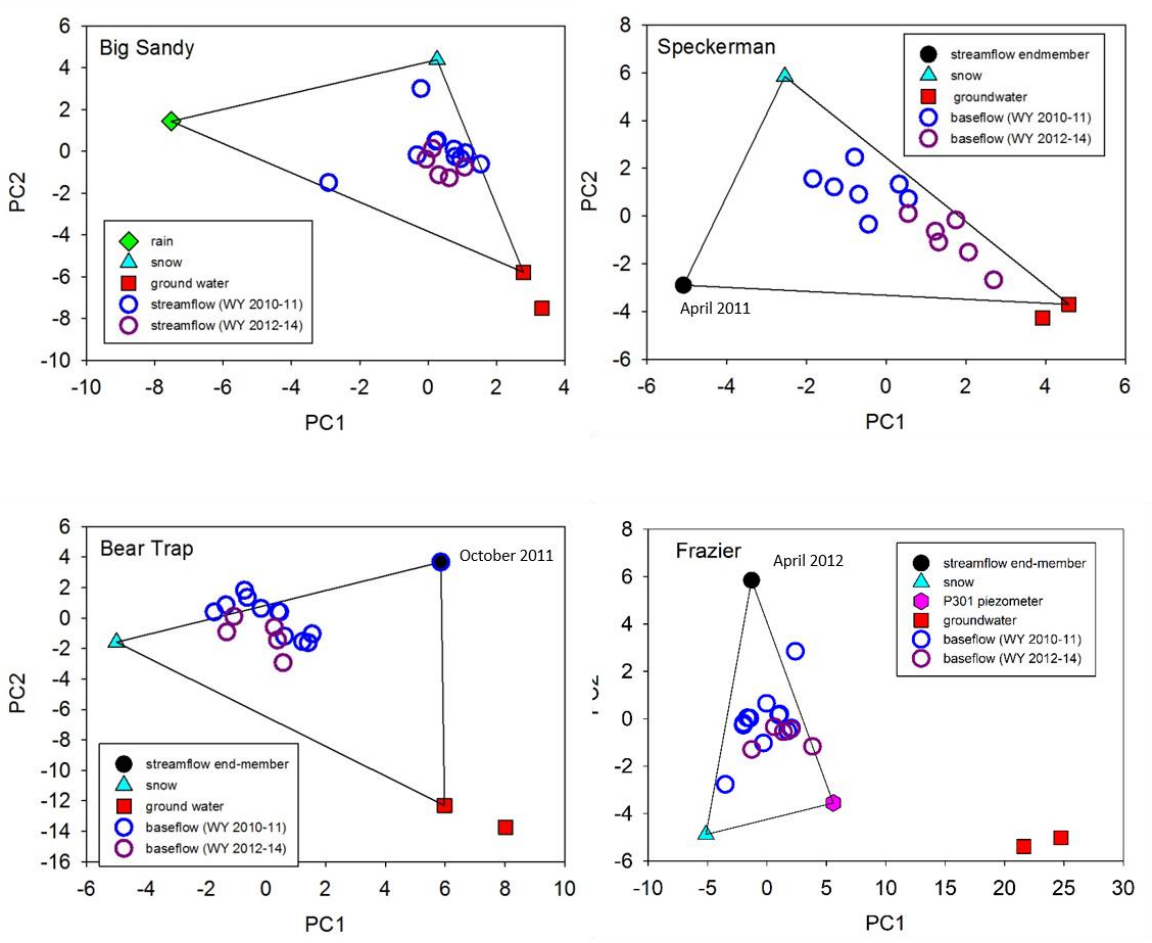

Figure 5.6. End-member mixing diagrams for study catchments showing end-members and summer baseflow stream samples in wet (blue circles) and dry (purple circles) years. Streamflow in all four catchments shifts toward the groundwater end-member during dry years.

The chosen end-members for Big Sandy, Speckerman, and Frazier Creek provided reasonably good fits to the data. Individual streamflow samples were used for one of the end-members in Speckerman and in Frazier. These samples both occurred in April three to four weeks after some of the largest spring discharge events of the year. It is suspected that these samples are representative of rain/shallow soil water. It should be noted that while the flowpaths for these end-members may be through the shallow subsurface, we included stable water isotopes as tracers for this analysis which are not expected to alter greatly through short subsurface pathways. Therefore, we believe end-members are more representative of source waters (i.e. rain) than of flow paths. The P301 piezometer end-member used for Frazier Creek is a shallow groundwater sample from KREW but may represent a deeper groundwater flow path present in the meadow; mixing analysis indicates that the groundwater end member contributing to Frazier Creek likely has a similar chemical signature.

Bear Trap Creek samples were the least well constrained by the available end-members. The chemistry of the Tenaya well samples does not represent groundwater for Bear Trap satisfactorily. This is reasonable as the Tenaya wells are not located near the Last Chance sites, nor are they in similar geology; they were used as no other deep groundwater samples were available. The Bear Trap end-member represented by one of the individual stream flow samples was from mid-October. While the precipitation event preceding it was not particularly large, stream flow at that time was very low so the ratio of rain water in the stream may be relatively large. This end-member is likely representative of rain and/or shallow soil water. For future work, additional rain, soil, and groundwater samples in closer proximity to the Last Chance sites will likely give a better constrained mixing diagram.

Fractional contribution of end members during summer baseflow suggests a shift toward groundwater, though with the caveat that statistically significant differences were not found between the means as sample sizes were limited and standard deviations high. Figure 5.7 shows the median, center quartiles, and range for baseflow samples in wet years and in dry years. A shift can be seen from greater snow and rain end-members in wet years to greater groundwater in dry years.

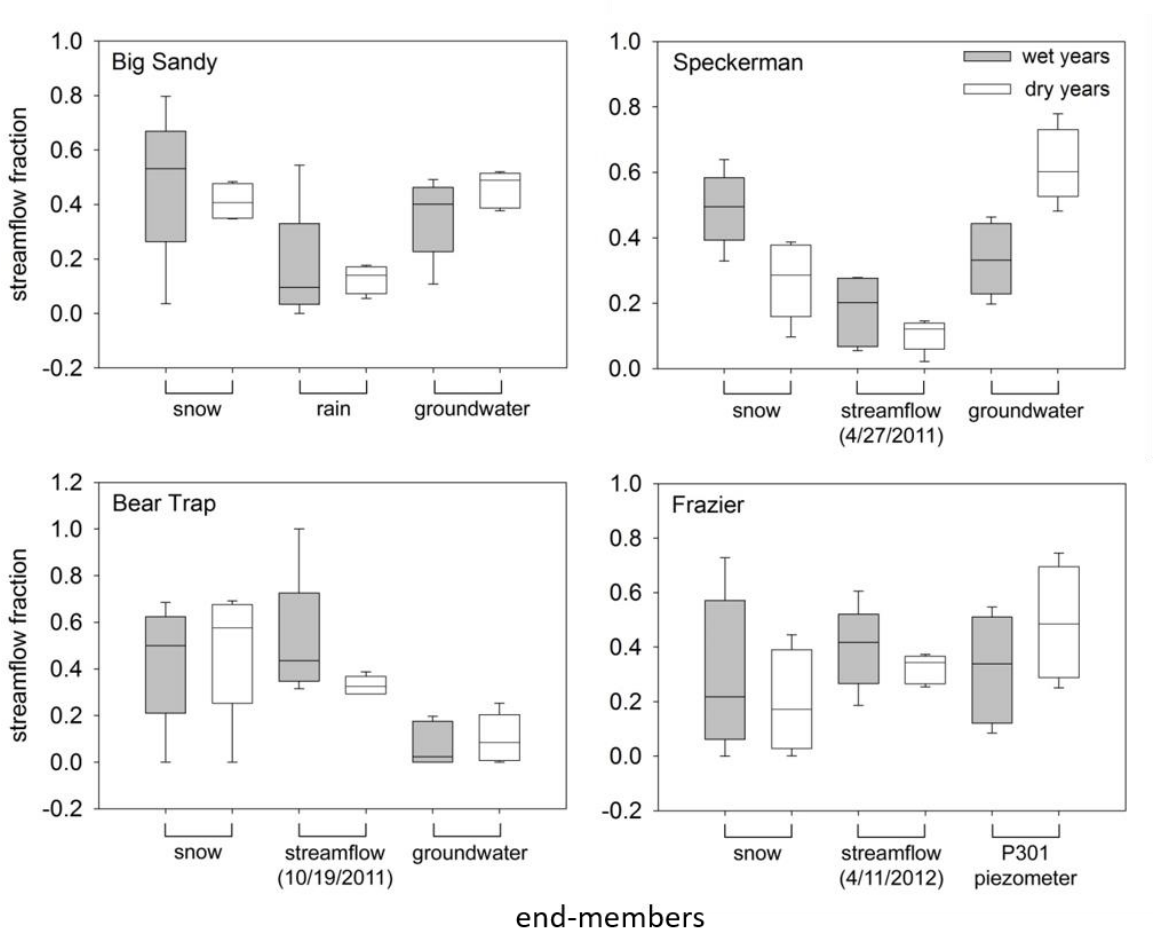

Figure 5.7. Fractional streamflow by end-member during summer baseflow in wet and dry years. Boxes show median and center quartiles; whiskers indicate range of values. From wet to dry years, the fraction of snow, rain, and/or streamflow end-members decreases and the groundwater (P301 piezometer for Frazier) end-members increase.

Discussion

Hydrologic Characteristics

The proximity and similar physiographic characteristics of catchments pairs in this study lead to very similar precipitation patterns. Hunsaker and Neary (2012) also showed similar precipitation patterns for catchments in close proximity at the nearby KREW catchments. Differences in elevation and in storm paths account for the differences in precipitation between the northern and southern sites. Big Sandy had a

higher percentage of snow than Speckerman because it had more high elevation area in the catchment. The two northern catchment pairs were roughly the same elevational distribution and thus the precipitation percentages were equal. Both northern catchments had more rain than snow most years due to being slightly lower elevation than the more snow influenced southern sites.

Stream flow in these catchments tended to respond quickly to precipitation or melt events, so the timing of discharge event peaks were fairly synchronous between pairs, but differences catchment characteristics generated notable differences in event peak magnitudes and drawdown rates. The greater discharges and flashier flows of Big Sandy are likely due to the larger watershed size compared to that of Speckerman. In the summer, however, Speckerman maintained baseflow more reliably than Big Sandy. Field observations revealed Speckerman's channel has shallower depths to bedrock and many springs feeding it. These springs maintained flow and the bedrock kept that flow near the stream bed surface in contrast to Big Sandy where the large amount of fine material (sands and gravels) in the channel likely allowed for more sub-surface stream flow. For the northern catchments, Bear Trap had greater annual discharge peaks and slightly faster drawdown after large events but also maintained more baseflow in channel during low flow periods. Like Speckerman, this may be due to shallower bedrock depths and less hyporheic zone storage. While Speckerman and Big Sandy catchments both have bedrock made up of Bass Lake tonolite a granodiorite batholith structure (Bateman, 1989), the northern sites have differing bedrock compositions which may lead to differences in subsurface flow and storage properties. Bear Trap's bedrock is predominately composed of the Shoo Fly Complex a metasedimentary sandstone and shale, while Frazier Creek is predominately volcanic material (Saucedo and Wagner, 1992). The highly crystalline metamorphic rock in Bear Trap can be assumed to have lower hydraulic conductivity and lower storage (Clow et al., 2003), while volcanics can vary in their potential for storage and flow based on structure and amount of weathering (Tague and Grant, 2004). Saksa (2015) noted that modeled differences in runoff and in a loss term (precipitation minus runoff thought to represent ET and changes in subsurface storage) between Bear Trap and Frazier may be due to these difference in subsurface storage and flow properties as well as due to vegetation changes.

Stream Water

Concentration data for conservative ions can give information about the makeup of bedrock and soil material as well as flow paths or residence times within the catchment (Soulsby et al., 2007). The relationship between stream water chemistry and catchment geology has been well established (Newton et al., 1987; Rochette et al., 1988; Jenkins et al., 1995; Horton et al., 1999; Soulsby et al., 2007; Praça Leite et al., 2010; LaPerriere Nelson et al., 2011; Kram et al., 2012; Kram et al., 2014). For example, similar K^+ concentration to conductivity ratios (ie. similar slope) for Big Sandy, Speckerman, and Frazier suggest that potassium contributes in the same fraction to stream conductivity in these three catchments. This may be due to similar bed rock and/or soil chemistry in regards to potassium. Speckerman plots in the low conductivity and low ion range (but

with the same concentration-conductivity ratio). This may be due to shorter residence times where water has less time to pick up ions from the soil and/or bedrock. Soulsby *et al*. (2006) showed that soil type was the strongest indicator of flow path and mean residence time of all the catchment characteristics tested. While Speckerman and Big Sandy have the same bedrock parent material, the extent of weathering and degree of soil development may also account for some of the differences seen in source water ratios.

Differences in streamflow ion concentrations vs conductivity were especially significant between the northern paired catchments. Frazier's concentration to conductivity ratios and end members were more similar to the southern sites than to its catchment pair Bear Trap, an occurrence also observed in the EMMA results. Bear Trap appeared to be the outlier in this study as its samples showed very little increase in Na^{+} or K^{+} concentration with increased conductivity suggesting that there were proportionally small amounts of these ions available in the soil or bedrock. In contrast, much of the stream conductivity was due to sulfate and to a lesser extent calcium as evidenced by steep regression line slopes. Dominant rock types within each basin likely account for these trends. Metamorphic material dominated Bear Traps substrate, typically gneisses and shales, containing visible pyrite inclusions. Pyrite FeS_2 can be a source for sulfate in the system (Joeckel et al., 2005).

Ion concentrations seen in this study fit within the range of values reported elsewhere in the Sierras. Meixner *et al*. (1998) reported values much more dilute than those in this study with approximate ranges from 5-15 μeqL^{-1}, 0-8μeqL^{-1}, and 2-14 μeqL^{-1} for Ca^{+2}, Cl^{-}, and SO_4^{-2} respectively for very small sub-alpine headwater catchments in Sequoia National Park. Streams inflowing to Emerald Lake in Sequoia National Park were also substantially more dilute than those in this study (Williams and Melack, 1991). The sum of all major cations ranged from 60 to 23 μeqL^{-1} at the Emerald Lake outflow during the snowmelt season. The summed average cation values for this study ranged from 170 μeqL^{-1} (Speckerman Creek) to 416 μeqL^{-1} (Big Sandy Creek). As the Sequoia National Park catchments were smaller and higher elevation the current study, the lower concentrations were not unexpected. In larger tributaries to the Merced River, Shaw (2009) reported average values of 183 μeqL^{-1}, 31 μeqL^{-1}, and 8 μeqL^{-1} for Na^{+}, Ca^{+2}, and Cl^{-} ion concentrations respectively. The Na^{+} values he reported are higher than those seen in this study. $Ca^{+2}$and Cl^{-} values were lower in the tributaries, but values in the main stem of the Merced River were higher (54 μeqL^{-1}) than those in this study. As the catchments from Shaw (2009) are much larger, with potentially deeper or older groundwater inputs it would be expected that concentrations would be higher. Our site's higher values may mean indicate that for the given catchment area there is proportionally more Ca^{+2} and Cl^{-} containing minerals in the soil and bedrock than in that of the Shaw (2009) tributaries. Liu *et al*. (2013) reported average values similar those in this study in the nearby Kings River Experimental watershed where catchments were of similar size, elevation, and vegetation cover to those in this study. Average values reported by Liu *et al*. (2013) for their 8 study watersheds were 45-171 μeqL^{-1} for Na^{+}, 74-325 μeqL^{-1} for Ca^{+2}, 21-85 μeqL^{-1} for Mg^{+2}, 15-35 μeqL^{-1} for K^{+}, 10-21 μeqL^{-1} for Cl^{-}, and 4-8 μeqL^{-1} for SO_4^{-2}.

Source Water

As would be expected in these mountain basins, snow is a consistent end-member for all four catchments. That streams typically remain perennial during the summer dry season with little to no precipitation input highlights the importance of sub-surface water storage in feeding dry season flow (Schwinning, 2010; Klos et al., in press). For Frazier Creek, the KREW P301 piezometer (a shallow groundwater sample) provides a better end-member fit than the deeper groundwater samples however the piezometer and groundwater samples occupy the same region (lower right) of the plots. While it is not expected that the Frazier groundwater is identical to the well and piezometer samples, EMMA indicates that there is similarity between the chemistry of the groundwater samples and that of one of the catchment end-members.

Shaw (2009) reported two distinct fractured bedrock aquifers in the Wawona area of Yosemite National Park approximately 10 kilometers northwest of the southern project site. A 1990's groundwater assessment for Wawona showed a shallow aquifer less than 100 meters deep with $\delta^{18}O$ and $\delta^{2}H$ that ranged from -11.7 to -12.2‰ and -81.5 to -86.5‰ respectively; in the deeper (below 100 meters) aquifer, values ranged from -13.3 to -13.6‰ and -94.5 to -99.5‰ for $\delta^{18}O$ and $\delta^{2}H$ respectively. Values from the groundwater wells used in this study were intermediary between the shallow and deep aquifer values from Wawona. This may be due to differences in the chemistry of the groundwater between the two sites, but more likely it represents a mixture of shallow and deep aquifer water due to screening of the wells in this study along the majority of their depth.

Liu *et al*. (2013) showed slightly different end-members at the KREW sites. As in this study, they found two of the end-members to be snowmelt and subsurface flow. Their third end-member they defined as fall storm runoff whereas in this study we make a case for the third end-member being more generally representative of rain. Variations in flowpaths can significantly alter water ion chemistry as a function of residence time and material the water contacts, however stable water isotopes (used as tracers in this study, but not at KREW) tend to undergo less alteration from precipitation to stream flow than nutrient solutes, especially in headwater basins with relatively short flow path lengths. The use of isotopes for 2 of our 3 conservative tracers means that end-members in this study are more representative of water sources than of flowpaths. While the single rain samples at Big Sandy and Fresno meteorological stations only provided an optimal end-member fit for Big Sandy Creek, the stream samples that were chosen as end-members are expected to approximate rain within the basin. The October streamflow sample chosen for Bear Trap had only a small rain event preceding the sample, but streamflow at the time was very low, so rain may have been a significant fraction of the sampled flow. The April sample dates chosen for Speckerman Creek and Frazier Creek were not immediately preceded by large rain events, but did have substantial rain events a few weeks prior. The samples may still be representative of these precipitation events as rain water may have had a slight lag time in reaching the stream through near surface flow pathways.

Nested catchment studies in the literature show considerable variability in end-member contributions across spatial scales and indicate a catchment scale dependence on

end-member mixing (Inamdar and Mitchell, 2007; Jung et al., 2009; Iwasaki et al., 2015). It remains important to tease out differences in vegetation, geology, and topography from flow/path residence time controlling factors. Flow path end-members may be more appropriate than source end-members in larger catchments (Uhlenbrook and Hoeg, 2003; Inamdar and Mitchell, 2007; Liu et al., 2008) where greater path lengths and residence times allow for more evolution of the waters and a greater differentiation between end-member chemistry.

Drought Signal

The shift toward a greater groundwater fraction in drought years was not surprising as perennial streamflow and lack of summer rain indicates there is subsurface storage in all four basins. The importance of groundwater in maintaining baseflow can be noted from the work of Winters (2007), who contends that the quantity and stability of baseflow is determined by the amount of groundwater discharge to the stream and by Dekker and Hughson (2014) who showed that the amount of groundwater storage was the most important factor in the persistence of ephemeral springs during drought years in mountainous areas of the Mojave Desert of California.

Interestingly, the shift toward greater groundwater fraction was only notable for baseflow stream samples. When EMMA stream water samples from the entire year were plotted, drought year samples from fall, winter, and spring were not substantially different than samples from the non-drought years. Even in years when rain and snow are low, wet season runoff still shows the higher snow and rain components typically seen in wet years. This suggests that precipitation is still an important contributor to flow in dry years, but that once this "newer" water is depleted, flow is maintained by groundwater stores. In a study at Sagehen Creek not far from this study's northern site, Rademacher *et al*. (2005) found that the mean residence time of water discharging to the channel was 15 years during the snowmelt period and 28 years during baseflow indicating proportionally more new water (i.e. snow) during spring and more old water (groundwater) during baseflow. Blumstock *et al*. (2015) during a drought in Scotland, saw homogeneous stream chemistry at the end of winter rains, but considerable variability during the recession and low flow periods for a small mountain catchment. For coastal mountain streams in northern California, decreased flows were seen in 60% of basins over the past 40-80 years by Sawaske and Freyberg (2014). Like in this study, the trends were only apparent during in late-summer low flows; no change in spring high-flow conditions could be identified for the study period.

When specifically looking at low flow season data, water chemistry measurements also support the model that drought years see a higher fraction of groundwater flow. During the summer baseflow seasons, higher conductivity values (Figure 5.8) and higher ion concentrations are observed in stream water in drought years as compared to the preceding wet years. Others have shown similar patterns of higher conductivity and ion concentrations due to increased groundwater fraction under drought conditions (Blumstock et al., 2015, Mosley et al., 2015).Higher conductivities and concentrations can be due to one of two reasons: 1) as the baseflow season progresses

there is an increasing fraction of sub-surface flow that had picked up dissolved materials while in contact with rock and/or soil, or 2) evaporation is occurring, increasing the concentration of dissolved material in the stream water.

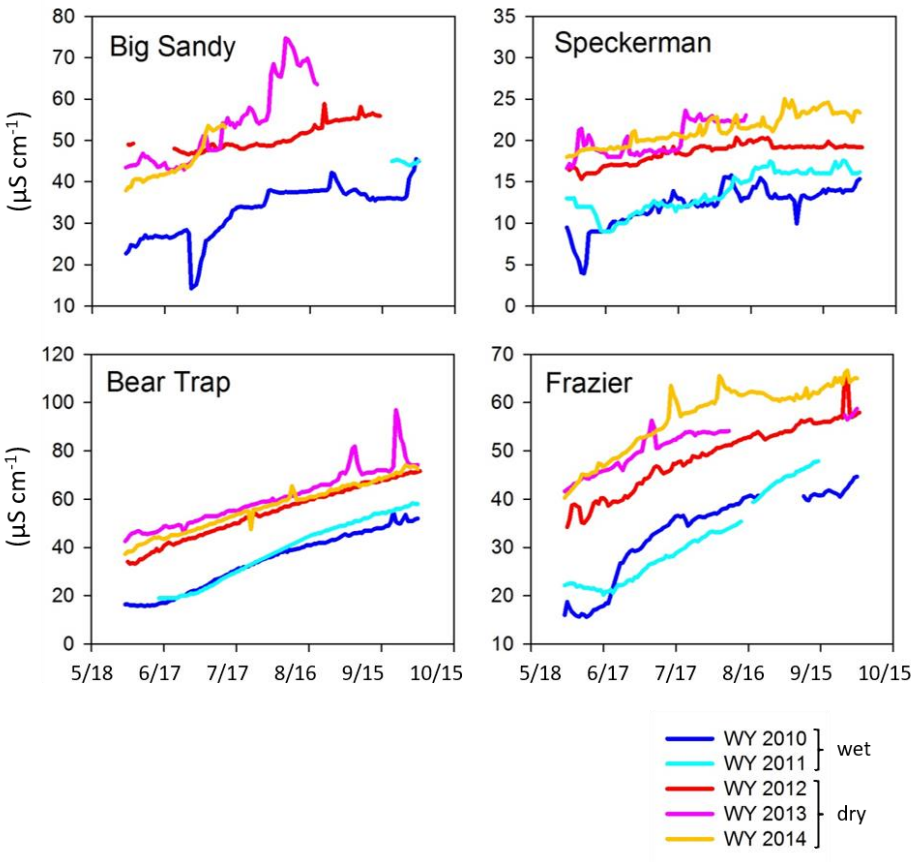

Figure 5.8. Baseflow stream conductivity data showing notably higher values during dry years vs wet years

Baseflow stable isotope data help to verify that the mechanism causing higher concentration and conductivity is increased groundwater rather than evaporation. Isotope values are based on the isotopic signature of precipitation falling on the watershed. These values vary considerably by storm, but contact with the subsurface does not typically alter the isotopic signature of the water, so even non-event water will plot along a localized meteoric waterline. Evaporation, however, will alter the isotopic signature as samples diverge from the LMWL at a shallow angle with increasingly less negative δ^2H and $\delta\ ^{18}O$ values (Figure 5.9). The baseflow data for the drought years (WYs 2012-13) did not show this evaporation signal so it can be concluded that increased conductivity and ion concentrations were due to a greater proportion of sub-surface water in the stream. A slight evaporation signal may have been present for a few samples in WY 2014, but could not be confirmed by the data. The trend was very minimal and later season samples did not show the same trend as the early summer samples. The presence of an evaporation signal can depend on the system. Boerner and Gates (2015) did not

find an evaporation trend in stable isotope data during a summer drought in the Platte River, NB. However, Blumstock *et al.* (2015) observed an evaporation signal in localized reaches during a low-flow, drought period in Scotland, and attributed it to evaporative losses from the near stream soils. They saw less of an evaporative signal in the downstream direction likely due to increased fractions of deep, non-fractionated groundwater.

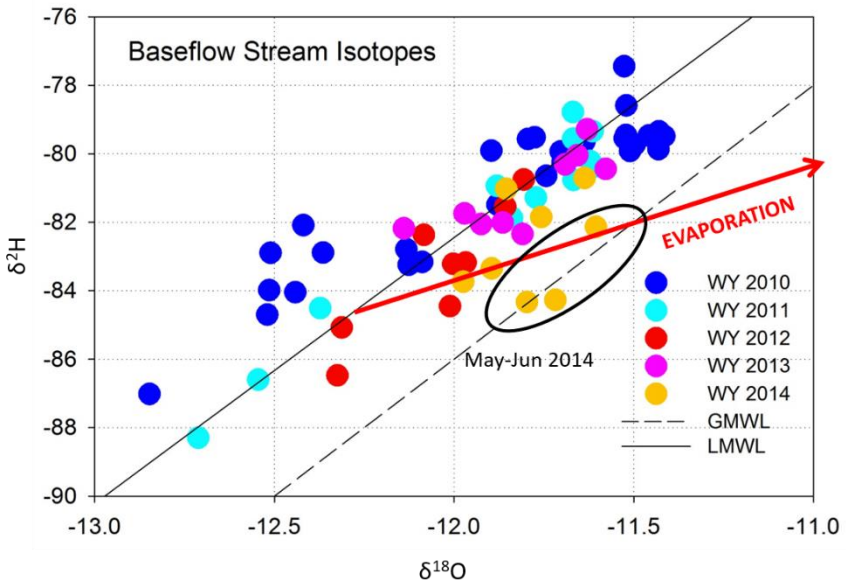

Figure 5.9. Baseflow (May through October) stream isotope data. Values generally plot along the local meteoric water line. A possible evaporation signal was only discernable in WY 2014, the third consecutive year of drought and driest year of the study period.

Low antecedent moisture after two preceding years of drought may have played a role in the particularly low annual water yield of 2014, highlighting the importance of antecedent conditions on hydrologic processes especially during an extended drought. For four rain-dominated, forested, mountain, river basins on the central coast of California with a Mediterranean climate similar to that in this study, Bart and Hope (2014) quantified the relationship between antecedent groundwater storage and baseflow recession rates. Their work emphasized the importance of antecedent conditions to baseflow recession in regions, like those in this study, which exhibit asynchronicity of precipitation and energy levels. In an examination of drought signals across Europe, Zaidman *et al.* (2001) found that for a 1976 drought event, the level of streamflow reduction couldn't be fully explained by low precipitation immediately preceding the event. Reductions in groundwater discharge, which they attributed to the low precipitation (drought) of several seasons prior, were found to also contribute to the observed streamflow reduction.

Drought and Forest Health

A greater reliance on deeper water sources to sustain baseflow in dry years combined with the cumulative effect of previous years of drought can have profound impacts on forest ecosystem health. While winter precipitation can accommodate wet-season ET even in dry years, the decreased precipitation totals result in lower subsurface recharge (Klos et al., in press). Additionally, higher dry season temperatures increase summer ET demands leading to greater deficits between storage and evaporative demand. The recent California drought was one of the warmest on record, increasing the water needs of forest vegetation during a time when water availability was already anomalously low (Griffin and Anchukaitis, 2014; Klos et al., in press).

Soil depths measured in this study ranged from 0 to ~1.5 m and during summer dry seasons of all years in this study, soil moisture was drawn down to field capacities similar to those reported by Ziemer (1964) for similar terrain at the Central Sierra Snow Laboratory. The exception to this was WY 2012 and 2013 where some isolated summer storms at the northern site raised soil moisture levels in the riparian zone leading to slightly higher site averaged soil moisture though hillslopes and ridges still saw full drying (Saksa, in press). To overcome the yearly lack of summer soil water, Sierra trees extend roots well beyond the limited soil layer (Schwinning, 2010; Fellows and Goulden, 2016; Klos et al., in press). While most years (wet and dry) see full drying of the soil layer, consecutive years of drought can begin to impact water storage in the saprolite and weathered bedrock layers below. When previous wet season recharge is less than dry season evaporative demand as seen in the 2012-2015 drought, progressively less water is available to plants and trees in the deep rooting zone (Klos et al., in press).

The substantial tree mortality across the Sierra by the end of the 4-year drought is a likely consequence of this rooting zone water deficit (Figure 5.10). On the Sierra National Forest where southern sites are located, the US Forest Service Aerial Detection and Monitoring Program mapped 33,000 acres as having tree mortality in 2012 (Heath et al., 2013). In the summer of 2016 at the end of the drought that number was 557,000 acres (42% of the Sierra NF) accounting for 18,563,000 dead trees (USDA Forest Service, 2012, Moore et al., 2017). On the Tahoe National Forest where the norther study sites are located, 19,445 acres were mapped in 2012 and in 2016 it was up to 99,000 acres (11% of the Tahoe NF) accounting for 358,000 dead trees (USDA Forest Service, 2012; Heath et al., 2013; Moore et al., 2017). More severe tree mortality around the southern site fits with forest treatment models run for the sites in this study by Saksa (2015) which pointed to forest vegetation being more limited in the southern Sierra Nevada than in the central Sierra Nevada. Areas that are already water limited are most likely to experience high tree mortality and ecosystem disruption.

Figure 5.10. Extensive tree mortality observed after multiple years of drought. Photo was taken approximately 3 miles south of the Sugar Pine sites (on the south side of Speckerman Mountain) in summer of 2016 courtesy of USDA Forest Service Aerial Detection Monitoring Program.

Conclusions

Knowledge of water sources throughout the year and shifts in end-member proportions from wet to dry years provides a better understanding of the effects of prolonged drought on forested mountain systems. In this study, a greater proportion of source water came from groundwater during the summer low flow period in dry years. Antecedent moisture conditions are important and multiple consecutive years of drought have greatly stressed forest vegetation (especially in more water limited southern site) resulting in significant tree die-off. These results highlight the importance of groundwater stores in maintaining flow and sustaining forested mountain ecosystems.

Data indicate that drought in these systems has the largest effect on summer low flows and that other times of year the effects of drought are difficult to detect in stream chemistry. Little difference in source water ratios were seen between high and low water years during the high flow season. Only during base flow were drought effects apparent. This work illustrates the fact that while high flow periods may drive geomorphic change

in a watershed, drought conditions and low flow periods are key to ecosystem stability especially in Mediterranean climates.

A solid understanding of these headwater systems is increasingly important as climate change brings more climatic variability. Decreased snow and earlier melt may mean less opportunity for groundwater recharge and subsequent reductions in downstream water. The system's reliance on groundwater sources for maintaining summer streamflow combined with the recently observed tree mortality should be a warning sign to land managers. Areas that are more water limited and already relying heavily on the deep groundwater sources will likely be most vulnerable to drought and climate change. In the face of these changes, properly managing water resources becomes even more critical.

References

Bart, R., & Hope, A. (2014). Inter-seasonal variability in baseflow recession rates: The role of aquifer antecedent storage in central California watersheds. *Journal of Hydrology*, *519*(PA), 205–213. https://doi.org/10.1016/j.jhydrol.2014.07.020

Bateman, P. C. (1989). *Geologic map of the Bass Lake quadrangle, west-central Sierra Nevada, California*.

Blumstock, M., Tetzlaff, D., Malcolm, I. A., Nuetzmann, G., & Soulsby, C. (2015). Baseflow dynamics: Multi-tracer surveys to assess variable groundwater contributions to montane streams under low flows. *Journal of Hydrology*, *527*, 1021–1033. https://doi.org/10.1016/j.jhydrol.2015.05.019

Boerner, A. R., & Gates, J. B. (2015). Temporal dynamics of groundwater-dissolved inorganic carbon beneath a drought-affected braided stream: Platte River case study, 1–14. https://doi.org/10.1002/2015JG002950.Received

Clow, D. W., Schrott, L., Webb, R., Campbell, D. H., Torizzo, a, & Dornblaser, M. (2003). Ground water occurrence and contributions to stream ow in an alpine catchment. *Colorado Front Range. Ground Water*, *41937e950*(7), 937–950. https://doi.org/10.1111/j.1745-6584.2003.tb02436.x

Craig, H. (1961). Isotopic Variations in Meteoric Waters. *Science*, *133*(3465), 1702–1703. https://doi.org/10.1126/science.133.3465.1702

Coplen, T. B., & Kendall, C. (2000). *Stable hydrogen and oxygen isotope ratios for selected sites of the U. S. Geological Survey's NASQAN and Benchmark surface-water networks.*

Dekker, F. J., & Hughson, D. L. (2014). Reliability of ephemeral montane springs in Mojave National Preserve, California. *Journal of Arid Environments*, *111*, 61–67. https://doi.org/10.1016/j.jaridenv.2014.07.008

Diffenbaugh, N. S., Swain, D. L., & Touma, D. (2015). Anthropogenic warming has increased drought risk in California. *Proceedings of the National Academy of Sciences*, *112*(13), 3931–3936. https://doi.org/10.1073/pnas.1422385112

Fellows, A. W., & Goulden, M. L. (2017). Mapping and understanding dry season soil water drawdown by California montane vegetation. *Ecohydrology*, *10*(1), 1–12. https://doi.org/10.1002/eco.1772

Griffin, D., & Anchukaitis, K. J. (2014). How unusual is the 2012 – 2014 California drought? *Geophysical Research Letters*, *41*, 9017–9023. https://doi.org/10.1002/2014GL062433.1.

Heath, Zackary; Moore, Jeff; Oblinger, Brent; Woods, M. (2013). *2012 Aerial Survey Results: California*. Retrieved from https://www.fs.usda.gov/Internet/FSE_DOCUMENTS/stelprdb5414677.pdf

Horton, T. W., Chamberlain, C. P., Fantle, M., & Blum, J. D. (1999). Chemical weathering and lithologic controls of water chemistry in a high-elevation river system: Clark's Fork of the Yellowstone River, Wyoming and Montana. *Water Resources Research*, *35*(5), 1643–1655. https://doi.org/10.1029/1998WR900103

Hunsaker, C. T., & Neary, D. G. (2012). Sediment loads and erosion in forest headwater streams of the Sierra Nevada, California. *Revisiting Experimental Catchment Studies in Forest Hydrology*, *353*(July 2011), 195–203.

Inamdar, S. P., & Mitchell, M. J. (2007). Contributions of riparian and hillslope waters to storm runoff across multiple catchments and storm events in a glaciated forested watershed. *Journal of Hydrology*, *341*(1–2), 116–130. https://doi.org/10.1016/j.jhydrol.2007.05.007

Iwasaki, K., Katsuyama, M., & Tani, M. (2015). Contributions of bedrock groundwater to the upscaling of storm-runoff generation processes in weathered granitic headwater catchments. *Hydrological Processes*, *29*(6), 1535–1548. https://doi.org/10.1002/hyp.10279

Jenkins, A., Sloan, W. T., & Cosby, B. J. (1995). Stream chemistry in the middle hills and the high mountains of Himalayas, Nepal. *Journal of Hydrology*, *166*, 61–79.

Retrieved from https://ac.els-cdn.com/002216949402600G/1-s2.0-002216949402600G-main.pdf?_tid=a1edd54c-c379-11e7-8470-00000aab0f26&acdnat=1510031463_e5878a41a79a886395d8d8e8c710c213

Joeckel, R. M., Clement, B. J. A., & Bates, L. R. V. (2005). Sulfate-mineral crusts from pyrite weathering and acid rock drainage in the Dakota Formation and Graneros Shale, Jefferson County, Nebraska. *Chemical Geology*, *215*, 433–452. https://doi.org/10.1016/j.chemgeo.2004.06.044

Jung, H. Y., Hogue, T. S., Rademacherr, L. K., & Meixner, T. (2009). Impact of wildfire on source water contributions in Devil Creek, CA: evidence from end-member mixing analysis. *Hydrological Processes*, *23*, 183–200. https://doi.org/10.1002/hyp.7132

Kang, D. H., Gao, H., Shi, X., Islam, S. U., & Déry, S. J. (2016). Impacts of a Rapidly Declining Mountain Snowpack on Streamflow Timing in Canada's Fraser River Basin. https://doi.org/10.1038/srep19299

Klos, P. Z., Goulden, M., Riebe, C., Tague, C., O'Green, A. T., Flinchum, B., Safeeq, M., Conklin, M, Hart, S., Berhe, A. A., Hartsough, P., Holbrook, W. S., Bales, R. (*in review*) Predicting plant-accessible water in the critical zone: mountain ecosystems in a Mediterranean climate. *WIREs Water*.

Krám, P., Farkaš, J., Pereponova, A., Nwaogu, C., Štědrá, V., & Hruška, J. (2014). Bedrock weathering and stream water chemistry in felsic and ultramafic forest catchments. *Procedia Earth and Planetary Science*, *10*, 52–55. https://doi.org/10.1016/j.proeps.2014.08.010

Krám, P., Hruška, J., & Shanley, J. B. (2012). Streamwater chemistry in three contrasting monolithologic Czech catchments. *Applied Geochemistry*, *27*, 1854–1863. https://doi.org/10.1016/j.apgeochem.2012.02.020

LaPerriere Nelson, M., Rhoades, C. C., & Dwire, K. A. (2011). Influence of bedrock geology on water chemistry of slope wetlands and headwater streams in the Southern Rocky Mountains. *Wetlands*, *31*, 251–261. https://doi.org/10.1007/s13157-011-0157-8

Liu, F., Hunsaker, C., & Bales, R. C. (2013). Controls of streamflow generation in small catchments across the snow-rain transition in the Southern Sierra Nevada, California. *Hydrological Processes*, *27*(14), 1959–1972. https://doi.org/10.1002/hyp.9304

Liu, F., Parmenter, R., Brooks, P. D., Conklin, M. H., & Bales, R. C. (2008). Seasonal and interannual variation of streamflow pathways and biogeochemical implications

in semi-arid, forested catchments in Valles Caldera, New Mexico. *Ecohydrology*, *1*, 239–252. https://doi.org/10.1002/eco.22

Martin, S. E., & Conklin, M. H. (in press). Tracking channel bed resiliency in forested mountain catchments using high temporal resolution channel bed movement. *Geomorphology*, *301*, 68–78. https://doi.org/10.1016/j.geomorph.2017.10.026

Martin, S. E., Conklin, M. H., & Bales, R. C. (2014). Seasonal accumulation and depletion of local sediment stores of four headwater catchments. *Water (Switzerland)*, *6*(7), 2144–2163. https://doi.org/10.3390/w6072144

Mishra, A. K., & Singh, V. P. (2010). A review of drought concepts. *Journal of Hydrology*, *391*, 202–216. https://doi.org/10.1016/j.jhydrol.2010.07.012

Meixner, T., Brown, A., & Bales, R. C. (1998). Importance of biogeochemical processes in modeling stream chemistry in two watersheds in the Sierra Nevada, California. *Water Resources*, *34*(11), 3121–3133.

Moore, J., Woods, M., Ellis, A., & Moran, B. (2017). *2016 Aerial Survey Results: California*. Retrieved from https://www.fs.usda.gov/Internet/FSE_DOCUMENTS/fseprd543943.pdf

Moore, R. D. (2003). Introduction to salt dilution gauging for streamflow measurement Part 1. *Streamline*, *8*(4), 20–23. https://doi.org/10.1592/phco.23.9.1S.32890

Mosley, L. M. (2015). Drought impacts on the water quality of freshwater systems; review and integration. *Earth Science Reviews*, *140*, 203–214. https://doi.org/10.1016/j.earscirev.2014.11.010

Newton, R. M., Weintraub, J., & April, R. (1987). The relationship between surface water chemistry and geology in the North Branch of the Moose River. *Biogeochemistry*, *3*(21), 21–35. Retrieved from https://link.springer.com/content/pdf/10.1007%2FBF02185183.pdf

Petrone, K. C., Hughes, J. D., Van Niel, T. G., & Silberstein, R. P. (2010). Streamflow decline in southwestern Australia, 1950-2008. *Geophysical Research Letters*, *37*(11), 1–7. https://doi.org/10.1029/2010GL043102

Praça Leite, M. G., Maria Augusta Gonçalves Fujaco, B., Hermínio Nalini Jr, B. A., & Paulo de Tarso Castro, B. A. (2010). Influence of geology in the geochemistry signature of Itacolomi State Park waters, Minas Gerais-Brazil. *Environ*, *60*, 1723–1730. https://doi.org/10.1007/s12665-009-0306-z

Rademacher, L. K., Clark, J. F., Clow, D. W., & Hudson, G. B. (2005). Old groundwater influence on stream hydrochemistry and catchment response times in a small Sierra

Nevada catchment: Sagehen Creek, California. *Water Resources Research*, *41*(2), 1–10. https://doi.org/10.1029/2003WR002805

Reinfelds, I., Swanson, E., Cohen, T., Larsen, J., & Nolan, A. (2014). Hydrospatial assessment of streamflow yields and effects of climate change: Snowy Mountains, Australia. *Journal of Hydrology*, *512*, 206–220. https://doi.org/10.1016/j.jhydrol.2014.02.038

Rochette, E. A., Drever, J. I., & Sanders, F. S. (1988). Chemical weathering in the West Glacier Lake drainage basin, Snowy Range, Wyoming: implications for future acid deposition. *Contributions to Geology*, *6*(1), 29–44.

Rood, S. B., Pan, J., Gill, K. M., Franks, C. G., Samuelson, G. M., & Shepherd, A. (2008). Declining summer flows of Rocky Mountain rivers: Changing seasonal hydrology and probable impacts on floodplain forests. *Journal of Hydrology*, *349*, 397–410. https://doi.org/10.1016/j.jhydrol.2007.11.012

Saksa, P. (2015). *Forest management, wildfire, and climate impacts on the hydrology of Sierra Nevada mixed-conifer watersheds*. University of California, Merced.

Saucedo, G. J., & Wagner, D. L. (1992). *Geologic Map of the Chico Quadrangle, Regional Geologic Map 7A*.

Sawaske, S. R., & Freyberg, D. L. (2014). An analysis of trends in baseflow recession and low-flows in rain-dominated coastal streams of the pacific coast. *Journal of Hydrology*, *519*, 599–610. https://doi.org/10.1016/j.jhydrol.2014.07.046

Schwinning, S. (2010). Ecohydrology Bearings - Invited Commentary: The ecohydrology of roots in rock. *Ecohydrology*, *3*, 238–245. https://doi.org/10.1002/eco.134

Shaw, G. D. (2009). *Investigating groundwater and surface water interactions using novel isotopes and geochemical tracers in the upper Merced River Basin, Sierra Nevada, California*. University of California, Merced.

Soulsby, C., Tetzlaff, D., Rodgers, P., Dunn, S., & Waldron, S. (2006). Runoff processes, stream water residence times and controlling landscape characteristics in a mesoscale catchment: An initial evaluation. *Journal of Hydrology*, *325*, 197–221. https://doi.org/10.1016/j.jhydrol.2005.10.024

Soulsby, C., Tetzlaff, D., Van Den Bedem, N., Malcolm, I. A., Bacon, P. J., & Youngson, A. F. (2007). Inferring groundwater influences on surface water in montane catchments from hydrochemical surveys of springs and streamwaters. *Journal of Hydrology*, *333*, 199–213. https://doi.org/10.1016/j.jhydrol.2006.08.016

Tague, C., & Grant, G. E. (2004). A geological framework for interpreting the low-flow regimes of Cascade streams, Willamette River Basin, Oregon. *Water Resources Research*, *40*(4), 1–9. https://doi.org/10.1029/2003WR002629

Tetzlaff, D., & Soulsby, C. (2008). Sources of baseflow in larger catchments - Using tracers to develop a holistic understanding of runoff generation. *Journal of Hydrology*, *359*(3–4), 287–302. https://doi.org/10.1016/j.jhydrol.2008.07.008

Uhlenbrook, S., & Hoeg, S. (2003). Quantifying uncertainties in tracer-based hydrograph separations: A case study for two-, three- and five-component hydrograph separations in a mountainous catchment. *Hydrological Processes*, *17*(2), 431–453. https://doi.org/10.1002/hyp.1134

USDA Forest Service. (2012). *Land areas of the National Forest System* (Vol. FS-383). Retrieved from https://www.fs.fed.us/land/staff/lar/LAR2011/LAR2011_Book_A5.pdf

USDA Forest Service Pacific Southwest Research Station. (2017). Tree Mortality in California. Retrieved November 6, 2017, from https://www.fs.fed.us/psw/topics/tree_mortality/california/index.shtml

Williams, M. W., & Melack, J. M. (1991). Solute chemistry of snowmelt and runoff in an Alpine Basin, Sierra Nevada. *Water Resources Research*, *27*(7), 1575–1588. https://doi.org/10.1029/90WR02774

Winter, T. C. (2007). The role of ground water in generating streamflow in headwater areas and in maintaining base flow. *Journal of the American Water Resources Association*, *43*(1), 15–25. https://doi.org/10.1111/j.1752-1688.2007.00003.x

Zaidman, M. D., Rees, H. G., & Young, A. R. (2001). Spatio-temporal development of streamflow droughts in north-west Europe. *Hydrology and Earth System Sciences*, *5*(4), 733–751. Retrieved from http://citeseerx.ist.psu.edu/viewdoc/download?doi=10.1.1.371.9105&rep=rep1&type=pdf

Ziemer, R. R. (1964). Summer evapotranspiration trends as related to time after logging of forests in Sierra Nevada. *Journal of Geophysical Research*, *69*(4), 615–620. https://doi.org/10.1029/JZ069i004p00615

Chapter 6. Conclusion

Study Results

Analysis of turbidity and discharge data showed that there was a seasonal pattern and that turbidity events were tied to higher flows. The predominately clockwise hysteresis patterns observed is indicative of nearby, easy to transport material (more material transported on the rising limb). This evidence along with no difference in turbidity seen between snow cover and non-snow cover periods points to in-channel rather than hillslope sediment sources. A reduction in turbidity peaks during last summer and early fall suggests that there is a seasonal accumulation and depletion cycle where erosion builds up material at the toe of banks during baseflow. That material gets transported during the winter-spring high flow season, but the material stores become progressively depleted leading to the observed shift to fewer clockwise hysteresis patterns during hydrograph drawdown.

The channel bed measurements build on this idea by connecting these seasonal accumulation and depletion cycles to downstream transport. Build-up and scour down of the channel bed occurs on event and annual scales. The amount of material on the channel bed represents a balance between sediment supply from the channel margins and conveyor-belt like transport in the thalweg. Not only are the rates of sediment production and transport important, but the seasonal connectedness between the margins and thalweg also acts as a key control on the accumulation rate of sediment stores at the toe of the banks and redistribution of sediment to the thalweg. When supply from the margins that *feeds* the conveyor-belt outpaces the rate of transport, material builds up. As supply stores are depleted and downstream transport outpaces supply, scour and a reduction of channel be elevation is observed.

During baseflow season and especially during baseflow of drought years, concentrations of major ions increased. End-member mixing analysis showed that stream water during summer base flow in drought years was maintained by a greater ratio of groundwater sources. This difference in source water ratios between drought and non-drought years was not observed during other times of year. Even after three consecutive years of drought, ratios of snow/rain to groundwater were within the same range as for wet years. These results imply that even in dry years recent precipitation (rain/snow) is sufficient to supply vegetation and streamflow during the wet season. Observations of extensive tree mortality in the Sierra Nevada after multiple years of drought emphasize the importance of groundwater stores in maintaining flow and baseflow hydrologic processes to ecosystem stability in forested mountain systems.

Management Implications and Water Quality

Both sediment and source water ratios have implications for hydrologic modeling and downstream infrastructure management and planning. Major ion concentrations measured in this study were relatively low and were not a concern to water quality downstream. For example, the US Environmental Protection Agency's Secondary Drinking Water Standard for sulfate is 5200 μeqL^{-1} and for chloride is 7100 μeqL^{-1} at least an order of magnitude higher than any stream sample in this study (US Environmental Protection Agency, 2017). Because of the naturally low concentration of chemical species and the limited potential for chemical pollution within the watersheds, sediment remains the main water quality concern.

An understanding of the controls on sediment allows us to better manage for it. The patterns and processes involved in sediment production and transport in forested, mountain basins have implications to local and regional water supplies as well as global sediment budgets. Most of the state's river systems contain dams, where storage area can be greatly reduced by accumulating sediment (Sierra Nevada Conservancy, 2011). Knowledge of sediment processes, and their temporal variability, gained in this work can inform sediment and water-quality modeling, and long-term planning for seasonal precipitation changes associated with climate change in forested, mountain basins world-wide.

A connection may exist between water sources and sediment production rates, but more work needs to be done to clarify the controls and processes. For example, a conceptual model in which precipitation water reaches the stream through a piston-type flow pathway could be tested through tracer studies. In these systems sediment production is dominated by bank erosion, accumulation of sediment occurs at the channel margins, and a seasonal connectedness exists between channel margins and the conveyor-belt like transport in the thalweg. Piston-flow is where precipitation falling on the landscape infiltrates into the shallow sub-surface and non-event is pushed into the channel through subsurface pathways ahead of event water. This mechanism implies that, rather than running overland, water enters the channel through the bed and banks, limiting sediment production to in-channel sources fitting with current results. The amount and duration of sub-surface flow (lateral flow and moisture content of the banks) determines the rate of sediment production at the channel banks. Both high rates of seepage and drying out of the banks may increase erosion rates.

Understanding of water sources and supply can also be important for resource management, downstream water quality, and ecosystem stability. Extremely low flows can lead to water quality issues such as stagnation, nutrient buildup, high temp, and low dissolved oxygen. Vegetation stress and tree mortality could lead to reduced vegetation cover, increased erosion, and increased fire risk. It should be noted though, that this work described here represents normal conditions and results may not applicable to catastrophic events (i.e. fire, intensive logging, mass wasting, or extreme precipitation events). For example, in the case of vegetation loss or fire, our assumption of no overland flow may not hold.

Future focus

There is a great need for understanding of patterns and variability of headwater systems and to be able to describe the underlying processes. While poor water quality is not a current concern for most Sierra Nevada headwater streams, climate change models predict an increase in extreme events in the future which have the potential to impact water quality. Data models may be necessary to predict future change and inform management, but model results can only be as good as their underlying data and it is important to base modeling on measured data.

Working in headwater systems (especially in forest mountain areas) is often difficult because of their remote locations but field data collection is critical to constrain models and inform management. Detailed data studies are needed, that illuminate and target sensitivity or vulnerable areas where management efforts can most efficiently affect change. Continued investment and improvements in new technologies that will allow better data collection would greatly aid these efforts. New sensors with improved accuracy and lower cost would allow for better data sets and distributed measurements. Advances in sensor robustness, power consumption, and data storage will improved the feasibility of measurements in remote headwater systems.

Finally, there is a great need for continued investment in long term monitoring studies that can capture year to year variability in parameters such as precipitation amounts/intensity, temperature, and timing. The management community needs to better understand shifting conditions and pressures of drought and climate change as existing baselines evolve. Recent record setting temp and precipitation patterns underscore the fact that we may no longer be able to rely on data of past conditions for current and future management (Millar et al., 2007). As catastrophic events (e.g. fire, pest outbreaks, drought, extreme hydrologic events) become more common, there is also an urgent need to understand their processes and effects. Long term studies are key to capturing data on these events and building our knowledge base. This knowledge is especially important in a changing future where previous long-term data sets may no longer be applicable.

References

Millar, C. I., Stephenson, N. L., & Stephens, S. L. (2007). Climate change and forest of the future: Managing in the face of uncertainty. *Ecological Applications*, *17*(8), 2145–2151. https://doi.org/http://dx.doi.org/10.1890/06-1715.1

US Environmental Protection Agency. (2017). Headwater Streams Studies. Retrieved November 11, 2017, from https://www.epa.gov/water-research/headwater-streams-studies